MAPPING SOIL PROPERTIES AND WATER TABLE DEPTHS USING ELECTROMAGNETIC INDUCTION METHODS

by

Fahad Sarwar Khan

Submitted in partial fulfilment of the requirements
for the degree of Master of Science

at

Dalhousie University
Halifax, Nova Scotia

in co-operation with

Nova Scotia Agricultural College
Truro, Nova Scotia

March 2012

DALHOUSIE UNIVERSITY

NOVA SCOTIA AGRICULTURAL COLLEGE

The undersigned hereby certify that they have read and recommend to the Faculty of Graduate Studies for acceptance a thesis entitled "MAPPING SOIL PROPERTIES AND WATER TABLE DEPTHS USING ELECTROMAGNETIC INDUCTION METHODS" by Fahad Sarwar Khan in partial fulfilment of the requirements for the degree of Master of Science.

Dated: March 15, 2012

Supervisor: _____

_____

Readers: _____

_____

_____

DALHOUSIE UNIVERSITY

NOVA SCOTIA AGRICULTURAL COLLEGE

DATE: March 15, 2012

AUTHOR: Fahad Sarwar Khan

TITLE: MAPPING SOIL PROPERTIES AND WATER TABLE DEPTHS USING ELECTROMAGNETIC INDUCTION METHODS

DEPARTMENT OR SCHOOL: Department of Engineering

DEGREE: MSc CONVOCATION: May YEAR: 2012

_____

Signature of Author

TABLE OF CONTENTS

LIST OF TABLES

LIST OF FIGURES

ABSTRACT

Detailed soil and water data are essential to ensure the optimum long-term management of fields. The objective of this study was to estimate water table depths, spatially variable and layered soil properties using electromagnetic induction methods. Soil samples were collected and analyzed within two wild blueberry, a soybean-barley and a pasture fields. Observation wells were installed. The DualEM-2 was calibrated to predict the soil properties and groundwater depths. The apparent ground conductivity (EC_a) and water table depths were measured simultaneously from each well, before and after every significant rainfall for three consecutive days. Comprehensive surveys were conducted in selected fields to measure EC_a with DualEM-2. Survey data were imported in C++ program to estimate layered soil properties using mathematical models. Regression models were developed to predict soil properties and groundwater depths. The predicted soil properties and groundwater table maps were generated. This information can help to develop variable rate technologies.

LIST OF ABBREVIATIONS AND SYMBOLS USED

ATV	All-terrain vehicle
BEEC	Bio-Environmental Engineering Centre
CEC	Cation exchange capacity
cm	Centimeter
CV	Coefficient of variation
CVs	Coefficient of variations
DEMs	Digital elevation models
DGPS	Differential global positioning system
DOE	Depth of exploration
EC	Electrical conductivity
EC_a	Apparent ground conductivity
EC_e	Saturated paste extract electrical conductivity
EC_p	Soil solid electrical conductivity
EC_w	Soil solution electrical conductivity
EMI	Electromagnetic induction
GIS	Geographical information system
GPS	Global positioning system
ha	Hectare
hr	Hour
HCP	Horizontal co-planar array
H_i	Induced magnetic field
H_p	Primary magnetic field
Hz	Hertz
IDW	Inverse distance weighting
km	Kilometer
kg	Kilogram
kHz	Kilohertz
m	Meter
Max.	Maximum
ME	Mean error
Min.	Minimum
mm	Millimeter
mS	Milli siemens
N	North
NSAC	Nova Scotia Agricultural College
PRP	Perpendicular co-planar array
PVC	Polyvinyl chloride
θ_v	Volumetric soil moisture content
%	Percent
^{o}	Degree
‘	Minute
r	Coefficient of correlation
R^2	Coefficient of determination
RMSE	Root mean square error

RTK-GPS	Real time kinematics global positioning system
ρ_b	Soil bulk density
SD	Standard deviation
SOM	Soil organic matter
TDR	Time domain reflectometry
µS	Micro siemens
W	West
WTD	Water table depth from soil surface
z_{in}	Depth to the interface

ACKNOWLEDGEMENTS

Undertaking the MSc programme at Nova Scotia Agricultural College, Truro, Nova Scotia, Canada in the past two years was a truly exceptional experience in my life. However, I could not achieve this work without the blessings of 'Almighty God' and support of different organizations and my near and dear ones.

First of all I would like to express my sincere indebtedness to the Almighty God, for his kindness to allow me to successfully complete my MSc course.

Throughout the course of this project I was privileged to have support from a number of people, to whom I am deeply grateful. First and foremost, I want to acknowledge the expert guidance I received from my supervisor, Dr. Qamar Zaman. I am very grateful to him for the time and effort he has invested in helping me to achieve this goal and for being an inspiration at every step of the way. Our time spent together was not only a chance to share technical information but to learn his philosophy and passion for life. Additionally, I also appreciate his kind cares about my family and personal life.

I equally thank to my co-supervisor, Dr. Arnold Schumann, for his support and encouragement of excellence in all phases of my research particularly his expertise on the EMI instrument and GIS. I also thank my supervisory committee members, Dr. Ali Madani and Dr. David Percival, for their profound understanding and insight about soils, soil moisture, water table depth and crop physiology, their intellectual guidance, consistent support, and endless efforts encouraged to progress and accomplish this project. I gratefully thank them both for their faith in me, and for their inspiration that never failed to lift my spirits and helped me persevere.

I also express my sincere gratitude to Dr. Qamar Zaman and Mrs. Afshan Qamar for providing extreme care, mental support and for helping me to accommodate at Truro from the very first day of my arrival. All my committee members have provided an unquantifiable amount of advice and inspiration during the past two years. I have been fortunate indeed to have such superb researchers in my supervisory committee.

I want to thank Dr. Gordon Brewster, Mr. Darrel Mullin, and Ms. Margie Tate for providing me the Lab facilities, Aitazaz Farooque and Hassan Chattha for helping me in plant growth measurements, Dr. Charlie Walls for his help and guidance in Arc GIS. I am very thankful to Aitazaz Farooque, Kelsey Laking, Travis Esau, Shoaib Saleem, Duncan Gibbs, Matthew Morrison, and Asena Yildiz for helping in laboratory and field data collection. I am also thankful to Aitazaz Farooque for his help in geo-statistical analysis, Dr. Young Chang for supporting and helping me in developing a C++ program in Microsoft Visual Studio software, Dr. Ilhami Yildiz, Dr. Peter Havard, Mr. David Langille, and Mr. Rick Taylor for every possible help, and Marie Law for her help and guidance during my stay at NSAC. I am very grateful to Oxford Frozen Foods, Nova Scotia Department of Agriculture Technology Development Program, and Wild Blueberry Producer Association of Nova Scotia for the financial assistance to complete this project.

I would also like to thank my other mentors Dr. William Philips, Dr. Charles Walls, Dr. Qamar Zaman, Dr. David Percival, Dr. Derek Lynch, Dr. Young Chang, and Dr. Gashaw Gobezie for their excellent teaching skills. I am grateful to Dr. Zaman and family for providing timely, affordable and peaceful accommodation, where I never feel home sick. I specially thank my all family members, my parents and brothers for their greatest trust

and support for me. I thank my beloved daughter (2 years) for her sacrifice and patience. Finally, I would specially like to thank my wife for her love, support, and encouragement while I was finishing my thesis.

CHAPTER 1 INTRODUCTION

One of the fundamental deficiencies in many agriculture production systems is the lack of detailed, up-to-date and pertinent geo-referenced soil and water information. Detailed spatial soil and water data are essential to ensure the optimum long-term management (fertility, irrigation, drainage) and sustainability of fields and associated agricultural crops (Schumann and Zaman, 2003).

Continuous measurement of soil properties as well as water status is expensive, time consuming and difficult. These measurements generally involve *in-situ* characterization and/or collection of soil profile sampling as well as determination of water table depths followed by considerable laboratory analysis.

Electromagnetic induction (EMI) is a technique that measures the apparent ground conductivity (EC_a) by inducing and then detecting an electrical current in the soil (Saey et al., 2009). The EMI instruments are cost-effective and are gaining wider use due to their non-destructive nature, rapid response, and ease of integration into a mobile platform, from which real-time measurements can be made (McNeill, 1980a; Hendrickx and Kachanoski, 2002; Abdu et al., 2007; Farooque et al., 2012). These instruments can be utilized to measure and map field-scale soil properties including soil moisture content (Kachanoski et al., 1988), soil texture (Williams and Hoey, 1987; Kitchen et al., 1999; Sudduth et al., 2005), soil nutrient status (Johnson et al., 2003; Corwin, 2005), water table depths (Schumann and Zaman, 2003), and the presence of restrictive soil layers (Doolittle et al., 1994). The EMI instruments can also provide information about subsoil properties at a range of depths that are important to plant growth, which makes EC_a unique for site-specific management because other methods of assessing soil properties

such as remote sensing and topographical information cannot directly provide information on subsoil properties (Kravchenko et al., 2003).

Specific field maps delineating water table depths as well as soil physical and chemical properties can be utilized to support several field management systems. Different management zones can be developed on the basis of variation in EC_a, coupled with the Geographic Information System (GIS), for the site-specific application of suitable fertilization, supplemental irrigation and its scheduling, and drainage design to reduce input costs and environmental impacts, and to increase productivity.

Ground conductivity measuring devices provide the simplest and least expensive measurement of soil variability (Farahani and Buchleiter, 2004). Among these instruments, the DualEM has been the primary instrument of choice for soil quality and site-specific applications of inputs (Irrigation, fertilization etc.) because its depth of penetration most closely corresponds to the root zone (Corwin and Lesch, 2005a).

The **hypothesis** proposed in this study was that the crop yield is affected by variability in water table depths and soil properties. If these patterns of variability can be measured and mapped quickly and non-destructively using EMI methods, it will then allow for the development of the variable rate technologies and site-specific management. Site-specific management can increase profitability of fields having large spatial variation in soil and water table.

1.1 Objectives:

The objectives of the study were to:

i) identify the relationship between selected spatially variable soil properties and EC_a,

ii) use mathematical models to process the EC_a outputs of the DualEM-2 for estimation of layered soil properties, and

iii) determine the accuracy of EMI in estimating water table drawdowns

CHAPTER 2 REVIEW OF LITERATURE

2.1 Soil Electrical Conductivity (EC)

There are four types of EC (Davis, 2007). Three EC laboratory methods are soil solution EC (EC_w), saturated paste extract EC (EC_e), and soil solid EC (EC_p). In the fourth method apparent soil EC (EC_a) is determined in the field (Rhoades, 1990b). In case of EC_w, soil solution is the pore water that is removed from soil samples by a variety of centrifuge and non-polar liquid displacement (Cook and Williams, 1998). EC_e is the EC measured on a soil-water paste. The solution from the paste is extracted and its EC is measured on the extract (Rhoades, 1990a; Brady and Weil, 2000). EC_p is due to the presence of exchangeable anions and cations on the surface of clay particles (Cook and Williams, 1998). The EC_p is measured by direct contact with the solid of the paste and not the extract (Rhoades, 1990a; Brady and Weil, 2000).

EC_a, also known as the bulk soil electrical conductivity or apparent ground conductivity, is the depth-weighted average of the soil EC (Greenhouse and Slaine, 1983; Cook and Walker, 1992). In other words, it is the average of the electrical conductivity readings made at different depths in the soil, these depths being dependent on the instrument used to make the measurement. EC_a includes the conductance through the soil solution, solid soil particles, and exchangeable cations that are located on the soil-water interface of clay minerals (Corwin and Lesch, 2003).

2.2 Factors Contributing and Affecting EC_a

The soil can exhibit different electrical properties, depending on its physical and chemical properties (Samouelian et al., 2005). Generally, soil solids and rocks have lower conductivity than electrolytes in soil moisture, which are the main contributors to EC_a

(McNeill, 1980a). Therefore, soil moisture content, salinity, and clay content, and mineralogy are the three main factors that contribute to soil EC_a (Nadler and Frenkel, 1980; Cook et al., 1989a). EMI can give a measurement of EC_a, which is an indirect indicator of such soil properties (Hedley et al., 2004).

When a voltage is applied to the soil moisture, electrons move toward cations causing an electric current (McNeill, 1980a). Soil moisture also has a characteristically high EC_a. In non-saline soils, the more water held in the soil, the higher the EC_a measurement (Rhoades et al., 1976; Kachanoski et al., 1988; McKenzie et al., 1997; Doolittle et al., 2000). However, when soils have high salt contents, an increase in water content will dilute the salt content and cause the EC_a to decrease (Samouelian et al., 2005). Allred et al. (2005) found that near-surface volumetric moisture content had the strongest effect on EC_a measurements.

EC_a can be affected by the electrolyte concentrations in the soil solution (Schumann and Zaman, 2003; Samouelian et al., 2005). Salts and their solutions have high EC. Therefore, when measuring EC_a of a soil containing salts, the readings naturally increase (Rhoades et al., 1976; Williams and Baker, 1982; Kachanoski et al., 1988; McKenzie et al., 1997).

Soil particle size is related to EC by influencing the charge density at the surface of the soil particles (Samouelian et al., 2005). EC_a increases with increasing clay content (Rhoades et al., 1976; Kachanoski et al., 1988; McKenzie et al., 1997) and as the particle size increases, EC_a decreases (Khakural et al., 1998; Fukue et al., 1999). Completely dry clay is an insulator. When water is added, clay becomes a conductor.

Factors affecting EC_a include soil moisture content (Freeland, 1989; Brune and Doolittle, 1990), salinity (McNeill, 1992; Geonics Limited, 1997; Rhoades et al., 1999), clay content (Friedman, 2005), organic compounds (Friedman, 2005), pore size distribution (Friedman, 2005), metals (Geonics Limited, 1997), temperature (McNeill, 1980a; Geonics Limited, 1997; Allred et al., 2005), cation exchange capacity (Friedman, 2005), concentration and mobility of dissolved ions (McNeill, 1980a) and bulk density (Friedman, 2005). Consequently, spatial patterns of soil properties can potentially be inferred from mapped EC_a (Hendrickx et al., 1992; Lesch et al., 1992; Doolittle et al., 1994; Doolittle et al., 2001; Fraisse et al., 2001; Inman et al., 2002; Kravchenko et al., 2002).

2.3 Working Principle of EMI Instruments

EMI instruments have a transmitter coil located at one end of the instrument to generate a primary magnetic field (H_p) (Abdu et al., 2007). This field creates eddy currents in the soil and these time-varying currents induce their own magnetic field (H_i) (McNeill, 1980b, Hendrickx et al., 2002). The induced field is superimposed over the primary field and a fraction of both H_p and H_i is intercepted by the receiver coil (McNeill, 1997), where the signal is amplified and formed into an output voltage that is linearly related to EC_a (McNeill, 1980b; Rhoades and Corwin, 1981; Slavich, 1990; Cook and Walker, 1992; Hendrickx and Kachanoski, 2002; Paine et al., 2004) (Figure 2-1). The distance between the transmitting and receiving coil determine how deep in the soil the electromagnetic field is measured (Cook and Williams, 1998; Paine et al., 2004). Also, most of the instruments have a horizontal and vertical dipole. This also determines how deep the instrument can measure EC_a (Schumann and Zaman, 2003).

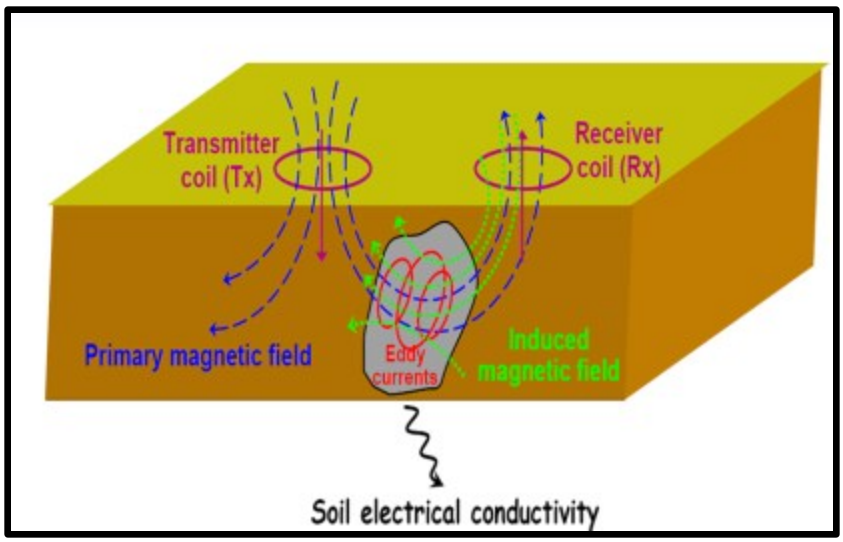

Source: EC-DIGISOIL PROJECT PM1 Paris, Sept 29-30th, 2009

Figure 2-1 Schematic diagram of EMI operation

2.4 DualEM-2

DualEM geo-conductivity meters simultaneously measure ground conductivity to two or more distinct depths of exploration (DOE). These meters can be useful to many kinds of agricultural, geological and environmental investigations. These comprise soil salinity mapping, the description of conductive contamination plumes from salts and acids, and investigation for groundwater and clay (DualEM, Inc. 2005).

These EMI meters include a transmitter that works at a fixed frequency (9 kHz) and at least one pair of receivers. The transmitter and one receiver of the pair have horizontal windings, and these components make a horizontal co-planar array (HCP). The other receiver has vertical windings; it combines with the transmitter to make a perpendicular array (PRP) (DualEM, Inc. 2005). The cumulative responses of PRP and HCP may be used as guides to DOE, in that they indicate the depths beyond which PRP and HCP are relatively insensitive to response from the earth. For the DualEM-2, the DOE of PRP is about 1 m, and the DOE of HCP is about 3 m (DualEM, Inc. 2005).

The DualEM can determine up to 3000 mS m^{-1} (DualEM, Inc. 2005). The data measurements are manual (discrete) as well as continuous at rates between 0.1 and 8 Hz (DualEM, Inc. 2005). The instrument data capacity is 65000 records of either measured quantities or GPS position (DualEM, Inc. 2005). The weight of the DualEM-2 is 10 kg with 0.089 m in diameter and 2.41 m in length (DualEM, Inc. 2005).

2.5 Estimating Soil Properties by EMI

Electromagnetic techniques are well suited for mapping EC_a of the soil profile (McNeill, 1990; Corwin and Lesch, 2005b). The ease and speed with which subsurface information can be acquired by EMI make the technology an ideal precursory investigative tool. When integrated with a global positioning system (GPS), copious amounts of data can be acquired rapidly, geo-referenced, and plotted by commercially available software programs (Kitchen et al., 1996). Research studies show that using EMI will reduce the amount of time spent in the field and will improve the accuracy and cost effectiveness of the soil survey (Cannon et al., 1994; Doolittle and Collins, 1998).

This technology allows for the detection of both lateral and vertical changes in soil subsurface properties. The success of an EMI survey depends upon the local soil morphological, physical, and chemical properties (McNeill, 1980b). EC_a can provide an indirect measure of soil properties (Davis et al., 1997).

Triantafilis and Lesch (2005) and Lesch et al. (2005) found that there is a high relationship between the predicted and measured clay contents. This was confirmed by Sudduth et al. (2005). It has been shown that the EC_a is moderately correlated with soil texture and organic matter, but not with porosity, bulk density, or hydraulic conductivity

(Banton et al., 1997). EC_a was positively correlated with clay content, laboratory measured soil EC, and pH (Johnson et al., 2001).

EC_a was used to map depths to claypans (Sudduth and Kitchen, 1993; Doolittle et al., 1994); and to determine depths to bedrock (Bork et al., 1998; Doolittle and Collins, 1998). More conductive soil overlain by sand allowed EC_a to estimate sand depth (Kitchen et al., 1996). Topsoil depth was estimated using EC_a (Sudduth et al., 2001). Coarse loamy and fine loamy soils were distinguished using EC_a to classify crop productivity (Anderson-Cook et al., 2002). Farooque et al. (2011) and (2012) reported that EMI data can be utilized to develop management zones for the application of fertilizers site-specifically in wild blueberry fields.

2.6 Estimating Soil Moisture Content and Water Table Depths by EMI

Rhoades et al. (1976) and Hendrickx et al. (1992) confirmed the relationship between soil moisture content and EC_a. Sheets and Hendrickx (1995) found a linear relationship between EC_a and soil moisture content in the upper 1.5 m in an arid region. Kachanoski et al. (1988) found a strong correlation ($R^2 = 0.77$) between measured volumetric moisture content and EC_a measurements at different depth intervals. EC_a has been modeled as a function of soil moisture content and bulk density (Rhoades et al., 1989). It has also been shown that EC_a could be used to control spatial variability of soil moisture content over large areas (Reedy and Scanlon, 2003).

EMI is a rapid and accurate tool not only in recharge-discharge of water table studies (Cook and Williams, 1998). But also can be used to estimate variations in water table recharge (Cook et al., 1989b) and evaluate the flow path of subsurface water (Scanlon et al., 1997). Schumann and Zaman (2003) used EC_a to map shallow groundwater in citrus

orchards. The unsaturated flow of soil moisture in an arid region was characterized with EC_a (Scanlon et al., 1999). EMI was also able to explain over 80% of the water table depth variation across a hill slope (Sherlock and McDonnell, 2003).

2.7 Limitations Using EMI during Recording Measurements

This technique does not work in all soil environments (Doolittle and Collins, 1998). One limitation is that the soil is not homogenous (Boettinger et al., 1997). There are various soil constituents that conduct electrical current. The more variability is in the soil, weaker the correlation (Doolittle et al., 2000). EMI is also greatly affected by the interference from proximate features like adjacent buildings, power lines, pumps and even bedrock (Doolittle and Collins, 1998; McNeill and Bosnar, 1999; Schumann and Zaman, 2003). Ground truthing is an important part of measuring EC_a using EMI (Scanlon et al., 1999; Freeland et al., 2001). It is the method to determine which soil components are more contributing to the electrical current flow (Freeland et al., 2001). Therefore, analysis of the soil is desired to determine which properties contribute to the EC_a. The designated DOE calculated by inter-coil spacing is a theoretical value (McNeill, 1986). There will always be deviations of penetration depth due to different soil properties.

2.8 Efficiency and Benefits of EMI

Measurements can be made and recorded as fast as the operator can move from one measurement location to another (McNeill, 1980a; Hendrickx et al., 1992). Large amounts of EC_a data can be collected using computer at a single time, thus eliminating several trips into the field (McKenzie et al., 1997). Measurement of EC_a using EMI also measures large volumes of soil, which reduces estimates and repeated trips to the field

(Hendrickx et al., 1992). The instrument is not required to disturb the soil medium; therefore, measurements can be recorded rapidly (McNeill, 1980a).

Computer generated maps are an alternative method for displaying soil information. They provide quantitative interpretations of EC_a data, which can improve understanding of soil distributions (Doolittle et al., 1996; Corwin and Lesch, 2003). Mapping EC_a is utilized by global positioning technologies (Jaynes et al., 1993; Mueller et al., 2004) which can be useful in site-specific management in order to characterize soil parameters such as soil salinity (Rhoades and Ingvalson, 1971), cation exchange capacity (CEC) (McBride et al., 1990), clay content (Williams and Hoey, 1987), topsoil thickness (Doolittle et al., 1994), and geologic strata (Zalasiewicz et al., 1985). Interpolation procedures are essential to generate maps quantifying EC_a values over continuous soil surfaces. Interpolation quality depends on measurement errors, variability of EC_a, and the procedures used to interpolate EC_a (Mueller et al., 2004). EMI also accurately measures small variations in conductivity (McNeill, 1980b) and conducts survey with excellent resolution (Geonics, 2005).

There have been many studies to map vegetation as well as hydrology using EMI. Low plant cover does not significantly affect the measurements of the instruments in taking EC_a readings (Hendrickx et al., 1992; Boettinger et al., 1997; Brevik et al., 2003). There was no significant effect on EC_a measurements in a forest soil (Cook and Williams, 1998). EMI is an investigative tool that can be used to direct more costly and time-consuming surveys (Doolittle et al., 2001; Inman et al., 2002). Most of the EMI instruments are lightweight and can be transported by a single person. This requires fewer people in the field at one time. Total man-hours are less when using EMI as compared to conventional methods (McNeill, 1980b).

2.9 Soil Sampling

Soil sampling is normally used to characterize the soil and its nutrient status of a field. There is no single optimal strategy for collecting soil samples due to differences among fields and management practices. Sampling on evenly spaced grids has become a common practice in precision agriculture (Lund et al., 1999). However, when very small grid sizes are used to adequately capture spatial variations, the practice can quickly become cost prohibitive. This experience has established the need to identify the variability in a field before soil samples are collected for analysis. Armed with knowledge of soil variability, sample locations can be chosen so that they are truly representative of the field. This designed set of sample points is referred to as directed sampling (Lund et al., 1999). Sampling according to soil variability coupled with an EC_a map can be more effective than grid sampling (Lund et al., 1998; Farooque et al., 2011, 2012).

2.10 Principle of Time Domain Reflectometry (TDR)

The underlying principle of TDR involves measuring the travel time of an electromagnetic wave along a waveguide. The speed of the wave in soil is dependent on the bulk dielectric permittivity of the soil matrix (Roberto and Guida, 2006). The fact that water has a much greater dielectric constant than air or soil solids is exploited to determine the volumetric moisture content (θ_v) of the soil. The θ_v measured by TDR is an average over the length of the waveguide.

Electronics in the TDR 300 generate and sense the return of a high energy signal that travels down and back, through the soil, along the waveguide composed of the two replaceable, stainless steel rods. The sampling volume is an elliptical cylinder that

extends approximately 3 cm out from the detecting rods of TDR. The high frequency signal information is then converted to θ_v (Campbell, 1990).

2.11 Global Positioning System (GPS)

The GPS is a space-based global navigation satellite system that provides reliable location and time information where there is an unobstructed line of satellites (Morgan and Ess, 1997). A GPS receiver determines the location of the point using pseudo random signals from at least four satellites; more satellite signals give higher accuracy (Morgan and Ess, 1997).

The development and implementation of precision agriculture or site-specific farming has been made possible by combining the GPS and geographic information systems (GIS). These technologies enable the coupling of real-time data collection with accurate position information, leading to the efficient manipulation and analysis of large amounts of geo-spatial data. GPS-based applications in precision agriculture are being used for farm planning, field mapping, soil sampling, tractor guidance, crop scouting, variable rate applications, and yield mapping (Hurn, 1993). The GPS technology also allows agricultural producers to work during low visibility field conditions.

Since the GPS locations are determined from the time taken by the signal from the satellite to reach the receiver, any deviation can cause error in the calculated location (Hurn, 1993). Differential Global Positioning System (DGPS) is a method of increasing the accuracy of positions derived from GPS receivers. The DGPS is used to compensate the timing errors, to reduce noise in the medium, and the electronic noise in the receiver (Saunders et al., 1996; Morgan and Ess, 1997).

2.12 Relationship between EC_a and Yield

Among the factors that affect crop yield, soil water holding capacity is usually a significant contributor. EC_a measurements in non-saline soils are driven primarily by soil texture and soil moisture. Same factors highly correlate to the soil water holding capacity. Thus, an EC_a map can serve as a proxy for soil water holding capacity, resulting in EC_a and yield maps that frequently exhibit similar spatial patterns (Lund et al., 2000). It is not surprising that soil physical properties and yield maps show visible correlation, because soil serves as the primary growth medium for crops. These properties affect significantly on water and nutrient holding capacity, which are main drivers of yield (Jaynes et al., 1995). The relationship between EC_a and yield has been reported by Kitchen and Sudduth (1996) and Fleming et al. (1998). They found that the non-linear relationship of EMI measurements to crop yield showed R^2 fairly low.

2.13 Geographic Information System (GIS)

The geographic information system (GIS) is the merging of cartography, statistical analysis, database and modeling technology. The GIS is also a powerful management tool which supports several interpolations and mapping techniques for evaluation and presentation of spatial variation (Schueller, 1992; Usery et al., 1995; Miller and Whitney, 1999).

2.14 Summary

Electromagnetic induction (EMI) is a broad precursory investigative tool that can be used to direct and focus the costly and time-consuming surveys. It can be used for obtaining high intensity, non-intrusive, spatially continuous soil information (Inman et al., 2002). EC_a patterns are largely governed by spatial variations in soil profile properties and water

table depth (Allred et al., 2005). EC_a mapping would be a useful tool in precision agriculture and it could be suitable for rapid and low-cost determination of soil variation over large areas (Ristolainen et al., 2009).

Effective and efficient management of water has a great importance for many agricultural communities (Gordon, 2005). Water conservation has advantages for society, environment, and agriculture. It is increasingly recognized that, although soil moisture content changes over time, the spatial pattern of its variability is fairly constant with time. Soil moisture content and water table levels are often the main reasons for yield variation. The movement and availability of soil water is greatly affected by soil structure and physical properties (Farkas et al., 2006). Interpretation of yield maps may improve by a good estimation of moisture content and its relationship to rainfall amount (Newton and Williams, 2006).

The soil moisture content is influenced by soil properties that relates to texture, structure, depth and organic matter of the soil and landscape features such as elevation and topography (Corwin, 2006). In general, EMI can provide spatially comprehensive information about soil texture, and temporally consistent monitoring of moisture, nutrients, salinity and water table depths (Eigenberg et al., 2006).

CHAPTER 3 MATERIALS AND METHODS

3.1 Description of Research Sites

The research was conducted on two blueberry fields, a pasture field and a field with soybean-barley rotations. Soil properties and water table depths were measured and mapped using the DualEM-2. The blueberry fields are located at Londonderry (45˚28′N, 63˚37′W) and North River (45˚27′N, 63˚12′W); both in central Nova Scotia, Canada. Both fields were in their fruit year of the biennial crop production cycle in 2010, and vegetative sprout year in 2011. The fields have not been under commercial management since 2010 and did not receive biennial pruning by mowing along with inorganic fertilizer, herbicides, fungicides, insects and disease management practices. While these practices greatly affect and contribute to the wild blueberry yield (Yarborough et al., 1986; Warman, 1987). The soils at the wild blueberry fields are classified as well drained sandy loam (Orthic Humo-Ferric Podzols) and are acidic in nature (Webb et al., 1991). The soybean-barley field is located at the Bio-Environmental Engineering Centre (BEEC), Bible Hill, Nova Scotia (45˚23′N, 63˚14′W), and the pasture field is at the Boulden Field (45˚22′N, 63˚15′W) at the Nova Scotia Agricultural College (NSAC). The soils of soybean, barley and pasture fields consist of "Debert 22" and "Pugwash 82" soil groups and have coarse loamy soil material (Webb et al., 1991). The BEEC and Boulden Fields have tile drainage systems. The diameter of the pipelines is 10 cm at both sites while the spacing between the pipes is 14 m and 7 m at BEEC and Boulden Sites, respectively.

3.2 Soil Sampling Strategy

The EC_a survey data collected by DualEM-2 (DualEM Inc., Milton, Ontario) was used to optimize the soil sampling strategy (Lund et al., 1998; Farooque et al., 2011, 2012).

Horizontal co-planar geometry (HCP) and Perpendicular co-planar geometry (PRP) were both utilized to develop a sampling strategy to collect soil, plant and fruit yield samples from all fields. The models of semivariogram were developed to best fit the HCP and PRP data. The grid size to collect soil, plant and fruit yield samples was then established based on the range of the influence from semivariogram. Kerry and Oliver (2003) suggested that the grid pattern for sampling is one third or half of the range of variability. Based on the range of the variability, a grid size was selected for sampling at all sites. Geo-statistical analysis was performed using GS+ Geostatistics for the Environmental Sciences Version 9 software (Gamma Design Software, LLC, Woodhams St, Plainwell, MI) to produce a semivariogram.

3.3 Collection of Soil Samples

In BEEC and Boulden Fields, soil samples were collected using a power auger during installation of water table wells (Figures 3-1 and 3-2) at 0-15 cm, 15-45 cm, 45-75 cm, ----- up to the water table below the soil surface at each water table well location. i.e., the sampling depths (at least 75 cm deep) were transient. The sampling depths varied from well to well on the basis of time dependent water table presence. In the wild blueberry fields, soil samples were collected using a ditch soil sampling auger at 0-15 cm depth (Figures 3-3 and 3-4). The samples were labeled and placed for two weeks for air drying. The air dried samples were grinded using a soil grinding machine (Nasco Farm & Ranch Co, WI), and passed through 2 mm sieve.

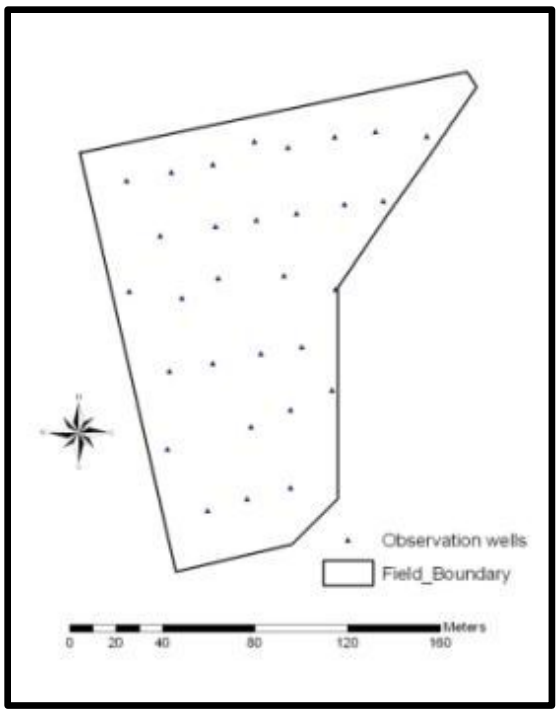

Figure 3-1 Field layout of BEEC Field, showing location of 30 observation wells and field boundary

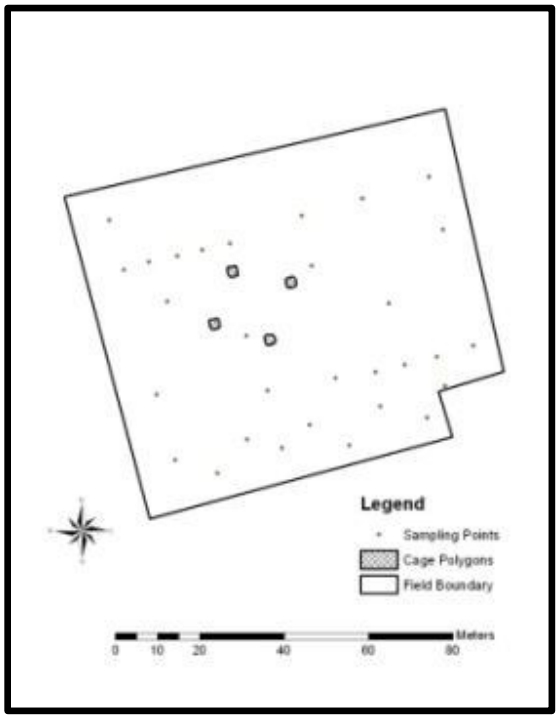

Figure 3-2 Field layout of Boulden Field, showing location of 30 observation wells and field boundary

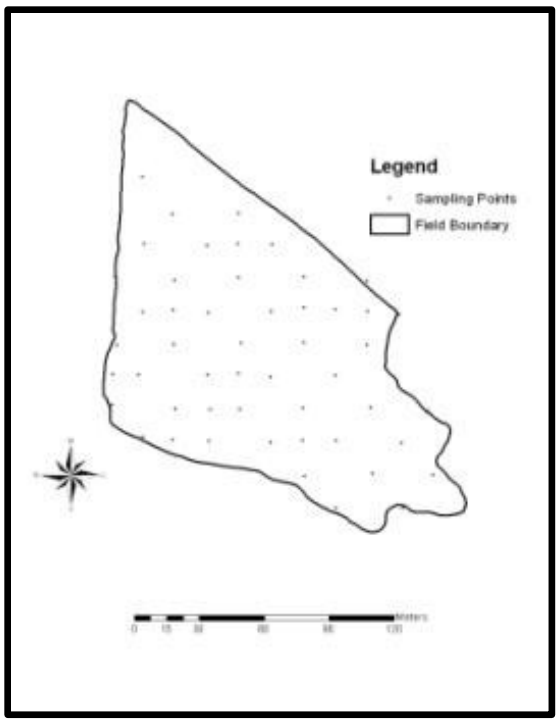

Figure 3-3 North River research Site and sampling design

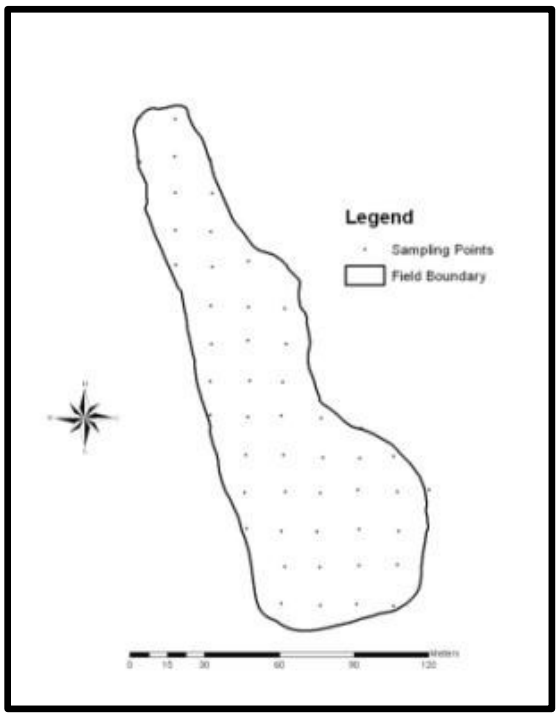

Figure 3-4 Carmel research Site and soil sampling design

3.4 Soil Analysis

All the air dried samples were analyzed for soil organic matter content (SOM) using the loss ignition method (Davies, 1974); soil texture, using the hydrometer method (Day, 1965; Gee and Bauder, 1986); soil volumetric moisture content (θv), using theTime-Domain Reflectometry (TDR) (Roberto and Guida, 2006); soil pH, using a standard pH meter (McLean, 1982; Mann, 2009); and soil electrical conductivity (EC), using a conventional meter (Rhoades, 1982; Mann, 2009). The soil samples were collected once in the first year of study (3rd week of June, 2010) and then sampling was repeated in last week of May, 2011. The coordinates of each sampling point, well location at two sites and the boundaries of the fields were recorded with the RTK-GPS.

3.5 Calibration of TDR

To calibrate the TDR probes, ten samples with the known volume of the soil were collected from the field and the θ_v was determined from the gravimetric method (wet-dry weight method). The θ_v was also determined from the same sampling points using TDR probes. The moisture content determined by the both method was analyzed using regression analysis to check the accuracy of the TDR, before using for the experiment.

3.6 Sieve Analysis of Coarse Aggregates

Since the wild blueberry fields are rocky in nature. In order to assess the effect of aggregates/ crystalline rocks on EC_a, the sieve analysis of coarse aggregates was performed to calculate the percentage of these rocks. The soil samples were collected from blueberry fields and air dried. The sieves were selected with suitable openings to achieve the information required. The sieves were nested in order of decreasing size of opening from top to bottom and the sample was placed on the top sieve. The sieves were

agitated by mechanical sieve shaker for 5 minutes. The mass of each size increment was determined on a scale or balance.

3.7 Apparent Ground Conductivity

Apparent ground conductivity (EC_a) measurements were made manually at each soil sampling and well point immediately after the soil samples were collected and the water table depths were measured. The DualEM-2 was used to measure EC_a at ground level in both the horizontal coplanar geometry (HCP) and perpendicular geometry (PRP), which corresponded with the vertical-dipole and horizontal-dipole modes of the EM38 instrument (Geonics Limited, Mississauga, Ontario, Canada), respectively (Abdu et al., 2007). The difference between the HCP and PRP readings indicates the distributions of salinity with depth (McNeill, 1980b). The difference is defined as the PRP reading minus the HCP reading. A negative difference indicates increasing salinity with depth whereas positive difference indicates decreasing salinity with depth (Chaves, 1995). Five EC_a values were sampled and averaged at each sampling and well location.

3.8 Elevation

A survey was conducted using RTK-GPS to measure and map surface elevation of each field. The elevation survey data were imported into ArcGIS 10 software (ESRI Redland, CA). These data were interpolated to develop smooth elevation contour maps and digital elevation models (DEMs) for additional slope derivations and calculations.

3.9 Water Table Measurement

Thirty water table observation wells were installed in June, 2010 in each of BEEC and Boulden Fields. Due to the rocky nature of soils in blueberry fields, no wells were installed. A 5 cm diameter polyvinyl chloride (PVC) pipe, perforated with small holes in

the lower section was installed, and its position was recorded using RTK-GPS. Each PVC well had a nylon fabric filter material to prevent soil entry. A PVC end-cap was placed over the top end of the pipe to prevent water or soil from entering. Measurements of water table depths and EC_a were made from June to October, 2010 and then repeated from May to October, 2011. These measurements were made immediately before and after significant rainfall for three consecutive days to record the rise and recession of water table levels. A water level sensor was used to measure depth to the water table.

3.10 EMI Surveys and Data Processing

An intensive DualEM survey was conducted at each field using the DualEM-2 to relate the EC_a to the water table depth fluctuations and selected soil properties variation. The instrument has a built-in DGPS. The EMI survey system consisted of the DualEM-2 mounted on a sled, towed behind an all-terrain vehicle (ATV) at a speed of approximately 5 km hr^{-1}. The DualEM-2 itself is housed in a thermoplastic case (with Styrofoam insulation on both ends). The DualEM-2 housing and sled maintains the DualEM-2 sensor approximately 15 mm above the soil surface and this small spacing is found to have no noticeable impact of instrument readings (Brevik et al., 2003). The surveys collected and recorded geo-referenced HCP and PRP values automatically after every 5 seconds during a survey. The lines of 5 m spacing were generated using ArcGIS software and EMI surveys were guided by a RTK-GPS on those lines. Customized Windows software on a laptop computer was used to merge the ground conductivity (HCP and PRP) data with corresponding GPS position coordinates through RS232 ports and these data were stored.

3.11 Program Development

A short program was written in Microsoft Visual Studio 2010 software for processing the two outputs of the DualEM-2 and to estimate the crystalline rock formation in wild blueberry fields, and water table depths at BEEC and Boulden Fields. The HCP, PRP, height of the instrument above the ground surface and the desired depth or thickness of upper layer of interest were used as an input and the ground conductivity of the upper desired layer and underlying earth were outputs of this program. This program was able to calculate the ground conductivities of two different layers below the soil surface and the depth to interface between these layers. The following equations, formulated by McNeill (1980a), and McNeill (1980b) cumulative response curves, were used in the program to calculate the layer conductivities and interface depth:

$HCP = H_y \times C_y + H_e \times C_e$ ---------- (1)

$PRP = P_y \times C_y + P_e \times C_e$ ---------- (2)

Where,

HCP = Horizontal component of ground conductivity measured by DualEM in mS m^{-1}

PRP = Perpendicular component of ground conductivity measured by DualEM in mS m^{-1}

H_y = Cumulative sensitivity of the HCP geometry to the upper layer

H_e = Cumulative sensitivity of the HCP geometry to the underlying layer

P_y = Cumulative sensitivity of the PRP geometry to the upper layer

P_e = Cumulative sensitivity of the PRP geometry to the underlying layer

C_y = Conductivity of an upper layer of fixed thickness in mS m^{-1}

C_e = Conductivity of an underlying layer in mS m^{-1}

3.12 Statistical Analysis

Descriptive statistics such as mean, minimum, maximum, median, standard deviation (SD), and coefficient of variance (CV) values were calculated using SAS 9.2 statistical software (SAS Institute Inc., NC, USA). The normality was tested using Anderson-Darling (A-D) test using Minitab 16 statistical software (Minitab Inc., NY, USA) at a significance level of 5% and the skewness and kurtosis coefficients were calculated (Farooque et al., 2011, 2012). Correlation coefficients were determined for soil properties and EC_a data. Regression models were developed to estimate soil properties and water table depths using EC_a. Transformed, linear, logarithmic, quadratic and cubic models of EC_a were evaluated to find the best-fitting models to estimate soil properties and water table depths. The accuracy of the water table depths and soil properties predicted from EC_a was estimated from the root mean square error (RMSE) (Coulibaly et al., 2001; Schumann and Zaman, 2003; Daliakopoulos et al., 2005; Vasquez-Amabile and Engel, 2005; Krishna et al., 2008; Arshad et al., 2009; Sethi et al., 2010 and Khan et al., 2011). The RMSE represents the average deviation of actual water table depths from the fitted regression models (Schumann and Zaman, 2003).

Classical statistics provides the overall variability of the property of interest; however, it does not provide the spatial trend. Therefore, semivariograms were calculated from the water table depths to determine the degree of spatial correlation. The first objective of this study was just to develop the relationship of soil properties and EC_a so the geostaistical and semivariogram data of soil properties were not reported and discussed in this study. These were reported only for WTD to see the spatial variability. The semivariograms were calculated using the GS+ Geostatistics for the Environmental

Sciences Version 9 software (Gamma Design Software, LLC, Woodhams St, Plainwell, MI). Each experimental semivariogram was fitted with linear, exponential, spherical and Gaussian models and the model of best fit was selected. The results of the fitting were plotted and the nugget, sill and the range were recorded. Nugget semivariance is the variance at zero distance; range is the lag distance between measurements at which one value of one variable does not influence neighboring values, i.e., the distance at which values of one variable become spatially independent of another; and sill is the asymptotic plateau of the semivariogram function and is used to estimate the range (Lopez-Granados et al., 2005). The ratio between the nugget and the sill characterizes the importance of the random component in the whole field spatial variability of the data and provides quantitative measures of spatial dependence at the chosen lag distance interval (Lopez-Granados et al., 2005).

3.13 Yield Estimation

The fruit yield was harvested manually using hand rakes from 0.5 x 0.5 m steel frame quadrant at each grid point in wild blueberry fields to measure the yield (Zaman et al., 2008). In Boulden Field, biomass was recorded using plate pasture meter (Farmworks Precision Farming Systems, Fielding, New Zealand) at the selected points (Flynn et al., 2006). A small combine harvester having 1 m cutting width was used to assess the yield variability at BEEC Field (Figure 3-6). Plots of 5 x 1 m were selected at sampling locations for this harvesting.

Figure 3-5 Harvesting at selected plots in BEEC Field

CHAPTER 4 DEVELOPMENT OF RELATIONSHIPS BETWEEN SELECTED SOIL PROPERTIES AND APPARENT GROUND CONDUCTIVITY

4.1 Introduction

Traditionally, farm managers consider fields as uniform and thus, fertilizers, pesticides, irrigation, seed rate etc., are applied without taking into account spatial variations in field characteristics. When fields are managed as uniform piece of land, it results in over-application or under-application in some areas within a field. Under treated zones do not reach optimum levels of exploitation whereas the over-treated ones there may pose risk of environmental pollution and an increase in costs (Bouma, 1997).

Features and inconsistency of soil parameters have been extensively examined in precision agriculture research and application (Hache, 2003). Different sensing technologies are under development and others are already being put on in order to gather data from the soils precisely and in actual. Soil properties differ from one study to another depending on the accessibility of sources for investigation, purposes, and awareness of field variability (Hache, 2003). For this present research, analyzed soil parameters were moisture content, organic matter, texture, pH, and electrical conductivity.

Soil moisture content states to the quantity of water held by the soil (Hache, 2003). Soil is a spongy medium, which contains different sizes of pores and the water that enters the soil either remains in the pores, percolates through them (Baver, 1961) or evaporates (Havlin et al., 2005). Organic matter presence in the soil aids to retain moisture content (Baver, 1961). Deficiency of moisture may cause a reduction in subsequent growth or may even be deadly during periods of active growth (Black, 1957). Plant growth is basically an increase in volume resulting from the creation and expansion of cells and if

there is deficiency of water the growth of shoot parts of plants is limited (Black, 1957). Waterlogging can also disturb plant growth and yield, given that water moves air from the pore spaces, inducing a stop in growth of roots resulting in a severe drop in the uptake and transport of mineral nutrients (Marschner, 1995).

Soil organic matter is the most critical soil property because of its effect on many biological, chemical and physical properties intrinsic in a productive soil (Havlin et al., 2005), and therefore its contribution to plant growth and improvement (Tatabatai, 1996). Organic matter in soils has two major functions: (a) a nutritional one causing from mineralization of organic nitrogen, sulphur and phosphorus (Tatabatai, 1996; Mengel and Kirkby, 2001) and (b) a physical one linking to the upgrading of physical properties (Mengel and Kirkby, 2001). It also gives a pH buffering action retaining a uniform soil pH (Havlin et al., 2005).

Texture defines the soil's internal geometry and porosity, its connections with fluids and solutes (Hillel, 1998). This time-invariant static parameter has a direct effect on the nature of the dynamic soil parameters. The most important dynamic soil property influenced by the time-invariant static soil physical properties is soil moisture content. Soil moisture status is serious to plant growth, crop quality, chemical fate and transport, and microbial processes (Abdu, 2009). Soil structure and texture are important properties monitoring the hydraulic conductivity and infiltration capacity of a soil system.

pH is a degree of soil acidity. It is a main chemical property because it disturbs the accessibility of nutrients to plants and the activity of microorganisms in the soil (Hache, 2003). Reduction in soil pH is affected by numerous factors including the use of

commercial fertilizers, especially NH_4^+ sources that make H^+ during nitrification and decomposition of organic residues (Havlin et al., 2005).

Electrical conductivity is a major soil parameter as it correlates to soil parameters influencing crop productivity (PPI, 1996). Some grain crops (e.g., rice, wheat, corn and barley) are relatively salt tolerant at germination and maturity but are very sensitive during early seedling and, in some cases, vegetative growth stages. In contrast, sweet potato, safflower, soybean, and many bean crops are sensitive during germination. This result depends on variety, especially with soybean (Marshner, 1995; Havlin et al., 2005). In precision agriculture some devices are being developed to record this soil parameter on real-time.

Soils are varied, and wide heterogeneity can occur even in fields that seem uniform (Havlin et al., 2005; Farooque et al., 2011, 2012). The first step in precision agriculture is to measure important factors that specify or influence the efficiency of the growing crop (Blackmore et al., 2002). Intensive soil sampling is the most valuable way to quantify variability (Havlin et al., 2005), but it demands human effort and time. Therefore, there exists the need for new methods that enable rapid measurement of soil parameters. The objective of this chapter was to develop relationship between selected soil properties and EC_a for predicting those soil properties in a rapid and non-destructive manner.

4.2 Materials and Methods

A soybean-barley, a pasture and two wild blueberry fields in central Nova Scotia were selected to develop relationships between soil properties and EC_a. A grid pattern of sampling points was established at each experimental site except at pasture field based on the range of influence of semivariograms to collect soil samples (Figure 4-1). The soil

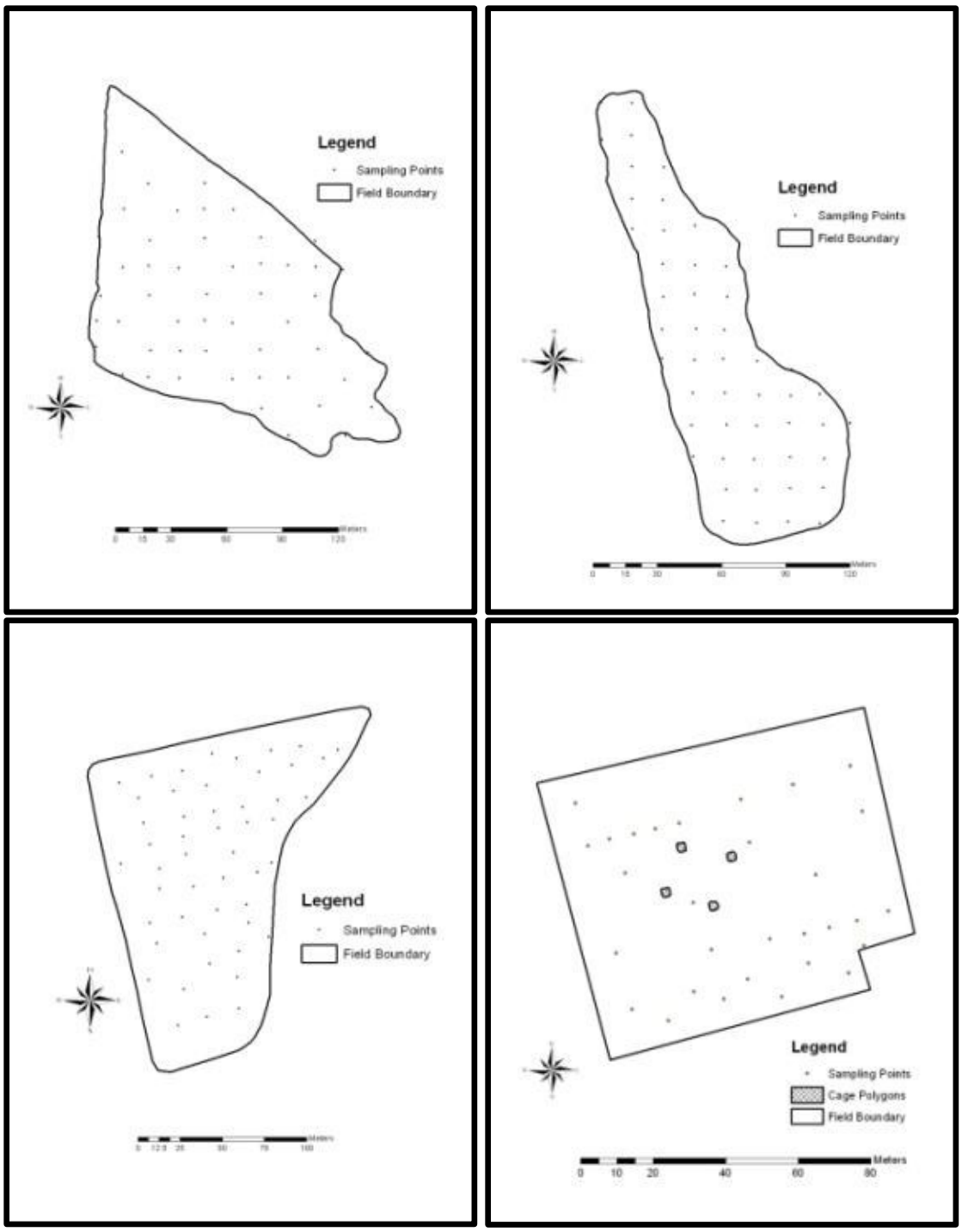

Figure 4-1 Research Sites and soil sampling design

samples were analyzed for SOM, texture, θ_v, pH, and EC using standard methods. The soil bulk density (ρ_b) was calculated using oven-dried mass of the sample divided by the sample volume (Blake and Hartge, 1986). Soil texture and pH were measured once at the

onset of the experiment since these parameters do not tend to change significantly in two monitoring years. Other soil properties were determined twice during 2 year study. The ground conductivity values (HCP and PRP) using DualEM were also recorded at each sampling point along with soil samples. The coordinates of each sampling point were recorded with a RTK-GPS. The boundary of the fields was also marked using a RTK-GPS. Samples were collected at 0 to 15, 15 to 45, and 45 to 75 cm soil depths. These sample depths were selected because we were most appealed in soil properties associated with the concept of soil quality, and these depths coincide with many previous similar investigations (Wander and Bollero, 1999; Brejda et al., 2000; Kettler et al., 2000; Johnson et al., 2001). The samples were air dried and ground to pass a sieve with 2 mm openings. Slope variability was measured and mapped with SMMS once at the beginning of experiment. Elevation was also measured and mapped once using RTK-GPS. Detailed materials and methods were discussed in Chapter 3.

4.3 Statistical Analysis

Means, minimums, maximums, medians, standard deviations (SDs), and coefficient of variations (CVs) of selected soil properties (soil texture, SOM, EC, pH, θ_v and coarse aggregate) were calculated using SAS 9.2 statistical software. Data normality was tested using Anderson-Darling (A-D) test using Minitab 16 statistical software at a significance level of 5% and the skewness and kurtosis coefficients were calculated. Pearson correlation coefficients were calculated for all pairs of soil property, yield and EC_a data. Regression models were derived to calibrate the DualEM-2 to predict soil properties using EC_a in each field separately (n = 50). Transformed, linear, logarithmic, quadratic, and cubic models of EC_a were evaluated to find the best-fitting models. Soil samples

(n=20) were obtained from the same field during the summer of 2011, analyzed in the laboratory using the same procedures indicated in Chapter 3. The calibration equations of first year for each selected field were used to predict soil properties in second year data for validation. Calibration and validation of regression equations/models, coefficient of determination (R^2) and root mean square (RMSE) were calculated using Minitab 16 statistical software.

4.4 Results and Discussion

4.4.1 Sampling Strategy

The apparent ground conductivity survey conducted by DualEM was utilized to develop a sampling strategy to collect soil samples from all fields except Boulden Field. The semivariogram for EC_a data were developed and gaussian and spherical models of semivariogram were found to best fit the data set in soybean-barley and wild blueberry fields, respectively. The grid size to collect soil samples was then established based on the range of the influence from semivariogram which was found to be around 54 m for BEEC and 60 m for blueberry fields (Fig. 4-2 to 4-4). The grid pattern for sampling is one third or half of the range of variability (Kerry and Oliver, 2003; Farooque et al., 2012). Based on the range of the variability, a grid size of 20 x 20 m was selected for sampling.

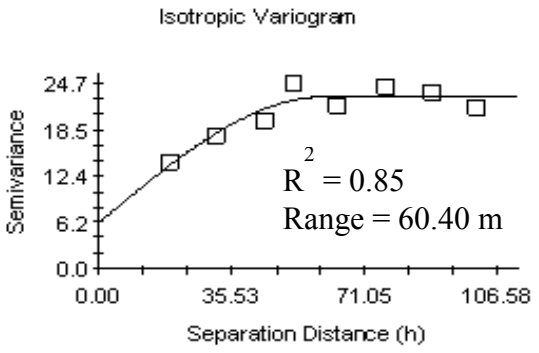

Figure 4-2 Semivariogram of EC_a at North River Site

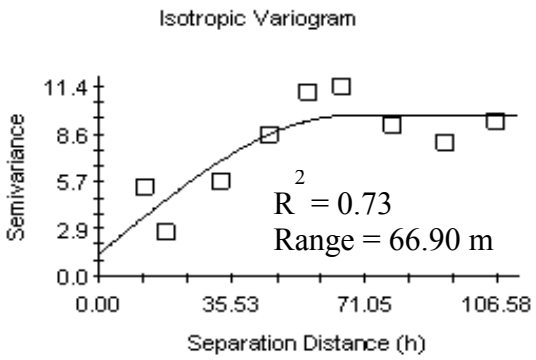

Figure 4-3 Semivariogram of EC_a at Carmel Site

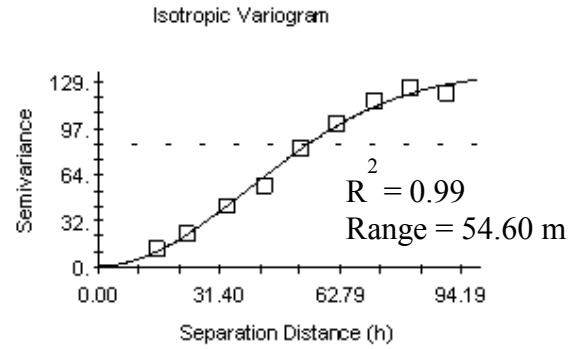

Figure 4-4 Semivariogram of EC_a at BEEC Site

4.4.2 Descriptive Statistics of Soil Properties and Crop Yield

Soil properties at the deepest sampling depth (45-75 cm) were generally more normally distributed than at the shallower sampling depths (Tables 4-1 to 4-4). Similarly, most soil property values at the deepest depth were noticeably different from the shallower sampling depths. For example, mean values of clay content and θ_v at the 45 to 75 cm sampling depth were higher than at shallower depths. Clay content at the deepest

Table 4-1 Descriptive statistics of soil properties at North River Site

Properties	n	Depth†	Min.	Max.	Mean	CV (%)	Skewness	Kurtosis
Clay, %	50	1	0.0	20.0	7.8	78.0	0.40	-0.9
	35	2	0.0	20.0	13.0	49.0	-0.50	-0.8
	7	3	12.0	30.0	17.0	33.0	2.10	5.1
Silt, %	50	1	15.0	43.0	28.0	25.0	0.20	-0.6
	35	2	12.0	44.0	27.0	24.0	0.10	0.2
	7	3	20.0	38.0	30.0	25.0	-0.30	-2.4
Sand, %	50	1	44.0	84.0	64.0	16.0	-0.01	-0.6
	35	2	38.0	80.0	60.0	17.0	-0.07	-0.7
	7	3	32.0	65.0	52.0	23.0	-0.70	0.2
Gravel, %	50	1	33.0	73.0	53.0	17.0	-0.20	-0.4
	35	2	32.0	79.0	56.0	17.0	-0.20	1.3
	7	3	26.0	52.0	39.0	29.0	0.06	-1.5
SOM, %	50	1	4.4	13.0	8.4	22.0	0.50	0.0
	35	2	4.4	11.0	6.6	23.0	0.90	1.2
	7	3	4.0	8.0	5.2	25.0	1.80	3.8
θ_v, $m^3\ m^{-3}$	50	1	5.9	35.0	22.0	31.0	-0.20	-0.3
	35	2	6.2	32.0	24.0	29.0	0.40	-0.7
	7	3	8.4	37.0	29.0	26.0	1.50	2.0
EC, $\mu S\ cm^{-1}$	50	1	36.0	103.0	54.0	24.0	2.10	4.4
	35	2	37.0	180.0	55.0	47.0	3.80	17.0
	7	3	37.0	55.0	45.0	16.0	0.30	-1.8
pH	50	1	5.0	6.2	5.6	10.0	3.10	10.5
	35	2	5.2	6.5	5.6	4.5	1.60	3.9
	7	3	5.5	6.6	5.8	6.9	2.30	5.5
PRP, $mS\ m^{-1}$	50		0.1	21.0	6.3	60.0	1.70	3.6
HCP, $mS\ m^{-1}$	50		0.1	20.0	6.2	76.0	1.00	0.4

† 1, 0 to 15 cm sampling depth; 2, 15 to 45 cm sampling depth; 3, 45 to 75 cm sampling depth
Note: Clay, silt, sand, SOM, EC, pH, and θ_v at 2nd and 3rd sampling depth were measured once in June, 2010. θ_v at 1st sampling depth was measured bi-weekly from June to October, 2010.

depth was more than twice that of the shallower sampling depths. The proportion of the sand and SOM were clearly higher at the 0-15 cm depth than the deeper sampling depths. Differences between the shallow sampling depth and the deeper sampling depths can be recognized to the following factors. First, tillage operations were primarily disc and field cultivation to a depth of 10 to 15 cm. Consequently, organic matter from plant residue assimilation as well as fertilizer amendments was mostly stratified within the surface

Table 4-2 Descriptive statistics of soil properties at Carmel Site

Properties	n	Depth†	Min.	Max.	Mean	CV (%)	Skewness	Kurtosis
Clay, %	50	1	1.0	14.0	7.4	41.0	-0.30	-0.40
	43	2	6.0	44.0	15.0	60.0	1.50	2.40
	9	3	9.0	29.0	18.0	38.0	0.60	-0.30
Silt, %	50	1	32.0	53.0	43.0	10.0	0.20	0.70
	43	2	2.0	40.0	24.0	34.0	-0.10	0.03
	9	3	14.0	43.0	28.0	35.0	0.30	-1.00
Sand, %	50	1	35.0	58.0	49.0	9.9	-0.90	1.20
	43	2	38.0	80.0	61.0	19.0	-0.30	-0.80
	9	3	28.0	77.0	54.0	27.0	-0.30	-0.20
Gravel, %	50	1	40.0	75.0	60.0	13.0	-0.10	0.30
	43	2	47.0	59.0	60.0	13.0	0.30	-0.80
	9	3	38.0	65.0	48.0	22.0	1.20	1.40
SOM, %	50	1	5.2	14.0	9.6	18.8	0.10	-0.02
	43	2	3.6	10.0	6.8	22.0	0.03	-0.60
	9	3	3.2	8.0	4.6	31.0	1.10	0.70
θ_v, $m^3\ m^{-3}$	50	1	10.0	34.0	26.5	15.4	-1.30	3.80
	43	2	14.0	37.0	30.8	19.0	0.70	4.30
	9	3	16.0	35.0	32.3	13.4	0.40	3.50
EC, $\mu S\ cm^{-1}$	50	1	60.0	78.0	68.3	8.5	0.30	-1.10
	43	2	40.0	76.0	53.0	20.0	0.90	-0.30
	9	3	40.0	52.0	45.0	9.2	0.20	-1.20
pH	50	1	4.6	5.4	5.1	4.3	-0.70	-0.20
	43	2	5.0	5.6	5.3	3.3	-0.70	-0.80
	9	3	5.3	5.7	5.5	2.4	-0.40	0.70
PRP, $mS\ m^{-1}$	50		0.7	7.5	3.8	44.0	0.02	-0.30
HCP, $mS\ m^{-1}$	50		0.0	11.8	5.4	53.0	-0.20	-0.40

† 1, 0 to 15 cm sampling depth; 2, 15 to 45 cm sampling depth; 3, 45 to 75 cm sampling depth

Note: Clay, silt, sand, SOM, EC, pH, and θ_v at 2nd and 3rd sampling depth were measured once in June, 2010. θ_v at 1st sampling depth was measured bi-weekly from June to October, 2010.

15 cm of soil but this factor is not applicable in wild blueberry fields because there is no tillage operation. Second, the 2nd and 3rd sampling depths were twice the thickness of the first sampling depth. Therefore, these deeper sampling depths had a greater possibility of including multiple horizons compared with the shallowest sampling depth. This second point is reinforced by the generally higher CV of most soil properties at the 15 to 45 and

Table 4-3 Descriptive statistics of soil properties at BEEC Site

Properties	n	Depth†	Min.	Max.	Mean	CV (%)	Skewness	Kurtosis
Clay, %	50	1	3.0	25.0	12.7	43.0	0.60	-0.60
	50	2	5.0	32.0	13.0	48.0	1.30	1.90
	50	3	2.0	28.0	13.0	50.0	0.60	-0.20
Silt, %	50	1	0.0	36.0	20.6	39.0	-0.10	-0.30
	50	2	5.0	38.0	22.5	32.0	-0.20	-0.20
	50	3	11.0	52.0	27.0	30.0	0.40	0.80
Sand, %	50	1	46.0	87.0	66.7	14.8	-0.10	-0.40
	50	2	42.0	83.0	65.0	14.0	-0.20	-0.03
	50	3	24.0	87.0	60.0	20.0	-0.40	0.50
SOM, %	50	1	2.8	16.0	4.2	23.0	0.70	2.90
	50	2	0.8	7.2	3.0	42.0	0.70	1.00
	50	3	0.4	6.6	2.0	58.0	2.30	7.40
θ_v, $m^3\ m^{-3}$	50	1	26.0	47.0	36.8	15.6	-0.10	-1.10
	50	2	29.0	49.0	38.0	17.0	0.30	3.00
	50	3	25.0	49.0	37.5	20.0	-0.09	-0.40
EC, $\mu S\ cm^{-1}$	50	1	67.0	262.0	112.0	31.0	1.70	5.10
	50	2	42.0	382.0	94.0	54.0	4.00	22.00
	50	3	29.0	144.0	80.0	29.0	0.50	0.50
pH	50	1	6.0	7.8	6.8	6.2	0.08	-0.70
	50	2	6.0	7.5	6.8	5.5	0.02	-1.00
	50	3	5.8	7.8	6.7	6.8	-0.40	-0.40
PRP, $mS\ m^{-1}$	50		5.0	37.0	21.0	44.0	-0.05	-1.10
HCP, $mS\ m^{-1}$	50		7.0	40.0	23.0	43.0	0.04	-1.00

† 1, 0 to 15 cm sampling depth; 2, 15 to 45 cm sampling depth; 3, 45 to 75 cm sampling depth
Note: Clay, silt, sand, SOM, EC, pH, and θ_v at 2nd and 3rd sampling depth were measured once in June, 2010. θ_v at 1st sampling depth was measured bi-weekly from June to October, 2010

45 to 75 cm depth samples compared with the shallowest depth (Tables 4-1 to 4-4) (Jung et al., 2005). The HCP and PRP were normally distributed for all four fields (Tables 4-1 to 4-4). HCP produced higher values compared with PRP at all sites except North River. Wild blueberry yield variability was high in 2010. Soybean-barley and pasture yield were moderately variable (Table 4-5).

Table 4-4 Descriptive statistics of soil properties at Boulden Site

Properties	n	Depth†	Min.	Max.	Mean	CV (%)	Skewness	Kurtosis
Clay, %	30	1	6.0	15.0	9.9	23.0	0.10	-0.20
	30	2	2.0	15.0	9.3	32.0	-0.20	0.20
	30	3	4.0	14.0	9.0	25.0	0.20	0.02
Silt, %	30	1	18.0	30.0	24.0	12.0	0.02	0.20
	30	2	16.0	34.0	23.0	20.0	0.70	0.30
	30	3	12.0	35.0	20.0	25.0	0.80	1.50
Sand, %	30	1	59.0	73.0	66.0	5.4	-0.01	-0.50
	30	2	56.0	78.0	68.0	8.6	-0.50	-0.20
	30	3	51.0	81.0	71.0	9.0	-1.20	2.80
SOM, %	30	1	2.8	6.6	4.6	20.0	0.20	-0.20
	30	2	1.6	5.6	3.8	24.0	-0.05	0.50
	30	3	1.2	5.0	2.2	38.0	2.00	5.00
θ_v, $m^3\ m^{-3}$	30	1	22.0	40.0	30.0	16.0	0.70	-0.40
	30	2	17.0	41.0	28.0	18.0	-0.80	0.50
	30	3	19.0	42.0	27.8	19.0	0.60	0.03
EC, $\mu S\ cm^{-1}$	30	1	48.0	121.0	83.0	19.0	0.30	0.30
	30	2	48.0	140.0	85.0	28.0	0.80	0.00
	30	3	43.0	691.0	104.0	99.0	5.10	17.00
pH	30	1	5.4	7.7	6.6	7.0	-0.30	1.00
	30	2	6.2	7.8	6.9	6.0	0.50	-0.40
	30	3	6.2	8.1	7.0	7.8	0.50	-0.60
PRP, $mS\ m^{-1}$	30		9.0	26.0	17.4	26.2	0.09	-0.80
HCP, $mS\ m^{-1}$	30		13.0	30.0	21.0	20.7	-0.07	-0.60

† 1, 0 to 15 cm sampling depth; 2, 15 to 45 cm sampling depth; 3, 45 to 75 cm sampling depth

Note: Clay, silt, sand, SOM, EC, pH, and θ_v at 2nd and 3rd sampling depth were measured once in June, 2010. θ_v at 1st sampling depth was measured bi-weekly from June to October, 2010.

Table 4-5 Descriptive statistics of crop yield ($kg\ ha^{-1}$) data

Field	Crop	Min.	Max.	Mean	CV (%)	Skewness	Kurtosis
North River	Blueberry	44	6532	1300	96	2.4	7.3
Carmel	Blueberry	180	6272	2085	67	1.1	1.7
BEEC	Soybean	1136	3456	2454	22	-0.4	0.2
	Barley	1248	3568	2101	23	0.7	0.2
Boulden	Pasture	1074	6140	4081	27	-0.5	0.6

4.4.3 Soil Properties Correlated and Regressed to EC_a

Statistically significant correlations between EC_a with the sensor at the soil surface (in both HCP and PRP array) and soil properties at the experimental sites were compared (Tables 4-6 to 4-9). The EC_a was significantly positively correlated with clay content with correlation values greater at the two deep sampling depths but low correlation value was observed. The low value of correlation is because of soil volume measured with DualEM-2 is larger than that used for soil sampling. In contrast, EC_a was negatively correlated with sand content except at BEEC site. Correlations of silt and sand

Table 4-6 Correlation coefficients among soil properties and EC_a at North River Site

Properties	n	Depth†	PRP	HCP
Clay, %	50	1	0.24*	0.36*
	35	2	0.64**	0.64**
	7	3	0.68**	0.26*
Silt, %	50	1	0.62**	0.44*
	35	2	0.26*	0.30*
	7	3	0.76*	0.14
Sand, %	50	1	-0.56**	-0.52**
	35	2	-0.58*	-0.58*
	7	3	-0.82**	-0.02
SOM, %	50	1	0.26*	0.36*
	35	2	0.32*	0.23*
	7	3	0.58*	0.80**
θ_v, $m^3\ m^{-3}$	50	1	0.63***	0.56***
	35	2	0.67**	0.59**
	7	3	0.72***	0.65***
EC, $\mu S\ cm^{-1}$	50	1	0.37*	0.39*
	35	2	0.66***	0.57**
	7	3	0.82**	0.62**
pH	50	1	0.00	-0.06
	35	2	0.60	0.42
	7	3	-0.06	-0.48

† 1, 0 to 15 cm sampling depth; 2, 15 to 45 cm sampling depth; 3, 45 to 75 cm sampling depth

* Significant at the 0.05 probability level

** Significant at the 0.01 probability level

*** Significant at the 0.001 probability level

content with EC_a were generally non-significant. These results were supported by the findings of Mueller et al. (2003).

Soil texture in the soil profile can be an important factor contributing to EC_a (Sudduth et al., 2003, 2005). Physical contact between soil particles allows for higher electrical conductivity and is known to be greater with clay than with sand- or silt-sized particles (Rhoades et al., 1976; Corwin and Lesch, 2003). Therefore, it is not surprising that correlations for clay are generally significant as compared to silt and sand contents.

Table 4-7 Correlation coefficients (r) among soil properties and EC_a at Carmel Site

Properties	n	Depth†	PRP	HCP
Clay, %	50	1	0.40**	0.24*
	43	2	0.16	0.02
	9	3	0.81**	0.65**
Silt, %	50	1	0.30*	0.28*
	43	2	-0.24	-0.36
	9	3	0.67*	0.59*
Sand, %	50	1	-0.42**	-0.32*
	43	2	0.22	0.31
	9	3	-0.81**	-0.68**
SOM, %	50	1	0.12	0.36*
	43	2	0.52*	0.60*
	9	3	0.56*	0.52*
θ_v, m^3 m^{-3}	50	1	0.64**	0.58**
	43	2	0.59**	0.55**
	9	3	0.67**	0.63**
EC, µS cm^{-1}	50	1	0.55*	0.52*
	43	2	0.43*	0.41*
	9	3	0.58*	0.50*
pH	50	1	-0.24	-0.22
	43	2	-0.26	-0.23
	9	3	-0.38	0.21

† 1, 0 to 15 cm sampling depth; 2, 15 to 45 cm sampling depth; 3, 45 to 75 cm sampling depth

* Significant at the 0.05 probability level

** Significant at the 0.01 probability level

*** Significant at the 0.001 probability level

The PRP component was generally more correlated at North River site as compared to HCP component (Table 4-6). It might be due to more rocky nature of soils at North River Site (Farooque, 2010). As the HCP has more sensing depth so the sand, underlying

gravels and crystalline rocks at the deeper depths contribute to HCP resulting weak and non-significant correlation with soil properties. The positive significant correlation coefficients indicated that with the increase in the soil property, the PRP also increases and vice versa. It also showed that DualEM can be used to predict the soil properties in a rapid and non-destructive manner. Soil pH was generally not well correlated to EC_a in all sampling depths, but it was significantly correlated in deepest sampling depth at Boulden site. θ_v was significantly positively correlated with EC_a in all of three sampling depths. As would be expected, EC_a is directly related to θ_v and clay (Increased clay and θ_v lead to wetter soil conditions while clay has greater water holding capacity and increased EC_a). EC was also significantly positively correlated and higher values in deeper depths as compared to the first sampling depth. Improved correlation was attributed in the deeper depths due to the fact that the clay contents were more in these two depths. Tillage also affects the first layer, but does not greatly affects the other two layers. EC_a was significantly positively correlated with SOM and the correlation values for SOM were higher in deeper sampling depths in blueberry fields (Tables 4-6 and 4-7) while these were higher in shallowest sample depth at BEEC and Boulden site (Tables 4-8 and 4-9). The low correlation coefficient and R^2 values somewhere can be explained as follows:

- It is possible that EC_a is highly governed by soil property (Allred et al., 2005) not listed in Tables 4-1 to 4-4 and it is clear on the basis of results that EC_a is not affected by a single soil property but more than one soil properties contributing and influencing the EC_a measurements.
- The EC_a measured with EMI methods is an effective value for a large soil volume, and the overall properties of this large volume might not be well

represented by a relatively small soil sample (Allred et al., 2005; Ristolainen et al., 2009).

Soil properties at each sampling depth were regressed against EC_a. Coefficients of determination, R^2, for linear and cubic regression model between EC_a and soil properties were calculated. Cubic regression models were found to be best fit to predict soil properties using EC_a.

Table 4-8 Correlation coefficients (r) among soil properties and EC_a at BEEC Site

Properties	n	Depth†	PRP	HCP
Clay, %	50	1	0.56*	0.56*
	50	2	0.51*	0.51*
	50	3	0.68*	0.59*
Silt, %	50	1	-0.24	-0.48*
	50	2	-0.06	-0.22
	50	3	0.54*	0.40*
Sand, %	50	1	0.26	0.46*
	50	2	0.04	0.16
	50	3	-0.54*	-0.36*
SOM, %	50	1	0.60**	0.70**
	50	2	0.002	0.08
	50	3	0.12	0.04
θ_v, $m^3\ m^{-3}$	50	1	0.74***	0.69***
	50	2	0.70***	0.65***
	50	3	0.78***	0.72***
EC, $\mu S\ m^{-1}$	50	1	0.22	0.22
	50	2	0.44*	0.42*
	50	3	0.74***	0.68***
pH	50	1	0.24	0.24
	50	2	0.16	0.10
	50	3	0.24	0.26

† 1, 0 to 15 cm sampling depth; 2, 15 to 45 cm sampling depth; 3, 45 to 75 cm sampling depth
* Significant at the 0.05 probability level
** Significant at the 0.01 probability level
*** Significant at the 0.001 probability level

At the deepest sampling depth, predictions of many soil properties were improved using a cubic model of EC_a instead of the simple linear regression. For example, prediction of clay content in the surface sample at Carmel Site was greatly improved by using the cubic model (coefficient of determination improved from 43 to 78 %). In general, soil

properties were better estimated from the EC_a cubic model. Using a similar approach, other transformations of EC_a were considered such as log, quadratic and exponential models. Regressions using these transformed terms almost always gave a coefficient of determination less than models using a cubic term.

Table 4-9 Correlation coefficients (r) among soil properties and EC_a at Boulden Site

Properties	n	Depth†	PRP	HCP
Clay, %	30	1	0.16	0.12
	30	2	0.74**	0.66*
	30	3	0.72*	0.40*
Silt, %	30	1	0.50*	0.14
	30	2	0.56*	0.56*
	30	3	0.72*	0.36*
Sand, %	30	1	-0.48*	-0.16
	30	2	-0.80**	-0.74**
	30	3	-0.86**	-0.44*
SOM, %	30	1	0.75***	0.80***
	30	2	0.69***	0.68***
	30	3	0.34*	0.23
θ_v, $m^3\ m^{-3}$	30	1	0.72***	0.89***
	30	2	0.78***	0.91***
	30	3	0.69***	0.83***
EC, $\mu S\ m^{-1}$	30	1	0.40*	0.74**
	30	2	0.76**	0.54*
	30	3	0.70*	0.84***
pH	30	1	0.32*	0.43*
	30	2	0.32	0.34
	30	3	0.43*	0.63***

† 1, 0 to 15 cm sampling depth; 2, 15 to 45 cm sampling depth; 3, 45 to 75 cm sampling depth

* Significant at the 0.05 probability level

** Significant at the 0.01 probability level

*** Significant at the 0.001 probability level

Table 4-10 Calibration models using EC_a to predict soil properties at North River Site

Depth†	Property	n	Model	R^2
1	Clay, %	50	$3.4+3.80HCP-0.24HCP^2+0.005\ HCP^3$	0.46
1	Silt, %	50	$25.3+1.80PRP+\ 0.007PRP^2\ -0.003PRP^3$	0.70
1	Sand, %	50	$81.3-4.2PRP+0.24PRP^2\ -0.006PRP^3$	0.61
1	SOM, %	50	$9.2+0.58HCP-0.12HCP^2+0.004HCP^3$	0.44
1	θ_v, $m^3\ m^{-3}$	50	$11.4+2.9PRP-0.05PRP^2-0.008PRP^3$	0.75
1	EC, $\mu S\ m^{-1}$	50	$47.7-0.4HCP+0.62HCP^2-0.03HCP^3$	0.45
2	Clay, %	35	$7.26+3.07HCP-0.8HCP^2\ +0.04\ HCP^3$	0.69
2	SOM, %	35	2.98 – 23.6 PRP	0.43
2	θ_v, $m^3\ m^{-3}$	35	$13.8+2.2PRP-0.07PRP^2-0.008PRP^3$	0.73
2	EC, $\mu S\ m^{-1}$	35	$51.7-8.6PRP+1.9PRP^2\ -0.12PRP^3$	0.72
3	Clay, %	7	$9.4+5.55HCP-0.63HCP^2\ -0.01\ HCP^3$	0.74
3	SOM, %	7	$2.7+3.56HCP-0.47HCP^2\ +0.09\ HCP^3$	0.88
3	θ_v, $m^3\ m^{-3}$	7	$23.2+4.5HCP-1.6HCP^2-0.07HCP^3$	0.82
3	EC, $\mu S\ m^{-1}$	7	$58.5-6.4HCP-0.71HCP^2\ +0.4HCP^3$	0.87

† 1, 0 to 15 cm sampling depth; 2, 15 to 45 cm sampling depth; 3, 45 to 75 cm sampling depth

Table 4-11 Validation models using 2nd year data at North River Site

Depth†	Property	n	Model	R^2	RMSE
1	Clay, %	20	$3.9-0.89HCP+0.39HCP^2-0.02\ HCP^3$	0.40	2.6
1	Silt, %	20	$32.9-2.98PRP+0.46PRP^2\ -0.02PRP^3$	0.55	3.7
1	Sand, %	20	$65.7+1.2PRP-0.33PRP^2\ +0.01PRP^3$	0.48	5.3
1	SOM, %	20	$8.9+0.40HCP-0.12HCP^2+0.01HCP^3$	0.39	0.7
1	θ_v, $m^3\ m^{-3}$	20	$10.9+2.9PRP-0.12PRP^2-0.001PRP^3$	0.77	3.0
1	EC, $\mu S\ m^{-1}$	20	$49.6+0.6HCP+0.52HCP^2-0.04HCP^3$	0.41	8.8
2	Clay, %	20	$8.8+1.8HCP-0.2HCP^2\ +0.006\ HCP^3$	0.55	2.1
2	SOM, %	20	$3.3+\ 0.06\ PRP-0.002PRP^2\ -PRP^3$	0.34	0.5
2	θ_v, $m^3\ m^{-3}$	20	$15.9+3.6PRP-0.04PRP^2-0.01PRP^3$	0.68	3.4
2	EC, $\mu S\ m^{-1}$	20	$56.5-5.6PRP+1.5PRP^2\ -0.06PRP^3$	0.59	6.8
3	Clay, %	7	$7.0+6.4HCP-0.47HCP^2\ -0.03\ HCP^3$	0.67	2.0
3	SOM, %	7	$1.4+1.05HCP-0.3HCP^2\ +0.03\ HCP^3$	0.82	0.4
3	θ_v, $m^3\ m^{-3}$	7	$21.2+3.9HCP-1.9HCP^2-0.04HCP^3$	0.78	3.1
3	EC, $\mu S\ m^{-1}$	7	$56.8-4.6HCP-0.37HCP^2\ +0.10HCP^3$	0.80	5.2

† 1, 0 to 15 cm sampling depth; 2, 15 to 45 cm sampling depth; 3, 45 to 75 cm sampling depth

The selected soil properties correlated significantly with EC_a in blueberry fields (R^2 varied from 0.43 to 0.90; $P < 0.05$), BEEC field (R^2 varied from 0.49 to 0.88; $P < 0.05$) and Boulden field (R^2 varied from 0.40 to 0.91) (Tables 4-10, 4-12, 4-14 and 4-16). The correlation between actual and predicted soil properties in blueberry fields (R^2 varied from 0.34 to 0.82; $P < 0.05$; RMSE ranged from 0.4 to 8.8), BEEC field (R^2 varied from

Table 4-12 Calibration models using EC_a to predict soil properties at Carmel Site

Depth†	Property	n	Model	R^2
1	Clay, %	50	8.6 + 20.9 PRP	0.48
1	θ_v, $m^3\ m^{-3}$	50	25.7 + 30.2 PRP	0.73
1	EC, $\mu S\ m^{-1}$	50	$68.4 - 5.6PRP + 3.50PRP^2 - 0.45PRP^3$	0.60
2	SOM, %	43	$4.2+0.86HCP -0.24HCP^2 +0.014HCP^3$	0.65
2	θ_v, $m^3\ m^{-3}$	43	$25.6-4.8HCP+3.2HCP^2 -0.05HCP^3$	0.70
2	EC, $\mu S\ m^{-1}$	43	$65.5-10.4PRP+3.8PRP^2 -0.22\ PRP^3$	0.47
3	Clay, %	9	$26.2-12.4PRP+4.56PRP^2 -0.44\ PRP^3$	0.90
3	SOM, %	9	$5.2+0.8HCP -0.38HCP^2 +0.04HCP^3$	0.61
3	θ_v, $m^3\ m^{-3}$	9	$22.5-9.9PRP+4.2PRP^2 -0.8\ PRP^3$	0.75
3	EC, $\mu S\ m^{-1}$	9	$44.8+ 4.2HCP - 0.88HCP^2 + 0.02\ HCP^3$	0.63

† 1, 0 to 15 cm sampling depth; 2, 15 to 45 cm sampling depth; 3, 45 to 75 cm sampling depth

Table 4-13 Validation models using 2^{nd} year data at Carmel Site

Depth†	Property	n	Model	R^2	RMSE
1	Clay, %	20	$6.4-0.5\ PRP+0.35PRP^2 -0.04PRP^3$	0.42	2.3
1	θ_v, $m^3\ m^{-3}$	20	$21.7+1.58\ PRP+0.03PRP^2-0.02PRP^3$	0.68	2.5
1	EC, $\mu S\ m^{-1}$	20	$70.2 -5.3PRP + 2.0PRP^2-0.18PRP^3$	0.51	5.6
2	SOM, %	20	$2.3+0.7HCP-0.14HCP^2 +0.008HCP^3$	0.59	0.5
2	θ_v, $m^3\ m^{-3}$	20	$23.8-5.3HCP+3.7HCP^2 -0.08HCP^3$	0.62	2.4
2	EC, $\mu S\ m^{-1}$	20	$58.9-11.9PRP+4.2PRP^2 -0.37\ PRP^3$	0.47	6.9
3	Clay, %	9	$23.3-10.6PRP+2.8PRP^2 -0.16\ PRP^3$	0.78	1.9
3	SOM, %	9	$2.6+0.5HCP -0.21HCP^2 +0.02HCP^3$	0.50	0.5
3	θ_v, $m^3\ m^{-3}$	9	$24.8-7.6PRP+3.0PRP^2 - PRP^3$	0.66	2.8
3	EC, $\mu S\ m^{-1}$	9	$41+3.8HCP-0.65HCP^2 +0.03\ HCP^3$	0.72	4.8

† 1, 0 to 15 cm sampling depth; 2, 15 to 45 cm sampling depth; 3, 45 to 75 cm sampling depth

Table 4-14 Calibration models using EC_a to predict soil properties at BEEC Site

Depth†	Property	n	Model	R^2
1	Clay, %	50	$5.22+3.4HCP-0.18HCP^2 + 0.005HCP^3$	0.61
1	SOM, %	50	$4 -0.06HCP+0.005HCP^2-0.00008\ HCP^3$	0.76
1	θ_v, $m^3\ m^{-3}$	50	$28.2-0.54PRP+0.03PRP^2 - 0.0007\ PRP^3$	0.81
2	Clay, %	50	10.55 + 28.68 PRP	0.56
2	θ_v, $m^3\ m^{-3}$	50	25.50 + 32.67 PRP	0.70
2	EC, $\mu S\ m^{-1}$	50	36.23 + 24.44 PRP	0.49
3	Clay, %	50	$3.55+4.5PRP-0.22PRP^2 +0.003\ PRP^3$	0.73
3	θ_v, $m^3\ m^{-3}$	50	$30.48-0.77PRP+0.12PRP^2 - 0.006\ PRP^3$	0.88
3	EC, $\mu S\ m^{-1}$	50	$16.2+10.8PRP-0.52PRP^2 +0.009PRP^3$	0.79

† 1, 0 to 15 cm sampling depth; 2, 15 to 45 cm sampling depth; 3, 45 to 75 cm sampling depth

Table 4-15 Validation models using 2nd year data at BEEC Site

Depth†	Property	n	Model	R^2	RMSE
1	Clay, %	20	$3.3+2.6HCP-0.12HCP^2+0.002HCP^3$	0.52	2.2
1	SOM, %	20	$3.0-0.20HCP+0.01HCP^2-0.001\ HCP^3$	0.65	0.6
1	θ_v, $m^3\ m^{-3}$	20	$36.9-1.6PRP+0.11PRP^2-0.002\ PRP^3$	0.74	2.7
2	Clay, %	20	$17.7-0.7\ PRP+0.02PRP^2-0.002PRP^3$	0.51	3.0
2	θ_v, $m^3\ m^{-3}$	20	$32.2-2.4PRP+0.2PRP^2-0.004\ PRP^3$	0.64	3.5
2	EC, $\mu S\ m^{-1}$	20	$86.0-2.3\ PRP+0.2PRP^2-0.003PRP^3$	0.47	13.8
3	Clay, %	20	$2.8+3.1PRP-0.15PRP^2+0.005\ PRP^3$	0.65	2.7
3	θ_v, $m^3\ m^{-3}$	20	$27.6-0.8PRP+0.18PRP^2-0.002\ PRP^3$	0.80	2.2
3	EC, $\mu S\ m^{-1}$	20	$61.0-0.04PRP+0.05PRP^2-0.002PRP^3$	0.58	9.1

† 1, 0 to 15 cm sampling depth; 2, 15 to 45 cm sampling depth; 3, 45 to 75 cm sampling depth

Table 4-16 Calibration models using EC_a to predict soil properties at Boulden Site

Depth†	Property	n	Model	R^2
1	SOM, %	50	$6.34-0.5HCP+0.07HCP^2-3.77\ HCP^3$	0.83
1	θ_v, $m^3\ m^{-3}$	50	$128-18.4HCP+0.88HCP^2-0.05HCP^3$	0.91
1	EC, $\mu S\ m^{-1}$	50	$312-32HCP+2.4HCP^2-0.045\ HCP^3$	0.84
1	pH	50	$8.22+17.4\ HCP$	0.47
2	Clay, %	50	$5.2+0.88PRP+0.042PRP^2-0.008PRP^3$	0.79
2	Sand, %	50	$50.4-34.6\ PRP$	0.70
2	SOM, %	50	$2.32+26.2\ PRP$	0.64
2	θ_v, $m^3\ m^{-3}$	50	$132-24.2HCP+0.56HCP^2-0.06HCP^3$	0.90
2	EC, $\mu S\ m^{-1}$	50	$212+46.6PRP-4.23PRP^2+0.08PRP^3$	0.80
3	Clay, %	50	$37+8.8PRP-0.58PRP^2+0.012PRP^3$	0.77
3	Sand, %	50	$134-20.3PRP+3.3PRP^2-0.05\ PRP^3$	0.90
3	SOM, %	50	$0.72+22.4\ PRP$	0.40
3	θ_v, $m^3\ m^{-3}$	50	$120-16.4HCP+1.44HCP^2-0.09HCP^3$	0.86
3	EC, $\mu S\ m^{-1}$	50	$318+52.2HCP-8.2HCP^2+0.04HCP^3$	0.89
3	pH	50	$10.2-0.66HCP+0.08HCP^2-HCP^3$	0.68

† 1, 0 to 15 cm sampling depth; 2, 15 to 45 cm sampling depth; 3, 45 to 75 cm sampling depth

0.47 to 0.80; $P < 0.05$; RMSE ranged from 0.6 to 13.8) and Boulden field (R2 varied from 0.39 to 0.83; $P < 0.05$; RMSE ranged from 0.4 to 9.7) was also significant (Tables 4-11, 4-13, 4-15 and 4-17).root mean square error (RMSE) between observed and predicted soil properties, are shown for these selected models (Tables 4-11, 4-13, 4-15 and 4-17). We conclude that the models derived from soil EC_a could provide reasonable estimates of these soil properties.

Table 4-17 Validation models using 2nd year data at Boulden Site

Depth†	Property	n	Model	R^2	RMSE
1	SOM, %	20	$9.1-1.0HCP+0.04HCP^2 - 0.001\ HCP^3$	0.77	0.4
1	θ_v, $m^3\ m^{-3}$	20	$161-19.8HCP+0.93HCP^2 - 0.01HCP^3$	0.83	2.6
1	EC, $\mu S\ m^{-1}$	20	$229- 24HCP + 1.1HCP^2 - 0.016\ HCP^3$	0.76	9.2
1	pH	20	$0.2+0.8\ HCP-0.03HCP^2 + 0.004HCP^3$	0.48	0.5
2	Clay, %	20	$5.3-1.0PRP+0.13PRP^2 -0.003PRP^3$	0.72	2.3
2	Sand, %	20	$58.3+2.0\ PRP-0.09PRP^2+0.0005PRP^3$	0.64	5.8
2	SOM, %	20	$0.87+0.24\ PRP-0.02PRP^2+0.005PRP^3$	0.58	0.5
2	θ_v, $m^3\ m^{-3}$	20	$144-27.2HCP+0.43HCP^2 - 0.03HCP^3$	0.82	2.4
2	EC, $\mu S\ m^{-1}$	20	$178+45.1PRP-2.6PRP^2+ 0.05PRP^3$	0.68	9.7
3	Clay, %	20	$33 +7.0PRP-0.38PRP^2 + 0.007PRP^3$	0.68	2.4
3	Sand, %	20	$171- 17.5PRP + 1.1PRP^2 - 0.02\ PRP^3$	0.67	4.5
3	SOM, %	20	$7.4-1.3PRP+0.08PRP^2-0.002PRP^3$	0.39	0.8
3	θ_v, $m^3\ m^{-3}$	20	$135-14.2HCP+2.6HCP^2 - 0.04HCP^3$	0.79	2.7
3	EC, $\mu S\ m^{-1}$	20	$472+75.5HCP-8.9HCP^2 +0.06HCP^3$	0.81	8.8
3	pH	20	$1.9+0.6HCP-0.02HCP^2 +0.004\ HCP^3$	0.60	0.4

† 1, 0 to 15 cm sampling depth; 2, 15 to 45 cm sampling depth; 3, 45 to 75 cm sampling depth

4.4.4 Soil Properties and EC_a Correlated to Crop Yield

Understanding the variability of soil properties and their effect on crop yield is a major component of site-specific management systems (Li et al., 2008). In agricultural fields, yield variability is partly caused by soil variability and topographic features of the field. Although yield is a function of many factors, including soil properties, topography, climate, biological factors, and management practices, in certain years as much as 60% or even more of the yield variability can be explained by a combination of soil properties and topographic features (Sanderson et al., 1996; Yang et al., 1998; Kravchenko and Bullock, 2000; Gagnon et al., 2003; Farooque et al., 2012). Soil properties can have a direct effect on crop growth and yield by redirecting and changing nutrients and water availability. Therefore, it is important to investigate the effect of soil properties on crop yield.

Statistically significant correlation coefficients of soil properties to crop yield are provided (Table 4-18). Silt and sand were correlated with yield at the 45 to 75 cm depth;

θ_v was more correlated at 0 to 15 cm depth than the other soil properties at different depths, and clay was correlated at 15 to 45 cm depth in North River Site. Silt, sand and SOM were correlated with yield in Carmel Site at the 45 to 75 cm depth; θ_v and pH were also correlated at 0 to 15 cm depth while clay was negatively correlated at 15 to 45 cm depth. In wild blueberry fields, soil properties were not generally significantly correlated to fruit yield at the 0 to 15 cm where the rhizomes of this crop present. But at the first depth, PRP, pH and θ_v showed negative significant correlation with wild blueberry yield indicating that increasing in these properties results in decreasing the yield. As this crop likes the sandy and well-drained soils, so the PRP and θ_v were higher in the clayey areas of the field because of more holding capacity of clay as compared to sand. There is several other factors affect yield variability, which have not been recorded and addressed. Disease and insect damage are obvious examples. Esau (2012) compared wild blueberry fields with control and fungicides application treatments, he found that fungicides significantly impact fruit yield. Weeds competing with wild blueberry, pollination, seasonal variability and winter kill can also negatively impact fruit yield (Farooque et al., 2011).

Silt and sand were correlated with yield at 0 to 15 cm depth in BEEC Site in 2010. θ_v and SOM were also correlated at 15 to 45 cm depth, and clay was correlated at 45 to 75 cm depth while EC and pH were not correlated at BEEC Site at any depth in 2010. In 2011, only sand, SOM, θv and EC were positively correlated with yield. The first three parameters were correlated at 0 to 15 cm and EC was at 15 to 45 cm depth. The parameters correlated at various depths at Boulden Site were similar as at BEEC Site in

Table 4-18 Correlation coefficients (r) among soil properties and crop yield

Properties	Depth†	Blueberry North River	Blueberry Carmel	Soybean BEEC	Barley BEEC	Pasture Boulden
Clay, %	1	-0.20	-0.46	0.10	0.20	0.14
	2	-0.74*	-0.87***	0.04	0.08	0.30
	3	-0.36	-0.72*	0.48**	0.06	0.62*
Silt, %	1	-0.58	0.05	-0.56**	-0.26	0.64*
	2	-0.26	-0.35	0.05	0.12	0.58
	3	-0.86*	-0.80**	0.22	0.18	0.20
Sand, %	1	0.48	0.32	0.40*	0.32*	-0.58*
	2	0.60	0.46	0.16	0.16	-0.34
	3	0.86**	0.89**	0.12	0.16	-0.40
SOM, %	1	0.28	0.06	0.38*	0.46*	0.18
	2	0.32	0.06	0.56**	0.02	0.34*
	3	0.46	0.81*	0.36	0.20	0.22
θ_v, $m^3\ m^{-3}$	1	-0.68**	-0.30*	0.05	0.36*	0.10
	2	-0.56	-0.26	0.44*	0.23	0.26*
	3	-0.47	-0.29	0.37	0.41	0.18
EC, $\mu S\ m^{-1}$	1	0.46	0.08	0.18	0.12	0.12
	2	0.44	0.60*	0.08	0.64*	0.26
	3	0.10	0.30	0.06	0.22	-0.30
pH	1	-0.36*	-0.34*	-0.08	-0.34	0.08
	2	-0.50	-0.26	-0.24	-0.26	0.30
	3	-0.81*	-0.56*	-0.10	-0.02	-0.52
PRP		-0.52*	-0.35*	-0.30*	-0.60**	0.22
HCP		-0.20	-0.21	-0.17	-0.34	0.20

† 1, 0 to 15 cm sampling depth; 2, 15 to 45 cm sampling depth; 3, 45 to 75 cm sampling depth

* Significant at the 0.05 probability level.

** Significant at the 0.01 probability level.

*** Significant at the 0.001 probability level.

2010. The PRP was negatively correlated at BEEC sites, but non-significantly correlated at Boulden Site. The results were supported by the findings of Jung et al. (2005). Correlation coefficient only indicates linear relationships but significant non-linear relationships may exist between soil properties and yield. Soil properties and crop yield vary spatially within field, among fields, and from year to year on a farm (Jaynes, et al., 1995). There are many factors including site characteristics, crop management, and climate, which can affect crop yield and quality (Patzold et al., 2008; Wong and Asseng,

2006). Factors other than soil properties were not measured like water holding capacity which is usually a significant contributor to crop yield (Lund et al., 2000). Jung et al. (2005) reported that rainfall affects yield more than variations in soil properties. Another factor that must be considered is that soil properties and yield correlations may invert from year to year, depending on rainfall (Jaynes, et al., 1995). This same phenomenon is one that must be dealt with when normalizing and averaging multiple years of yield data (Kitchen, et al., 1999). It has been shown that 7 to 10 years of yield data may be needed in order to develop yield goals effectively based solely on soil properties maps (Lutticken, 1998), and other research has discovered that yields are not steady after six years of examining (Colvin, et al., 1997).

4.4.5 Interpolation and Mapping of Soil Properties

The soil properties, fields boundary and EC_a data were imported into ArcGIS 10 software (ESRI, Redlands, CA) and shape files were created for visual display of North River Site (Figures 4-5 and 4-6), Carmel Site (Figures 4-7 and 4-8), BEEC Site (Figures 4-9 and 4-10) and Boulden Site (Figures 4-11 and 4-12).

GIS combined with geo-statistics was applied to analyze the spatial variability in soil properties for all fields. Soil parameters were interpolated using kriging combined with semivariogram parameters to generate detailed maps. Schumann and Zaman, (2003) showed that the kriged estimates were very close to the measured estimates in Florida citrus groves. The kriging interpolation is considered to be more accurate and reliable than other methods such as inverse distance weighting (IDW) or trend surface models (Mulla et al., 1992). The maps of soil properties were generated using ArcGIS 10

software at the same scale and equal number of classes in order to allow easier comparison.

The interpolated maps of HCP, PRP, θ_v, EC, SOM, sand, silt and clay at North River Site (Figures 4-5 and 4-6) showed gradual spatial variability with significantly different values across the field. Spatial patterns of variation for PRP, HCP, θ_v, EC, silt and clay (Figures 4-5 and 4-6) were almost similar, showing higher value in the northwest, north central region, and medium values were generally observed in the south eastern region of the field. The lower values were observed in the center of the field. The variation in soil properties might be due to the variation in elevation with the high values of these soil parameters in low lying areas and vice versa. These results were in agreement with the findings of Farooque et al. (2011).

The map of SOM (Figure 4-6) at North River Site indicated the substantial variation across the field. The map of sand content showed lower values in the northwest and southeast region of the field. Higher values were observed in southwest, southeast and south central region indicating textural variation within field. It was observed that most of the crop areas were contained with more sand than clay for North River Site. The ground inspections revealed that the areas with higher clay content within field were weeds, bare spots and grasses.

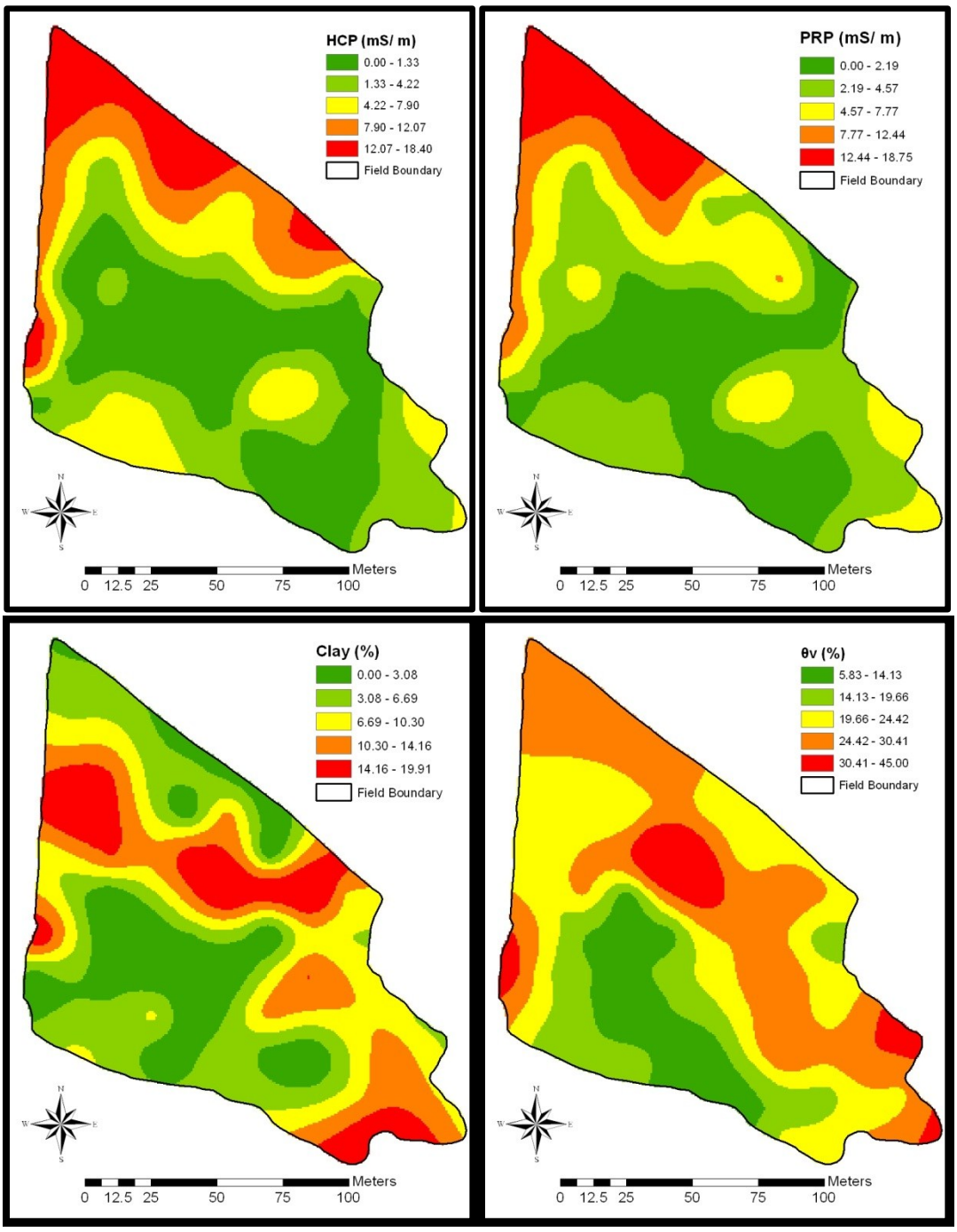

Figure 4-5 Maps of HCP, PRP, clay and θ_v for North River Site

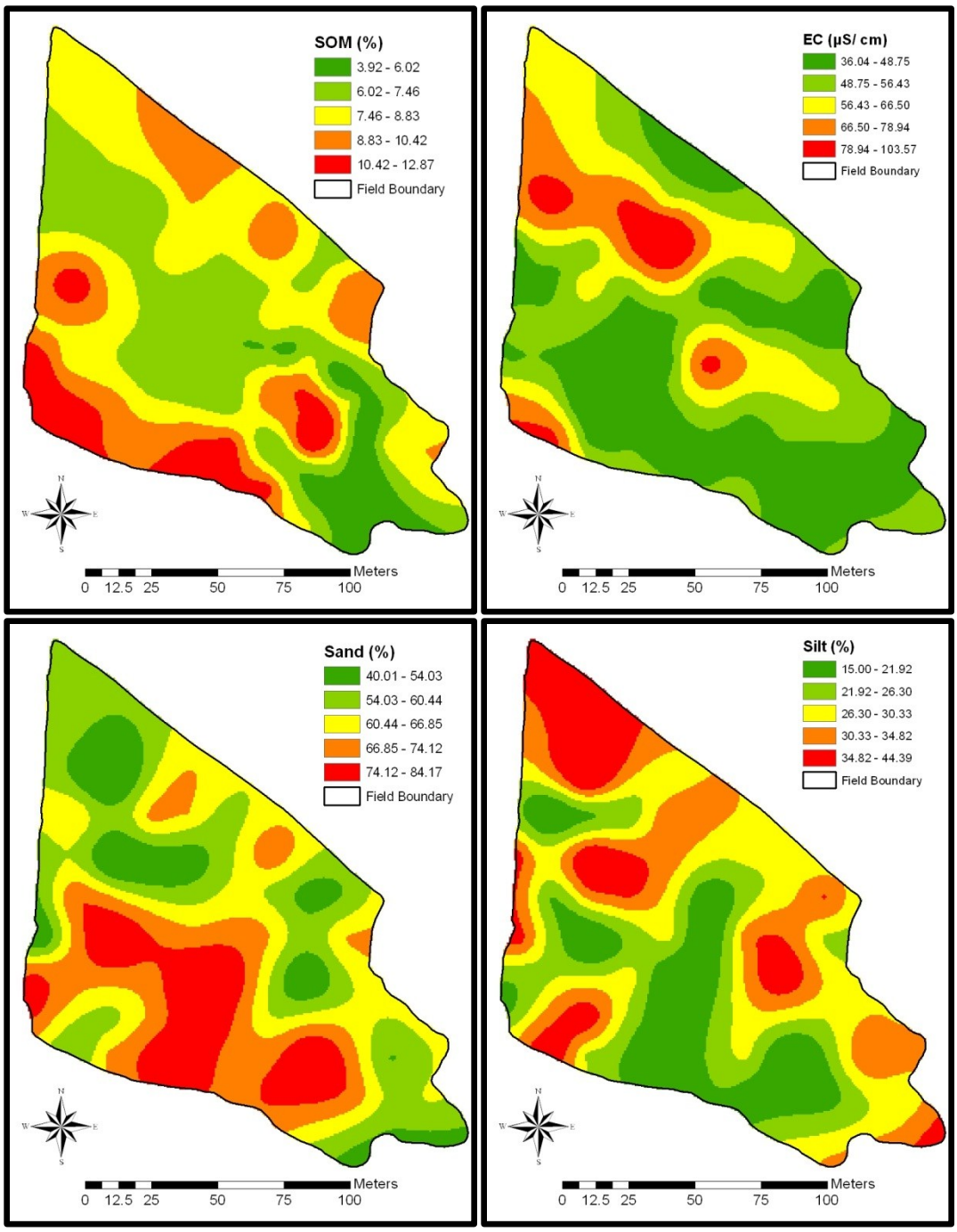

Figure 4-6 Maps of SOM, EC, sand and silt for North River Site

The interpolated maps of HCP, PRP, pH, EC, SOM, sand, silt and clay at Carmel Site (Figures 4-7 and 4-8) showed gradual spatial variability with significantly different values across the field. Spatial patterns of variation for HCP, PRP, SOM and sand (Figures 4-7 and 4-8) were almost similar, showing higher value in the north and lower

values in the southwest and south central part of the field. The medium values were observed in the center of the field. The maps of HCP, PRP, SOM, clay and EC indicated the large spatial variability of these soil properties within field.

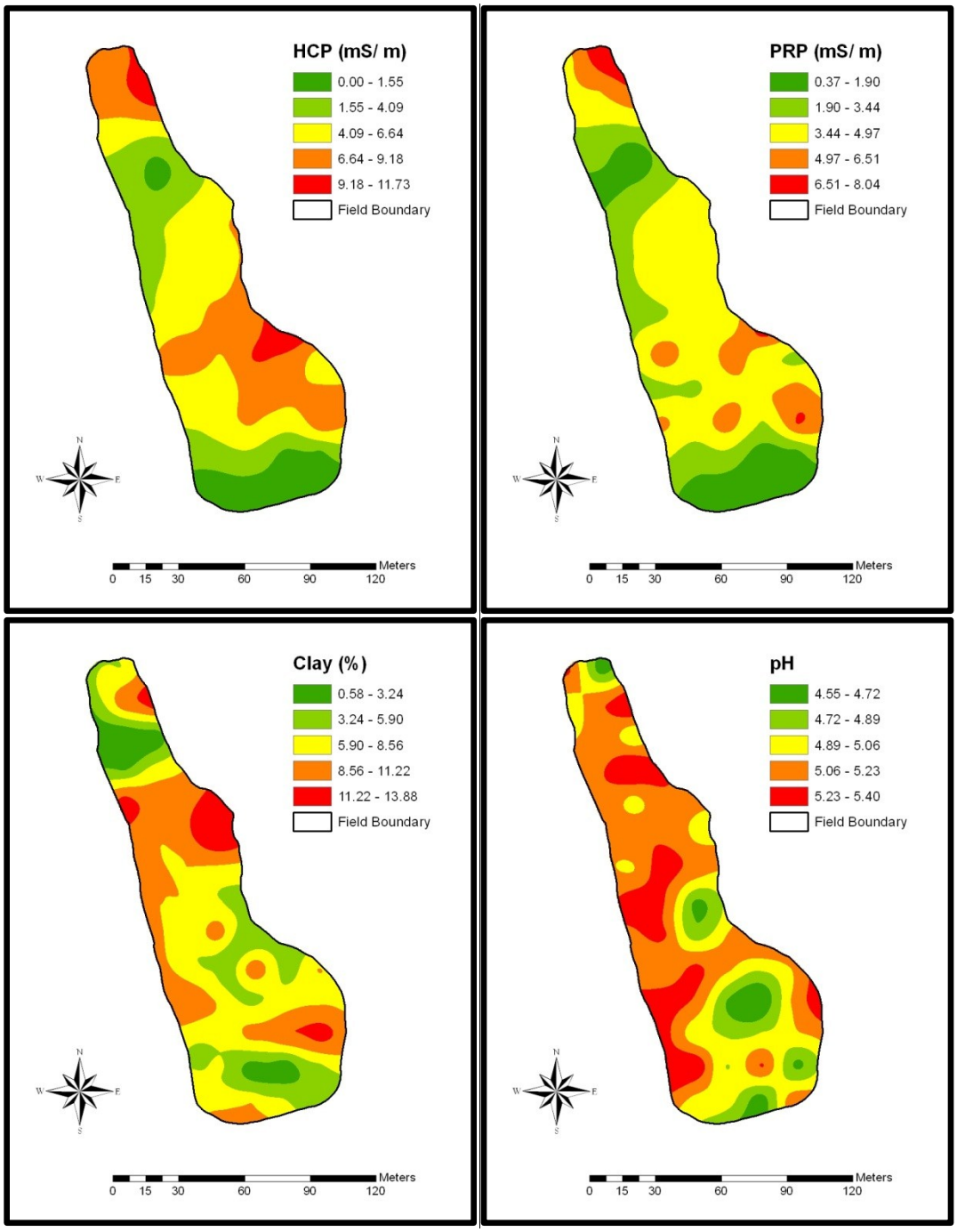

Figure 4-7 Maps of HCP, PRP, clay and pH for Carmel Site

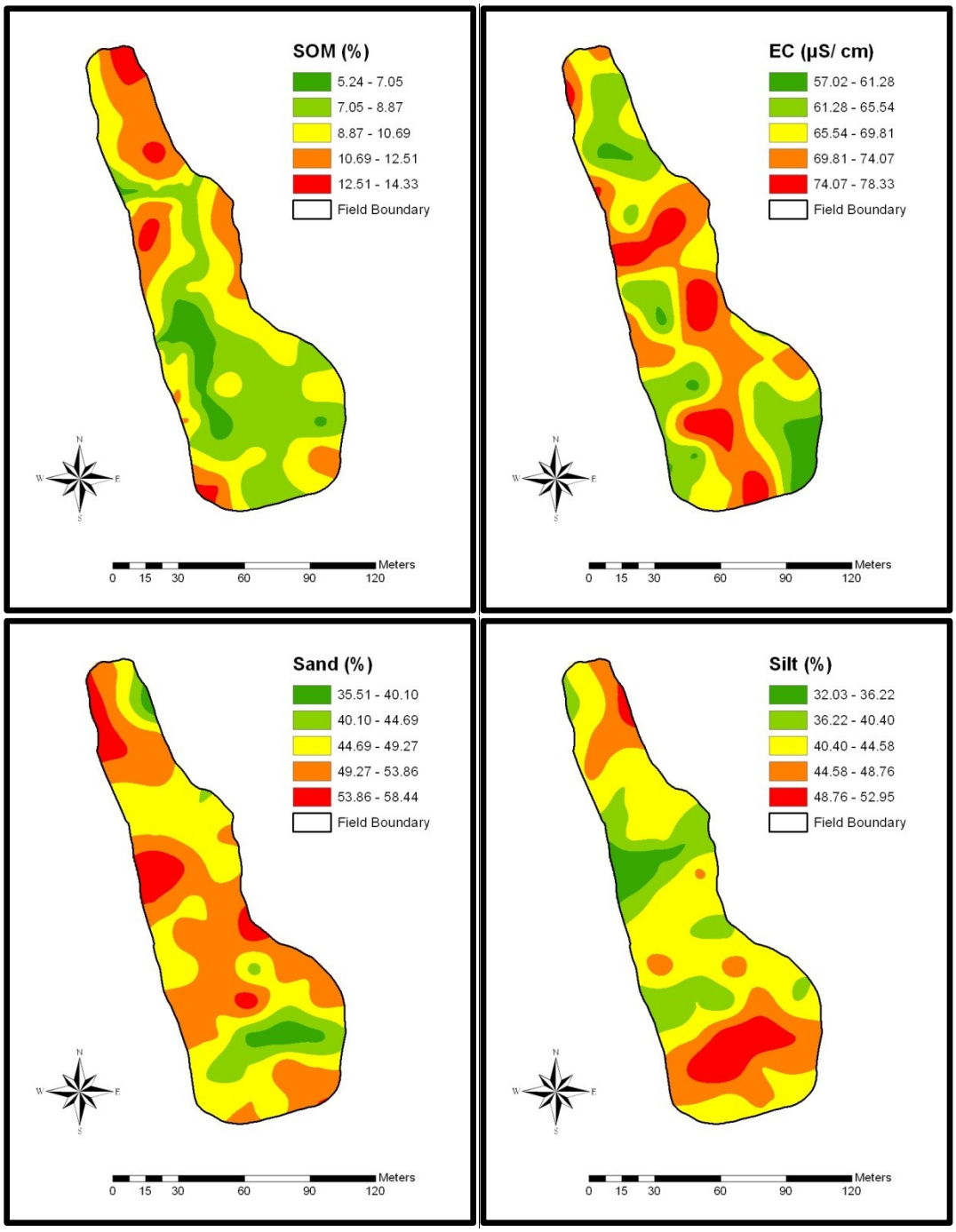

Figure 4-8 Maps of SOM, EC, sand and silt for Carmel Site

The map of silt content indicated that this soil property was less variable as compare to the other soil properties (Figure 4-8). The lower values for the pH were observed in the south part of the field, and higher values were observed in the upper center of the field. The soil pH map indicated that the most of the Carmel Site having the pH ranging from

5.05 to 5.40 (Figure 4-7). Overall the maps of soil properties indicated the large spatial variation within field.

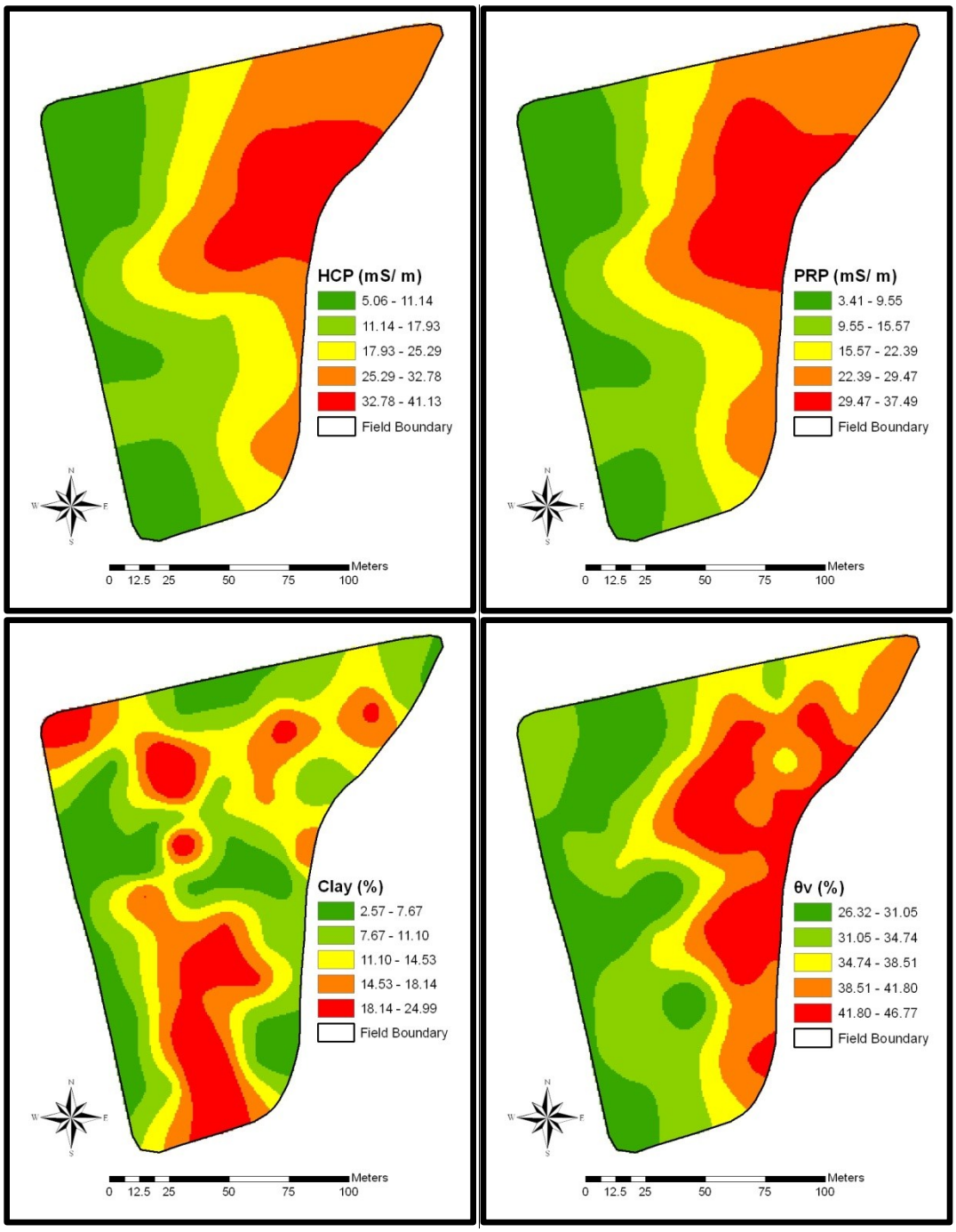

Figure 4-9 Maps of HCP, PRP, clay and θ_v for BEEC Site

The interpolated maps of HCP, PRP, θv, EC, SOM, sand, silt and clay at BEEC Site (Figures 4-9 and 4-10) showed gradual spatial variability with significantly different values across the field. Spatial patterns of variation for PRP, HCP and θv (Figure 4-9) were almost similar, showing higher value in the northeast and north region, and medium values were generally observed in the center of the field from north to south. The lower values were observed in the northwest and west of the field. The variation in soil properties might be due to the variation in elevation with the high values of these soil parameters in low lying areas and vice versa.

The map of SOM, sand and silt (Figure 4-10) at BEEC Site indicated the substantial variation across the field. The map of SOM content showed lower values in the northwest and north region of the field. Higher values were observed in northeast region indicating variation within field.

The interpolated maps of HCP, PRP, θ_v, EC, SOM, sand, silt and clay at Boulden Site (Figures 4-11 and 4-12) showed gradual spatial variability with significantly different values across the field. Spatial patterns of variation for HCP, PRP, SOM, θ_v and EC (Figures 4-11 and 4-12) were almost similar, showing higher value in the north and south, and lower values in the west and east part of the field. The medium values were observed in the center of the field. The maps of HCP, PRP, SOM, clay, θ_v, sand, silt and EC indicated the large spatial variability of these soil properties within field.

The lower values for the sand content were observed in the central part of the field, and higher values were observed in the northeast and northwest of the field. The HCP and PRP maps indicated that the most of the Boulden Site having the apparent ground

conductivity ranging from 18.00 to 30.00 (Figure 4-11). Overall the maps of soil properties indicated the large spatial variation within field.

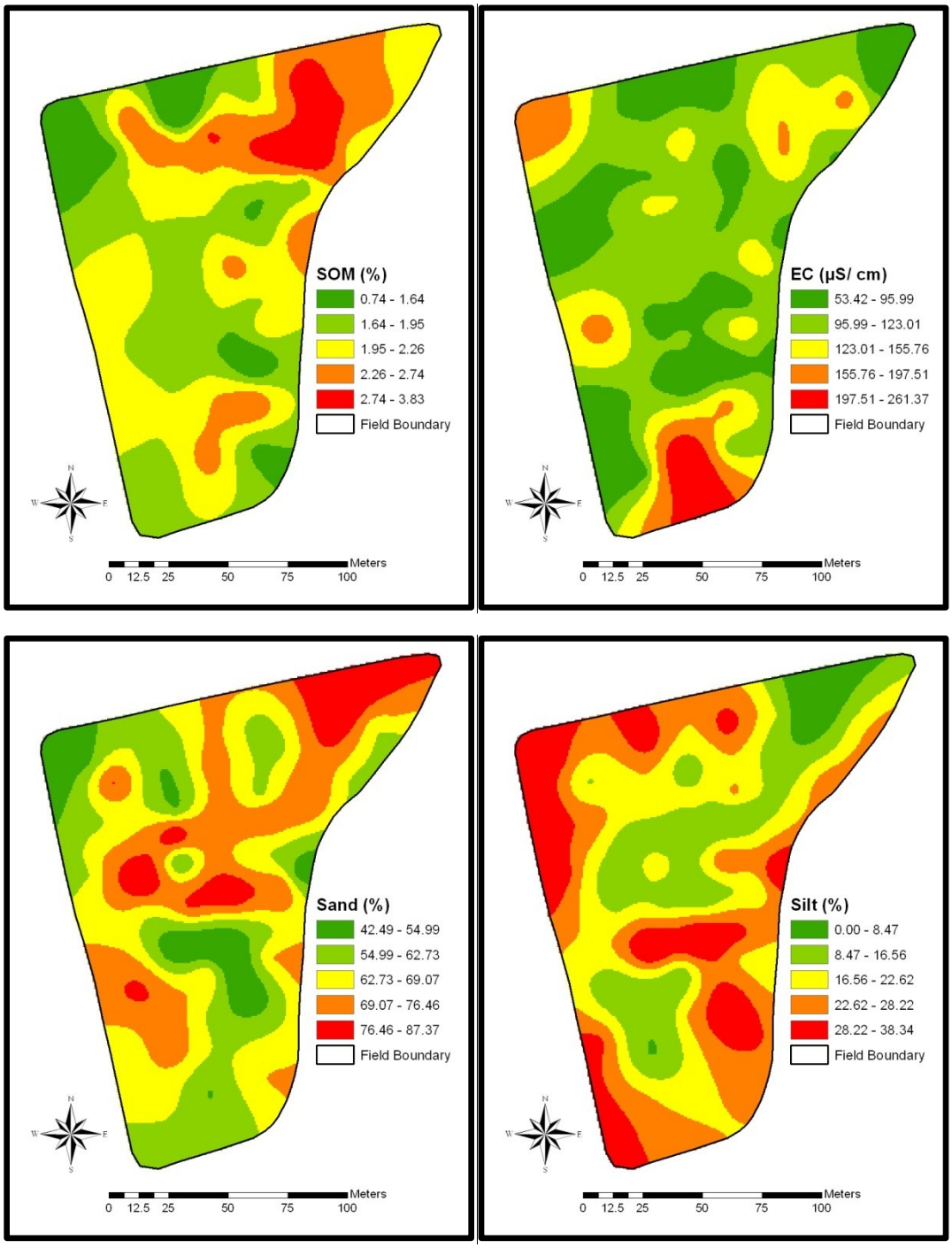

Figure 4-10 Maps of SOM, EC, sand and silt for BEEC Site

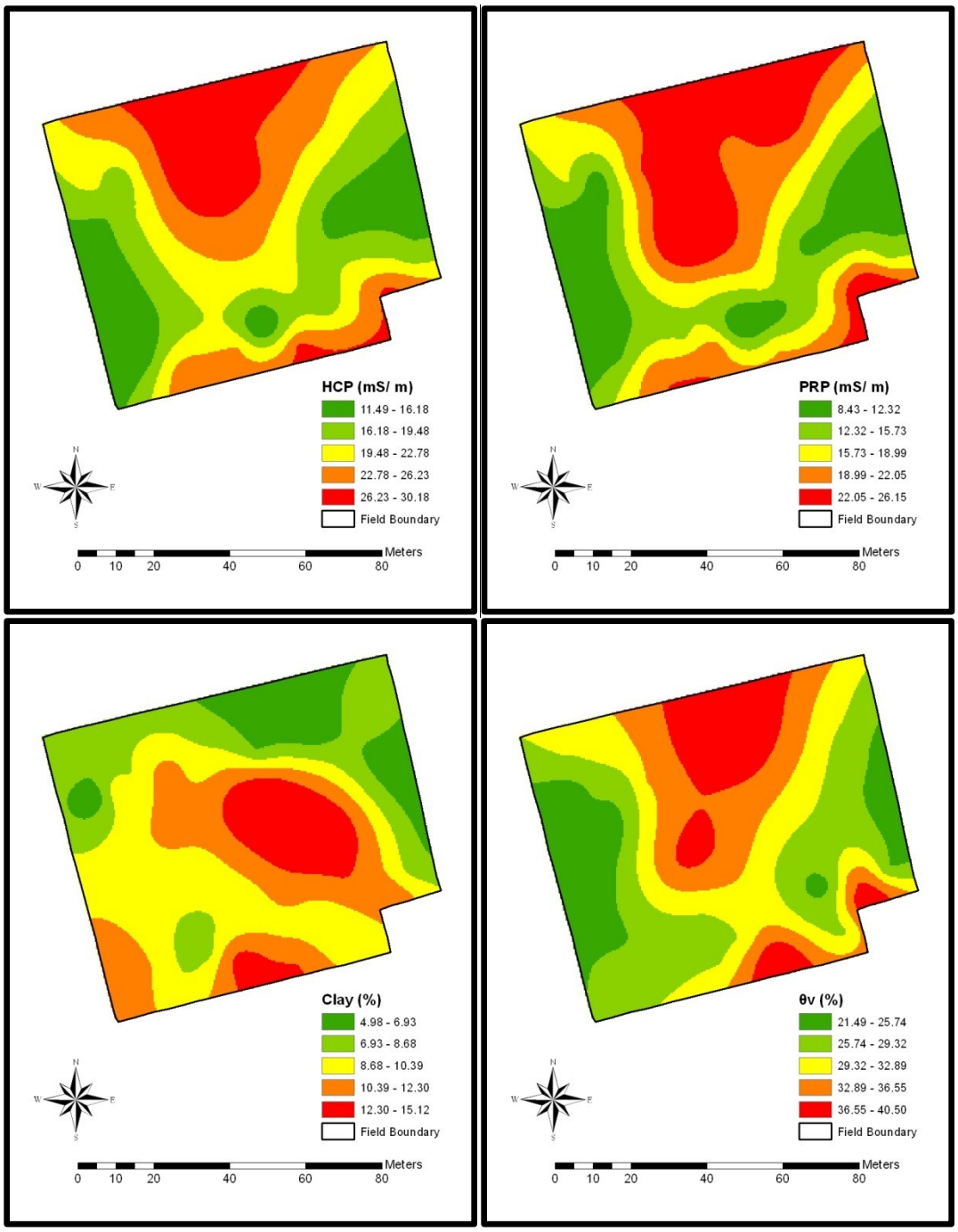

Figure 4-11 Maps of HCP, PRP, clay and θ_v for Boulden Site

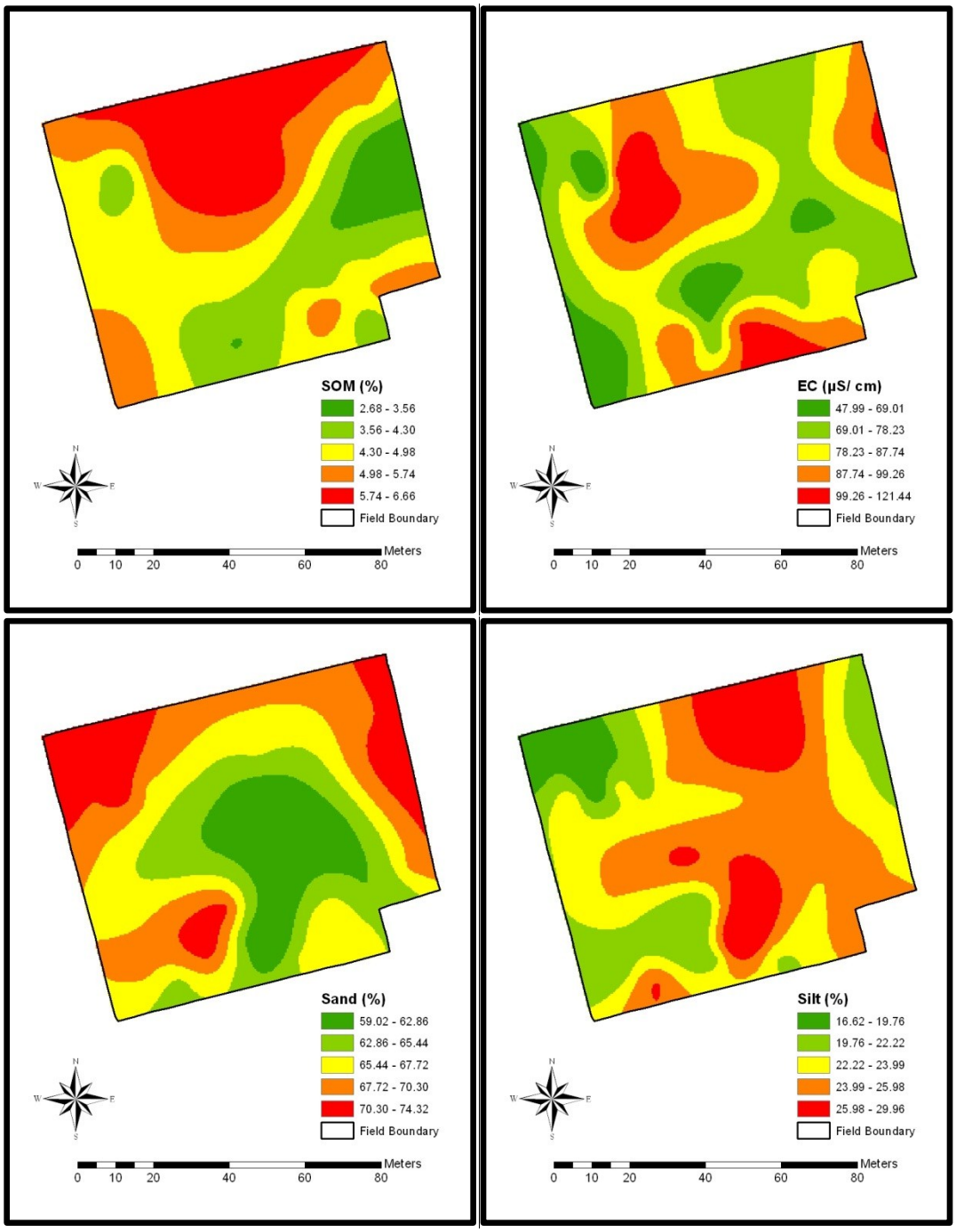

Figure 4-12 Maps of SOM, EC, sand and silt for Boulden Site

4.5 Conclusion

The procedure of measuring EC_a using DualEM provided the best relationship between EC_a and soil properties with the top 75 cm on a field. The EC_a can provide important information for characterizing soil properties. In this study, we compared soil physical

and chemical properties to EC_a during two years for four agricultural fields. We found that EC_a was significantly correlated to some soil properties (clay content, θ_v, SOM, and EC). Most regressions were significantly improved using a cubic term in EC_a, when using EC_a to predict soil properties. Approximately 60-90% of the variation in clay for the 45 to 75 cm depth could be predicted using EC_a. Regression models were validated with soil sample data set (n = 20). Soil properties were similar between measured and predicted soil properties.

This study showed that while soil properties varied greatly by depth, EC_a were significantly correlated with soil properties, especially some physical properties that impact crop yield. It was concluded that EC_a has the ability to serve as a soil quality indicator for soil productivity.

CHAPTER 5 ESTIMATION OF LAYERED SOIL PROPERTIES

5.1 Introduction

EMI is a method that measures the EC_a by inducing an electric current in the soil (Saey et al., 2009). EC_a is controlled by a combination of soil properties, such as moisture content, concentration of dissolved electrolytes in the soil solution, and the quantity and composition of colloids (McNeill, 1980a). The main benefits of EMI are: (i) non-invasive and (ii) a rapid response. These properties have made EMI instruments very famous for the inventory of lateral variations in subsurface soil properties. Generally, EMI is most popularl in areas with a single dominant factor of soil variability. Changes in EMI response can be directly related to variations in the dominant property (Doolittle and Collins, 1998).

Previous studies linked the EC_a to the depth and thickness of soil horizons (Doolittle et al., 1994; Bork et al., 1998; Inman et al., 2002; Saey et al., 2008), soil moisture content (Brevik et al., 2006; Huth and Poulton, 2007), clay content (McBratney et al., 2005; Triantafilis and Lesch, 2005), and soil salinity (Lesch et al., 1998; Amezketa, 2006, 2007). In all of these investigations, single coil spacing was used to develop a relationship between the property of interest and EC_a. The depth of investigation in EMI is measured by the coil spacing, coil orientation and frequency of the induced current (Gebbers et al., 2007). Most of the EMI instruments have a fixed frequency, the only option to measure the depth of investigation is coil orientation and coil spacing. Therefore, co-localized instruments attributed to multiple coil spacing or coil orientations provide more information in depth (Saey et al., 2009). Triantafilis et al. (2003) utilized the ratio between EC_a measurements of EM31 and EM38 instruments, which vary in coil spacing and frequency, to conclude a subsurface clay layer underlying sandier sediments

in a previous stream channel. Less research has been done to utilize the possibilities of the DualEM geo-conductivity sensors. Mostly, these have multiple coil spacing and multiple coil orientations, providing simultaneous measurements with different depth sensitivity (Saey et al., 2009).

It was observed during the soil sampling there was a compact gravel layer below the soil surface in selected wild blueberry fields. It was also found that the compaction of gravels was gradually increased as the sampling depth increased. Wild blueberries develop best in acidic, infertile and well drained soils. Soil textures vary from sandy to very coarse gravelly material (Eaton and Jensen, 1996). Soil erosion in blueberry fields occurs as a result of rainfall and runoff water moving fine soil particles away from blueberry plants and depositing them in lower areas of the field, causing the appearance of increased amount of gravels (Eaton and Jensen, 1996). Due to continuous erosion, the gravel layer reaches near to soil surface until the blueberry rhizomes and roots exposes to air. After exposing, blueberry roots and rhizomes quickly wither and die. The phenomenon is most evident in Nova Scotia and Maine. In order to estimate the interface to these gravels, the soils at blueberry sites were considered as two layer (i.e., the first layer was above the gravel formation and the second was underlying the first one). Similarly, two layer soils was assumed and considered at BEEC and Boulden site with respect to water table. In this case, the first layer was the unsaturated zone above the water table and the second layer was the saturated zone below the water table. The objective of this chapter was to characterize the depth to the interface between two contrasting soil layers with the help of EMI.

5.2 Materials and Methods

5.2.1 Study Sites and their Geology

The research sites were located in central Nova Scotia, Canada. The soil at both the North River and Carmel Sites is classified as sandy loam (Orthic Humo-Ferric Podzols), which is a well-drained acidic soil. These acidic soils, known as "Truro 52", are mostly found in the Colchester County of Nova Scotia, Canada (Webb et al, 1991). These soils have developed on fine sandy glaciofluvial sediments. They are found on level to strong slopes (0-30%). They are non-stony to slightly stony, and non-rocky. These soils have 50-80 cm of friable, coarse loamy, soil over loose, fine sandy lower soil material. The soil at BEEC Site consists of "Debert 22" and "Pugwash 82" soil groups (Webb and Langille, 1996). Debert 22 soils have 20-50 cm of friable, coarse loamy soil over firm, coarse loamy, lower soil material. They are imperfectly drained and are found on very gentle slopes (2-5%). Pugwash 82 soils are well drained and have greater than 80 cm of friable, coarse loamy, soil over firm, coarse loamy, lower soil material. These are also found on very gentle slopes. The soil at Boulden Site is of "Debert 52" soil group (Webb et al., 1991). These soils have 50-80 cm of friable, coarse loamy, soil over firm, coarse loamy, lower soil material. They are also imperfectly drained and are found on level to very gentle slopes (0-5%).

5.2.2 Cumulative Depth Response of EMI Sensors

For the DualEM-2, the cumulative response of a layered medium up to a depth z (m) below the sensor was given by Wait (1962) and McNeill (1980b), for the horizontal [$R_h(z)$] and perpendicular [$R_p(z)$] modes:

$$R_h(z) = 1 - \left[4\frac{z^2}{s^2} + 1\right]^{-0.5} \qquad (1)$$

$$R_p(z) = 2\frac{z}{s}\left[4\frac{z^2}{s^2} + 1\right]^{-0.5} \qquad (2)$$

with s being the transmitter-receiver spacing. Two different cumulative depth response profiles were established based on the different spacing between the transmitter and receiver coils.

The cumulative response relative to an increase in z of the two coil configurations (horizontal [R_h] and perpendicular [R_p]) of the DualEM-2 was developed (Figure 5-1). The general shape of all cumulative sensitivity distributions as developed by Callegary et al. (2007) was similar to that predicted by McNeill (1980a), especially at deeper depths. Under electrically conductive conditions, lower cumulative responses were detected by Callegary et al. (2007) than McNeill (1980a), especially at deeper depths. Therefore, the models expressed by McNeill (1980a) gave a truthful representation of the depth to the interface at a shallow depth between two layers.

Based on the exponential form of the cumulative response curves, the depth of exploration (DOE) can be described as the depth where 70% of the response is attained from the soil volume above this depth. This DOE increases for the various coil configurations: PRP, 1 m and HCP, 3.18 m (Figure 5-1).

5.3 Results and Discussion

5.3.1 EMI Survey

The summary statistics of the DualEM-2 EC_a measurements recorded at the study sites are provided (Table 5-1). The means of the EC_a values recorded with coil configurations that gave a larger weight to deeper soil layers were the largest: HCP > PRP. The CV of these signals was smaller at BEEC and Boulden Sites. This designates

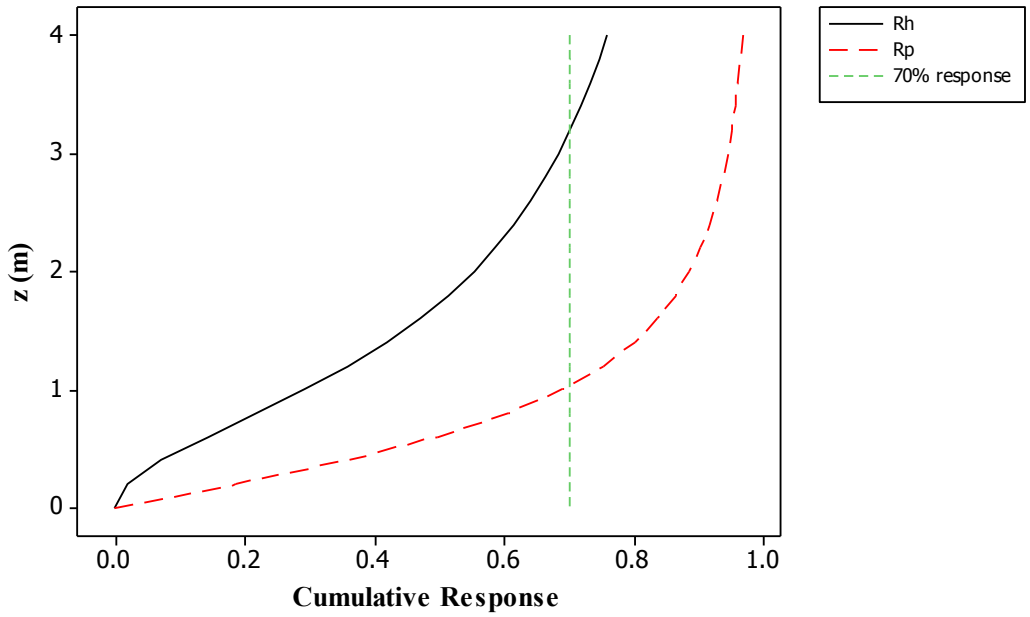

Figure 5-1 Cumulative response as a function of the depth z for the DualEM-2 in the 2.1-m perpendicular and 2-m horizontal configurations

that at these sites, the subsoil can be considered more conductive and less heterogeneous than the top soil. While the CV of the EC_a was higher at North River and Carmel Sites directing that the subsoil can be more heterogeneous than the topsoil (Saey et al., 2009).

Table 5-1 Descriptive statistics of the EC_a for the different coil configurations of the DualEM-2

Site	Coil configuration	Min.	Max	Mean	CV (%)	Skewness	Kurtosis
North River	HCP	0.0	24	4.4	86	0.90	0.7
	PRP	0.0	24	3.4	86	1.50	3.5
Carmel	HCP	0.0	12	5.4	50	-0.20	-0.4
	PRP	0.0	11	2.9	57	0.30	0.1
BEEC	HCP	3.4	44	22.0	39	0.30	-0.6
	PRP	0.0	48	19.0	43	0.40	-0.6
Boulden	HCP	9.1	34	22.0	20	0.02	-0.4
	PRP	7.7	30	17.0	24	0.40	-0.2

5.3.2 DualEM-2

To calibrate HCP and PRP with the depth to the interface (z_{in}) between the upper layer material and gravel substrate, and unsaturated and saturated layers, manual measurements of gravel and water table depths were used. The locations for manual measurements were selected in such a way that both highest and lowest EC_a value areas within the fields were covered. The depth to the gravel was measured at 50 observation points in each of the North River and Carmel sites and the depth to water table was measured at 30 observation points in each of the BEEC and Boulden sites.

The relationship between the EC_a measurements and z_{in} observations was formed using the McNeill (1980b) cumulative response curves. The major assumptions of this model were a double-layered soil and a constant EC_a of the upper and lower layers throughout the field. The cumulative response from the upper soil and the gravel substrate in blueberry fields can be computed as $R(z_{in})$ and $1 - R(z_{in})$, respectively, for the horizontal and perpendicular arrays (Eqs. [1] and [2]). For every HCP and PRP measurement, the predicted z_{in} (z_{in}^*) can be determined by solving a system of non-linear equations. Therefore, a C++ program was, written in Microsoft Visual Studio 2010 (Microsoft, Redmond, WA, USA) software, used given the conductivity values of the upper layer ($EC_{a\ upper}$) and the gravel subsoil ($EC_{a\ gravel}$) at North River and Carmel sites; and the unsaturated ($EC_{a\ unsaturated}$) and saturated ($EC_{a\ saturated}$) layer at BEEC and Boulden sites:

$$HCP = [R_h (z_{in}^*)]\ EC_{a\ upper} + [1 - R_h(z_{in}^*)]\ EC_{a\ gravel} \quad (3)$$

$$PRP = [R_p (z_{in}^*)]\ EC_{a\ upper} + [1 - R_p(z_{in}^*)]\ EC_{a\ gravel} \quad (4)$$

$$HCP = [R_h (z_{in}^*)]\ EC_{a\ unsaturated} + [1 - R_h(z_{in}^*)]\ EC_{a\ saturated} \quad (5)$$

$$PRP = [R_p (z_{in}^*)]\ EC_{a\ unsaturated} + [1 - R_p(z_{in}^*)]\ EC_{a\ saturated} \quad (6)$$

To fit these theoretical relationships to the z_{in}-EC_a data, the sum of the squared differences between z_{in} and z_{in}^* was minimized:

$$\sum_{i=1}^{n}[z_{in} - z_{in}^*(i)]^2 = \min \qquad (7)$$

with n being the number of observations. The parameters $EC_{a\ upper}$, $EC_{a\ gravel}$, $EC_{a\ unsaturated}$ and $EC_{a\ saturated}$ were iteratively corrected to attain the smallest sum of the squared differences between z_{in} and z_{in}^*. The obtained values of $EC_{a\ upper}$ and $EC_{a\ gravel}$ at North River Sites were 35.5 and 2.1 mS m^{-1} and at Carmel Site, these were 25.6 and 13.1 mS m^{-1}, respectively. Similarly, the obtained values of $EC_{a\ unsaturated}$ and $EC_{a\ saturated}$ at BEEC Site were 62.8 and 4.4 mS m^{-1}, respectively and at Boulden site, 8.7 and 34.2 mS m^{-1}. So at each measurement point, HCP and PRP were related to z_{in}^* by using Eq. (1), (2), (3), (4), (5) and (6) as

$$\mathrm{HCP} = 35.5 - \frac{75.2}{\left(4z_{in}^{*2}+4\right)^{0.5}} \qquad \text{(North River Site)}$$

$$\mathrm{PRP} = 2.1 + \frac{66.6\ z}{\left(4z_{in}^{*2}+4.41\right)^{0.5}} \qquad \text{(North River Site)}$$

$$\mathrm{HCP} = 25.6 - \frac{77.4}{\left(4z_{in}^{*2}+4\right)^{0.5}} \qquad \text{(Carmel Site)}$$

$$\mathrm{PRP} = 13.1 - \frac{24.95\ z}{\left(4z_{in}^{*2}+4.41\right)^{0.5}} \qquad \text{(Carmel Site)}$$

$$\mathrm{HCP} = 62.8 - \frac{134.4}{\left(4z_{in}^{*2}+4\right)^{0.5}} \qquad \text{(BEEC Site)}$$

$$\mathrm{PRP} = 4.4 - \frac{116.5\ z}{\left(4z_{in}^{*2}+4.41\right)^{0.5}} \qquad \text{(BEEC Site)}$$

$$\mathrm{HCP} = 8.7 - \frac{85.8}{\left(4z_{in}^{*2}+4\right)^{0.5}} \qquad \text{(Boulden Site)}$$

$$\mathrm{PRP} = 34.2 - \frac{50.9\,z}{\left(4z_{in}^{*2}+4.41\right)^{0.5}} \qquad \text{(Boulden Site)}$$

This system was solved for z_{in}^{*} with C++ program.

An independent validation was accomplished to assess the predictive quality of this model. Two indicators were used as validation criteria: the mean error (ME) and the root mean square error (RMSE). The ME and RMSE were acquired from:

$$\mathrm{ME} = \frac{1}{n}\sum_{i=1}^{n}\left[z_{in}^{*}(i) - z_{in}(i)\right] \qquad (8)$$

$$\mathrm{RMSE} = \sqrt{\frac{\sum_{i=1}^{n}\left[z_{in}^{*}(i) - z_{in}(i)\right]^{2}}{n}} \qquad (9)$$

with n representing the total number of validation observations. The observed depths were compared with the model predictions (Figures 5-2 to 5-5). A strong correlation between predicted and measured depths and RMSE (0.27 m, North River Site; 0.2 m, Carmel Site; 0.4 m, BEEC Site; and 0.5 m, Boulden Site) showed that this procedure was good enough in predicting z_{in}^{*} in a very rapid and non-destructive way.

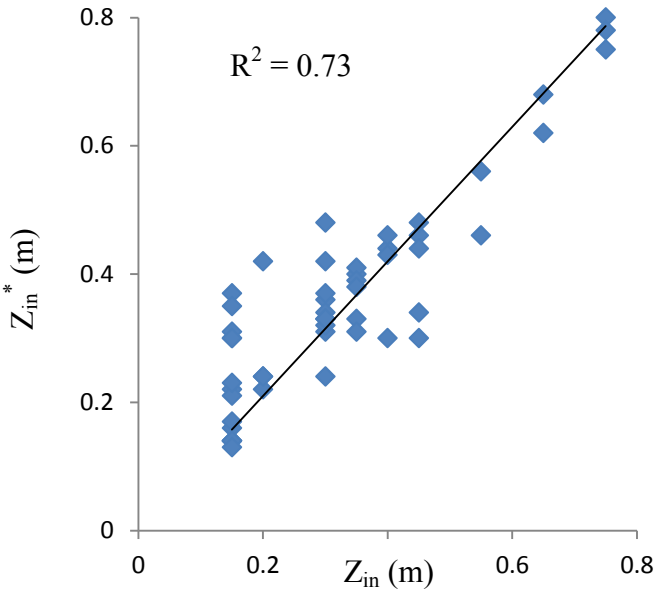

Figure 5-2 Scatter plot of predicted interface depth (z_{in}^*) vs. the measured depth (z_{in}) at North River Site

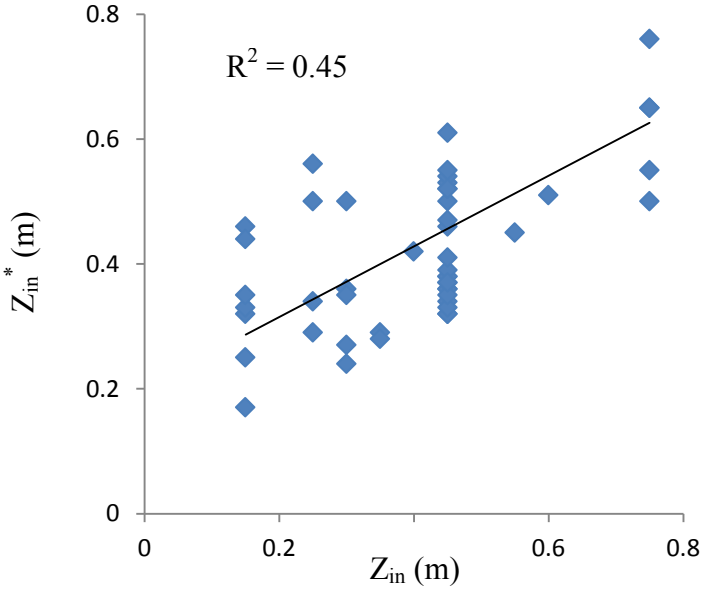

Figure 5-3 Scatter plot of predicted interface depth (z_{in}^*) vs. the measured depth (z_{in}) at Carmel Site

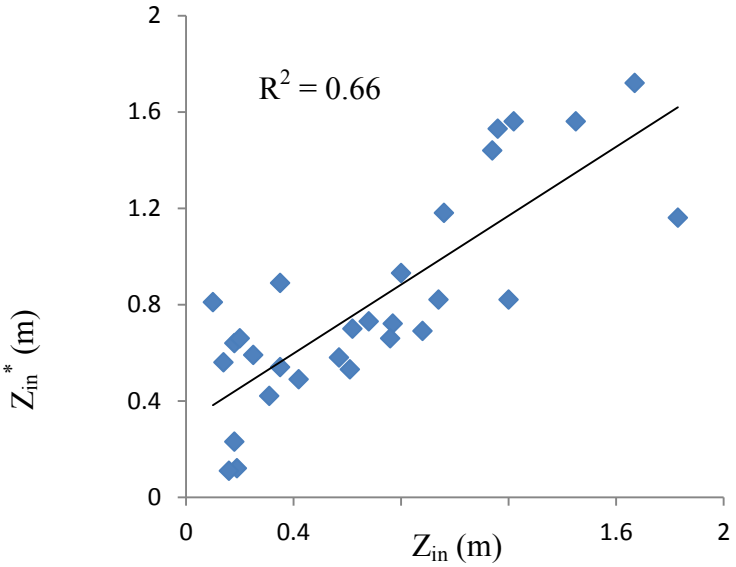

Figure 5-4 Scatter plot of predicted interface depth (z_{in}^*) vs. the measured depth (z_{in}) at BEEC Site

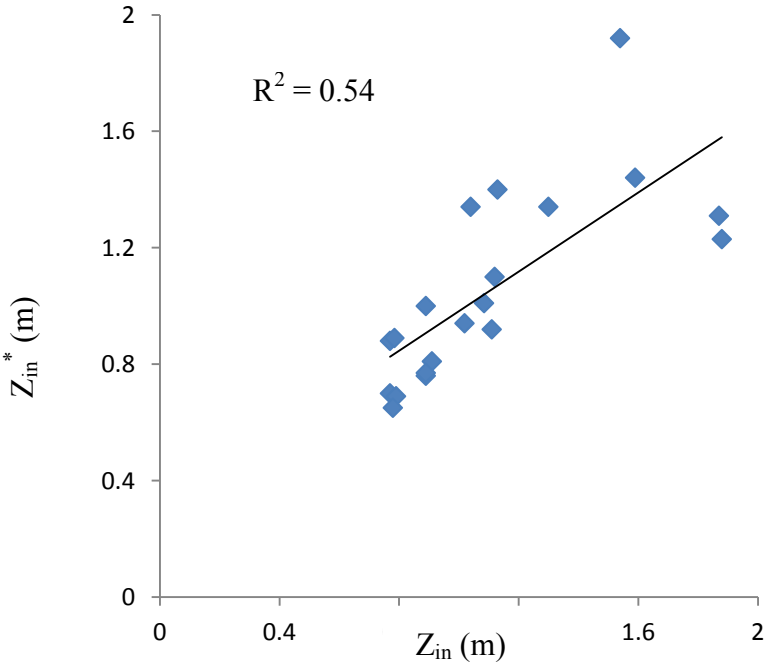

Figure 5-5 Scatter plot of predicted interface depth (z_{in}^*) vs. the measured depth (z_{in}) at Boulden Site

5.3.3 Construction of the Interface Depth

The predicted interface depths (z_{in}^{*}) as produced by the DualEM-2 procedure were interpolated using kriging. Depths to interface surfaces (Figures 5-6 to 5-9), exhibited a strong variability of the interface between the upper layer and gravel layers, and the unsaturated and saturated layers. For plants, gravel or crystalline rock layer is often indicative of the rooting limit (Shenk, 2008) and this information is significant for determining the shape of a root system (Ganatsas and Spanos, 2005; Shenk and Jackson, 2002), soil water availability and crop production potential. Therefore, it is important to detect the gravel layer in wild blueberry fields because if it is present in the root zone depth, it may affect and impede the rhizomes of the crop and may result in low yield due to less nutrient and moisture uptake through rhizomes (Eaton and Jensen, 1996). Microorganisms might also move from shallow gravel areas which also contribute to crop yield. As the gravel layer was more porous, the water after the rain may infiltrate very rapidly causing the plants in moisture stress. In this way, this gravel depth detection may be useful to improve wild blueberry production.

The shallow gravel layer was generally observed in the high elevation areas while the deeper gravel layer was found in flat areas and low elevation areas of the wild blueberry fields. It might be due to soil erosion from high to low elevation parts of the fields. Visual observations revealed that blueberry plants were less dense with grasses and weeds in some areas of the fields having the shallow (0 to 15 cm) gravel depth. Similar observations were also reported by Eaton and Jensen (1996). Maps of yield, grasses and bare spots of North River Site were displayed side by side for comparison. These maps showed shallow gravel depth affect the blueberry yield (Figures 5-9 and 5-10) because of

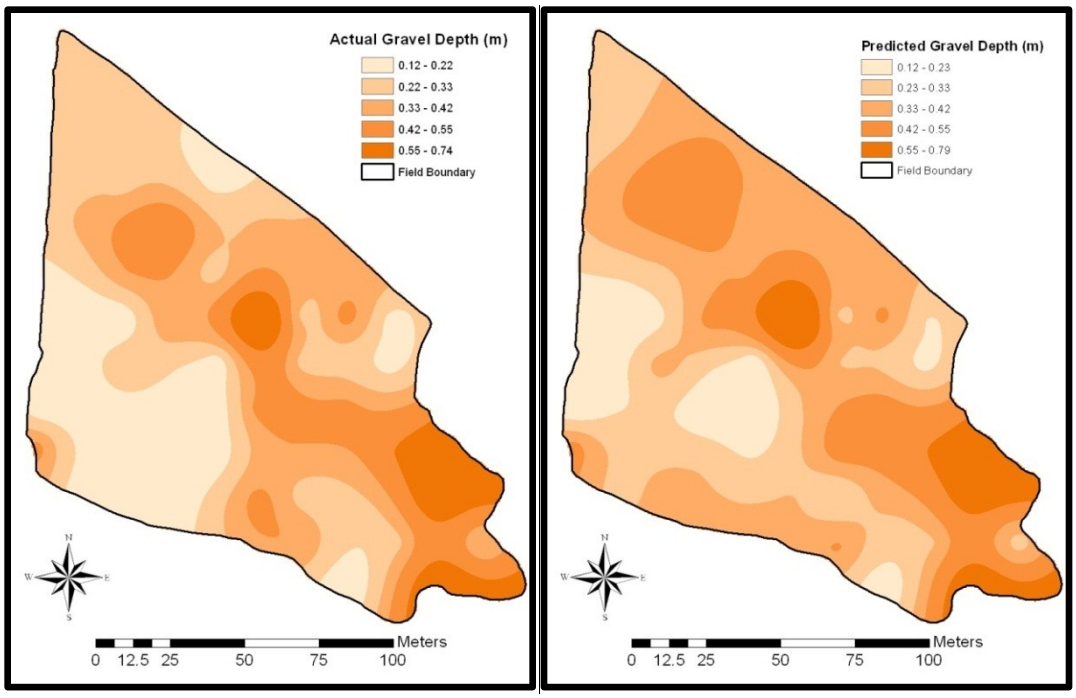

Figure 5-6 Interface depth predicted by the DualEM-2 at North River Site

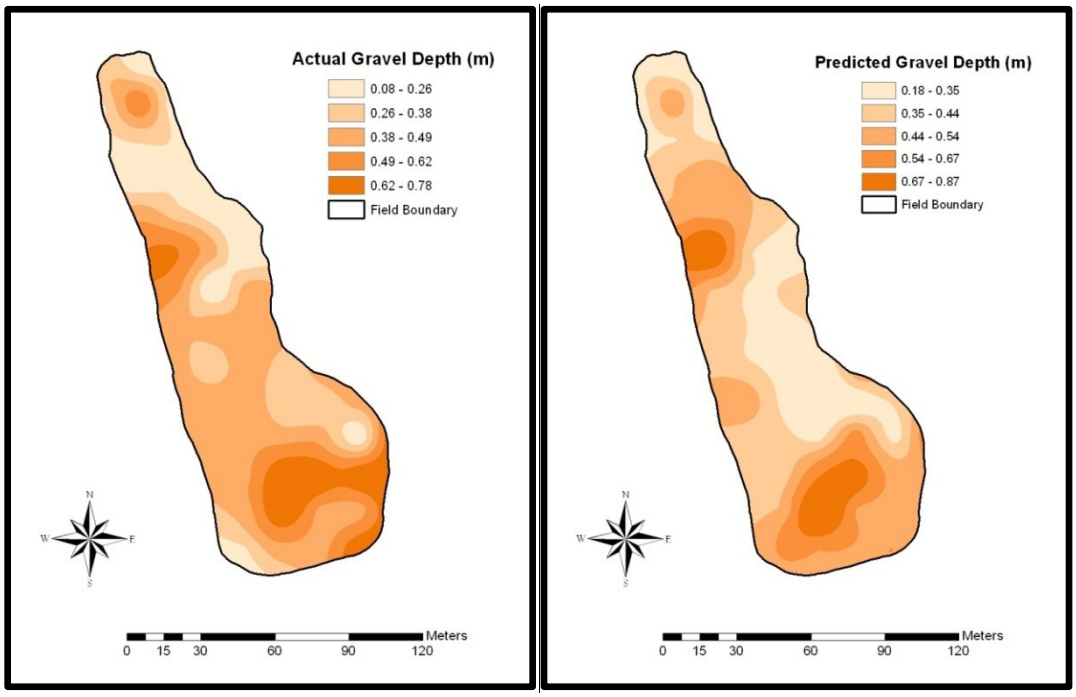

Figure 5-7 Interface depth predicted by the DualEM-2 at Carmel Site

the resistance to the root growth. It may cause fewer stems to flower and reduction in yield. Correlation coefficients also supported these maps. When the gravel layer reaches the soil surface due to soil erosion, develops the bare-spots. Gravel layer between 0-15

cm adversely affect fruit yield due to less density of plants within wild blueberry fields. The interpolated maps of actual and predicted gravel depths (Figures 5-6 and 5-7) showed substantial variation and almost similar patterns. The shallow gravel layer at North River site was found in southwest part of the field. The deeper gravel layer was observed in southeast and northwest region. The gravel depth maps at Carmel Site showed moderate variation. The shallow gravel layer was in north and center part of the field while deeper values were in south part of the field. The predicted WTD maps at BEEC and Boulden sites also indicated substantial variation in WTD. Actual and predicted maps were almost similar. The shallow WTD at BEEC Site was found in low lying areas (east and northeast region) of the field. Higher values of WTD were observed in high elevation areas (west and northwest region) of the field. Similar pattern was observed for Boulden Site with respect to elevation.

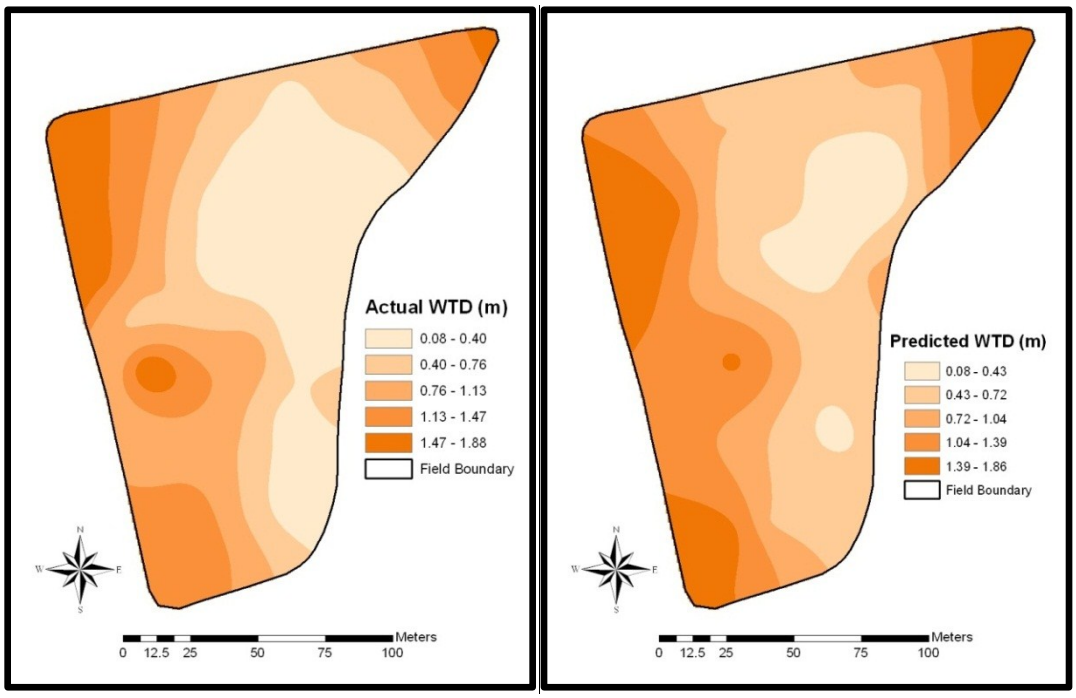

Figure 5-8 Interface depth predicted by the DualEM-2 at BEEC Site

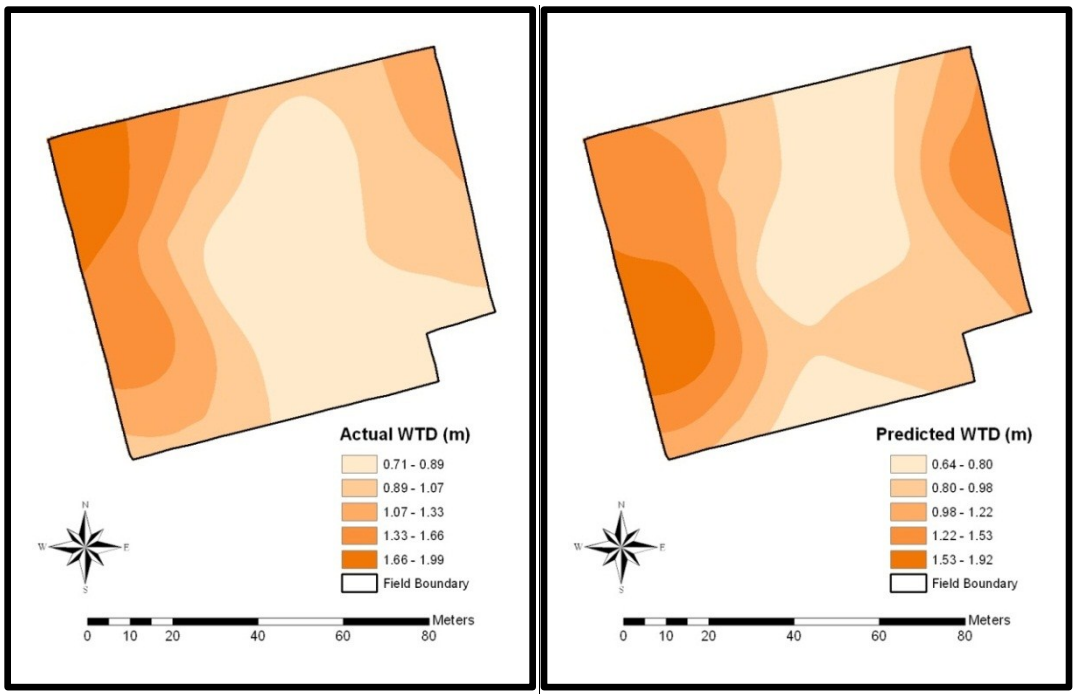

Figure 5-9 Interface depth predicted by the DualEM-2 at Boulden Site

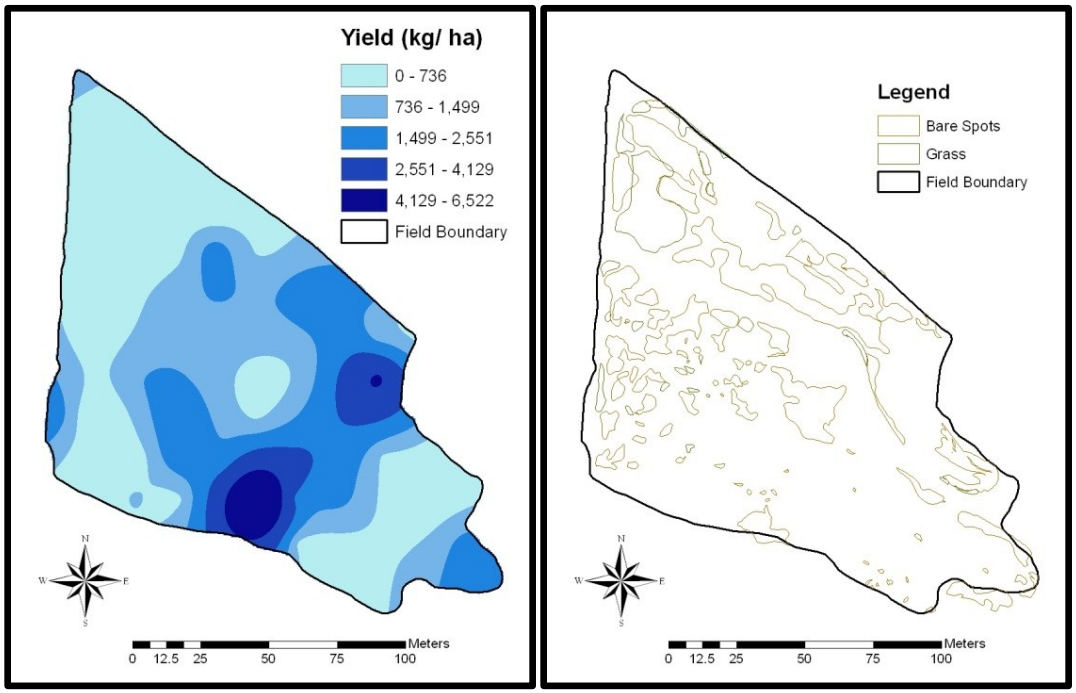

Figure 5-10 Yield, bare spots and grass maps of North River Site

5.4 Conclusion

The DualEM allowed prediction of depth to interface (z_{in}) in a two-layered soil in a rapid, effective and non-destructive manner. With the DualEM-2, a number of soil auger

observations are required to calibrate the EC_a measurements in respect to z_{in}. The quadruple-array EMI instruments like DualEM-21S would be better to estimate z_{in} because these sensors avoid the need for calibration augering and their rich information enables a quantification of z_{in} with a good predictive accuracy. Additionally, these may provide inventories of the spatial variability in top and subsoil conductivity.

In order to compute interface and water table depth within two-layered soil profile based on the theory of McNeill, (1980a), using the outputs of DualEM, this procedure was found efficient and rapid. It can also be used as real-time if some necessary modifications are made. Based on the results, it can be concluded that gravel layer in wild blueberry fields can be estimated and these may restrict infiltration influence the lateral movement of soil water and agrochemicals, and limit crop production if the gravels are present within root zone depth. In addition to other parameters that affect and contribute to blueberry yield, gravel layer is another important factor which can be considered along with various soil properties, fertilizers, herbicides, fungicides, etc. Mapping of variations in gravel layer and water table depths may be important components for crop production. EMI methods can provide large quantities of data in a relatively short period of time.

CHAPTER 6 ESTIMATION OF WATER TABLE DRAWDOWNS

6.1 Introduction

Large precipitation quantities not only produce extra flow in streams but also produce increases in soil moisture content, as well as rising groundwater tables, in areas not nearby to rivers or streams (Vazquez-Amábile and Engel, 2005). These influences are especially significant on flat areas, where the stream network is not always well defined and water surpluses are not quickly removed by runoff. These influences may create immediate damage. Rises in groundwater table can decrease the total yield of the watershed by lessening the farming area, influencing the growth process of the crops, and delaying or stopping field work (tillage, planting, and harvesting), and they can degrade the soil properties for the subsequent crop season (Pivot et al., 2002). Shallow water tables may affect growth due to inadequate aeration through the pores. The water table study can provide data on variation of the water table, the amount and path of movement of groundwater and a sign of water resources (Gundogdu and Degrimenci, 2006). In the long run, groundwater table rises may cause about soil salinization, depending on the groundwater quality. Salinization of soil and water is a mutual problem in arid and semiarid regions around the world (Ghassemi et al., 1995); its impact is felt in many agricultural provinces. Soil salinization reduces crop yields, increases runoff and soil erosion, and causes to desertification (Banin and Fish, 1995). Salinization pollutes surface water and groundwater supplies, limits irrigation, needs treatment for municipal and industrial uses, causes freshwater plants to be replaced by salt-tolerant ones, and influences recreational and commercial fisheries (Paine, 2003). Salt-affected land differs considerably spatially across the field and over the year in both levels of soil salinity and

water table depth (Bennett et al., 2009). Water table depths are nearest to the surface in winter and soil salinity levels are lowest at this time (Smith, 1962).

There have been studies on EC_a mapping as a tool for gauging the magnitude and spatial variability of soil salinity (Doolittle et al., 2001) and water table depths (Schumann and Zaman, 2003; Allred et al., 2005). A combination of topographic features and EMI data was used to map soil drainage classes (Kravchenko et al., 2002) and to define claypan soil management zones (Fraisse et al. 2001). Johnson et al. (2001) evaluated EC_a mapping for delineating soil physical and chemical properties. Kachanoski et al. (1988) observed significant correlation among spatial variation of soil water content, soil solution electrical conductivity and EC_a measured by EMI methods. Studies about the effects of shallow hydrology on EC_a are relatively limited. Sheets and Hendrickx (1995) documented a positive linear relationship between EC_a and moisture content. Khakural et al. (1998) found a positive linear relationship between EC_a and soil profile water storage. Sudduth et al. (2001) concluded that soil moisture need to be considered when using EC_a to estimate top soil depth. Therefore EC_a can be affected by shallow hydrologic conditions (Allred et al., 2005).

Specific field maps delineating water table depths can be utilized to support several field management systems. Different management zones can be developed on the basis of variation in EC_a, coupled with the geographic information system (GIS), for the site-specific application of suitable fertilization to reduce input costs and environmental impacts, and increase productivity. In general, EMI can provide spatially comprehensive information about soil texture, and temporally consistent monitoring of moisture,

nutrients, salinity and water table depths (Schumann and Zaman, 2003; Eigenberg et al., 2006).

Knowledge of water table depth is a critical element in several hydrological studies, including agricultural salinity management, landfill characterization, chemical seepage movement, and water supply studies (Buchanan and Triantafilis, 2009). Water table depth measurements are inherently expensive and time consuming, particularly during the installation process, which requires drilling a well. Consequently, the number of measurements that are available in a given area is often relatively sparse and does not reveal the actual level of variation that may be present.

The problem of sparse sampling data is not rare to water table studies. It is a subject that influences our capability to map the distribution of many natural resources where sampling is either costly or time consuming, including industrial pollutants and aquifer and soil properties (Buchanan and Triantafilis, 2009). Increasingly, researchers are dealing the issue by relating an inexpensive, high resolution ancillary data set to a limited set of calibration measurements. Using statistical techniques, it is then feasible to make high-resolution forecast of the property of interest.

Today, there are numerous sources of relatively inexpensive ancillary data that might be helpful in predicting the water table depth. EMI techniques have been used widely in hydrological investigations but not generally as a direct predictor of water table depth. It is used more commonly to detect associated processes, such as deep drainage (Triantafilis et al., 2003, 2004), unsaturated flow characteristics (Scanlon et al., 1999), and recharge (Cook et al., 1992). The objective of this chapter was to test the DualEM-2 for estimating

the water table depths rapidly and assessing the variation in EC_a readings recorded by the DualEM-2 affected due to the fluctuations of water table levels.

6.2 Materials and Methods

6.2.1 Study Area

Two fields were selected (soybean-barley rotation and pasture) in central Nova Scotia, Canada to predict the water table depths in a non-destructive manner using EMI method. The soybean-barley field (Figure 6-1) was located at BEEC Site (2.78 ha; 45.38^{o}N, 63.23^{o}W) and the pasture field (Figure 6-2) was at the Boulden Site (0.76 ha; 45.37^{o}N, 63.25^{o}W). Both fields had tile drainage system. Soybean and barley were grown at BEEC in 2010 and 2011, respectively. Small cages were installed in Boulden Field for other on-going experiment (Figure 6-2). The soil at BEEC Site is classified as coarse loamy, but half of this is an imperfect drained acidic soil, commonly known as "Debert 22" while a well-drained acidic soil exists on the other half of the site, commonly known as "Pugwash 82". The soil at Boulden site is also classified as coarse loamy which is an imperfect drained acidic soil, commonly known as "Debert 52" (Webb and Langille, 1996). The field boundary was mapped using Real time kinematics (RTK)-GPS (Topcon Positioning Systems Inc., Livermore, CA, USA).

6.2.2 Water Table Measurements

The EMI survey data, HCP and PRP, were utilized to develop an installation strategy of observation wells in BEEC Field. The gaussian models of semivariogram were found to best fit the HCP and PRP data. The grid size to install wells was then established on the basis of the range of influence from semivariogram which was found to be around

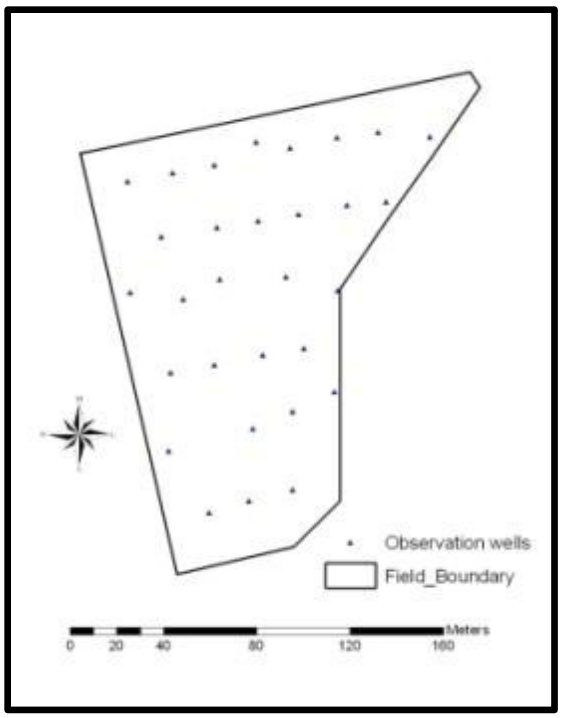

Figure 6-1 Field layout of BEEC Field, showing location of 30 observation wells and field boundary

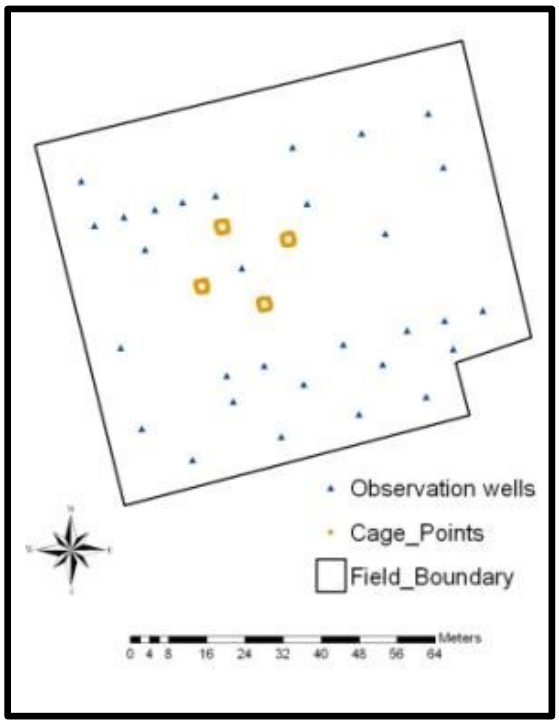

Figure 6-2 Field layout of Boulden Field, showing location of 30 observation wells and field boundary

50 m for BEEC Field (Figure 4-7). The grid pattern for sampling is one third or half of the range of influence (Kerry and Oliver, 2003). Therefore, a grid size of 20 x 20 m was set for installing wells at BEEC field. The wells were installed as an irregular grid at Boulden Field because it was very small field. i.e. almost one fourth of BEEC Field. Schumann and Zaman, (2003) also installed the wells as an irregular grid in one field and as regular in the other. Thirty water table observation wells were installed using an earth auger (Andreas Stihl AG & Co., Waiblingen, Germany) in each field. Each well was divided into two sections and they were coupled using threading. The joint was around 30-40 cm below the soil surface (Figure 6-3). It was favorable during harvesting and other management practices of crop in the fields because only the upper section was removed before these operations and there was no need to install wells again in second year. A 5-cm diameter polyvinyl chloride (PVC) pipe, perforated with small holes in the lower section was installed, and its position was recorded using the RTK-GPS. The PVC wells had a nylon fabric filter material around the bottom end and a PVC end-cap over the top end of the pipe to prevent water or soil from entering.

Measurements of water table depths and EC_a were made from June to October, 2010 for three consecutive days after every significant rainfall event and then from May to October, 2011, one day before and three days after significant rainfall event to assess the rise and recession of water table levels. Three datasets were collected in each year. An acoustic water level sensor was used to measure water table depth (WTD) below soil surface.

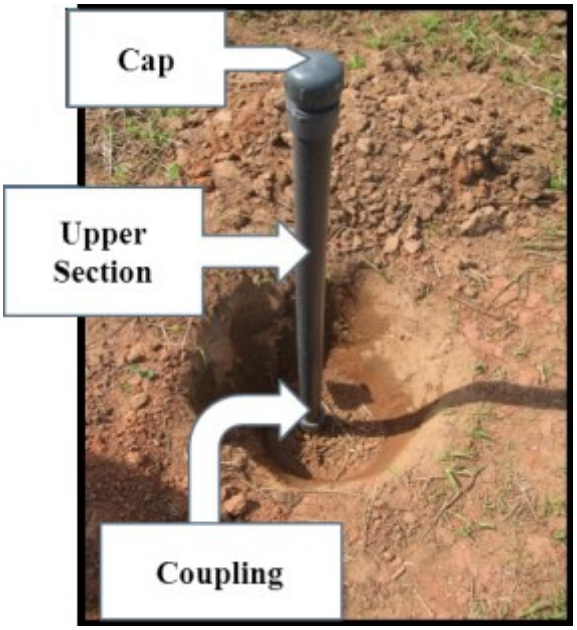

Figure 6-3 Installation of wells

6.2.3 Apparent Ground Conductivity Measurements

6.2.3.1 Manual Data Collection

EC_a measurements were collected manually at each well when WTD were measured after every significant rainfall for three consecutive days to visualize the recession of water table level simultaneously. A DualEM-2 (DualEM, Milton, Ontario, Canada) instrument was used to measure EC_a at ground level in both the horizontal coplanar (HCP) geometry and perpendicular (PRP) geometry (Figure 6-4). Five EC_a values were sampled and averaged at each well location.

6.2.3.2 EMI Surveys

Intensive EMI surveys were conducted at each field with the DualEM-2 instrument in 2010 and 2011. The instrument was hanged over the shoulders because the crop was tall during first year while during second year of study before sowing and after

Figure 6-4 Manual measurement of apparent ground conductivity at well location

harvesting of barley, comprehensive EC_a surveys were conducted in each field with the DualEM-2 instrument mounted on a sled behind an ATV at a speed of approximately 5 km hr^{-1}. The instrument was towed 5 m behind a four-wheel-drive vehicle equipped with a Garmin GPS18x LVC (Garmin International, Inc., Olathe, KS, USA) (Figure 6-5). Customized Windows software on a laptop computer was used to merge the ground conductivity (HCP and PRP) data with corresponding GPS position coordinates through RS232 ports, and these data were saved to the fixed hard disk. The HCP and PRP data were recorded automatically after every second during a survey. The lines of 5 m spacing were generated using ArcGIS 10 (ESRI, Redlands, CA) software and EMI surveys were guided by a RTK-GPS on those lines. At the end of each survey, WTD were measured manually in the field. These WTD were used to calibrate with the nearest HCP values collected during the survey, and the resulting calibration models were used to predict the WTD for each surveyed position in the field.

Figure 6-5 Automated DualEM Survey

6.3 Statistical Analysis

The data of 30 WTD of each field and the corresponding EC_a were analyzed by regression with Minitab 16 statistical software to obtain calibration models for predicting WTD using EC_a. Transformed, linear and logarithmic models of EC_a were evaluated to find the best-fitting models to predict WTD. The performance of these models was verified through the coefficient of determination (R^2) and root mean square error (RMSE). The RMSE represents the average deviation of actual WTD from the fitted regression model, in units of WTD (cm). The survey data files of HCP readings were imported into ArcGIS 10 software for mapping. The data surfaces were interpolated from the calculated WTD data using kriging. Means, minimums, maximums, skewness, kurtosis, standard deviations (SD) and coefficient of variations (CVs) of manually measured data for WTD and HCP were also calculated but it is not suitable to provide the spatial trend and, location of high and low values (Schumann and Zaman, 2003). Therefore, geo-statistical analysis was performed using GS+ Geostatistics using the

Environmental Sciences Version 9 software (Gamma Design Software, LLC, Woodhams St, Plainwell, MI) to characterize the WTD and EC_a. The semivariogram were produced for every WTD and EC_a data before and after rainfall to attain the degree of spatial variability between the observations.

6.4 Results and Discussion

The Anderson-Darling (A-D) normality test at a significance level of 5% using Minitab software (Farooque, 2010), of WTD and HCP data suggested that all parameters were normally distributed ($p>0.05$) except WTD of 2nd and 3rd data set in 2010 and 3rd data set in 2011 for BEEC site. WTD for all three data set were not normally distributed ($p<0.05$) for Boulden site in 2010 while in 2011, WTD measured on May 8th, June 16th, August 3rd and 4th were not normally distributed but all HCP data were normally distributed in both years. The reason for normal and non-normal distributions of some WTD data at both fields is unknown, but precipitation, temporal effects and management practices may be the real causes (Farooque et al., 2012).

The descriptive statistics for both BEEC and Boulden Sites for both years is reported in Tables 6-1 and 6-2. It is reported by Wilding (1985), if the CV < 15%, soil properties are least variable, 15 to 35% indicates moderate variability and CV > 35% suggests most variable. Summary statistics showed that both WTD and HCP had high CVs showing high variability at BEEC Site. The WTD data were moderate to highly variable at Boulden Site in both years while the HCP data were moderately and least variable in 2010 and 2011, respectively. Mean values of WTD were observed lower in 2010 for BEEC Site as compared in 2011. This may be due to more precipitation (heavy rainfall) in 2010 (Figure 6-6). In Boulden Field, mean WTD were observed higher in 2010 in

comparison with 2011 mean WTD data. Sophocleous (1991) indicated that the water table fluctuations could be misleading if these fluctuations are confused with those resulting from pumping, drainage and other causes. The reason behind this may be that Boulden Field has control drainage system while BEEC field has no control drainage system. In this study, water collection data by drainage systems were not recorded.

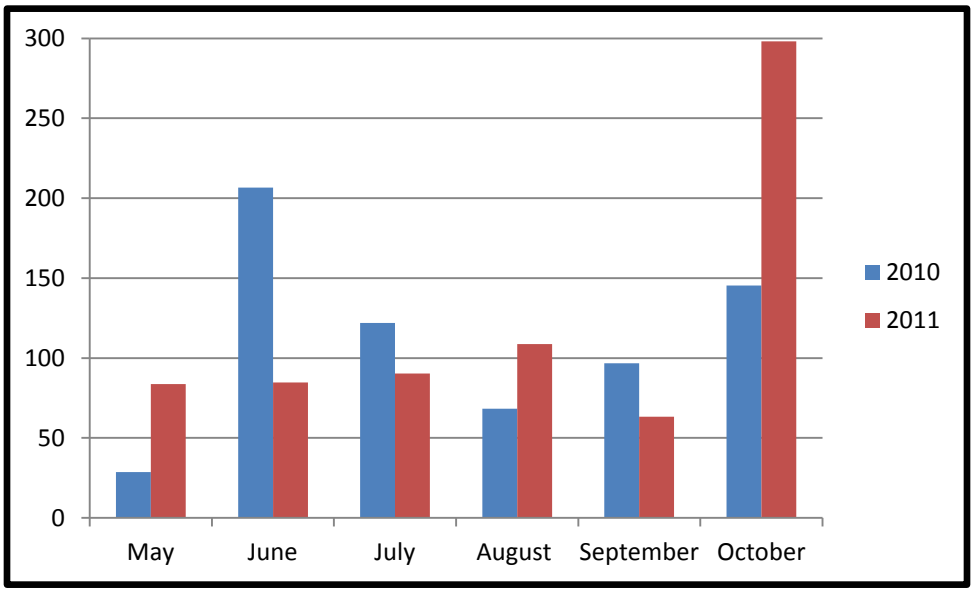

Figure 6-6 Total monthly precipitation (mm) during data collection period (Source: http://www.climate.weatheroffice.gc.ca/climateData/)

The HCP component was used to correlate with water table depth because of the greater sensitivity of this component in deeper layers of soil (Schumann and Zaman, 2003). Correlations between WTD and HCP in both fields were highly significant (BEEC: R2 = 0.76 to 0.93, Boulden: R2 = 0.58 to 0.85) (Tables 6-3 and 6-4). Data could only be collected from 29 wells in BEEC field for first and third data set because the

Table 6-1 Descriptive statistics for BEEC and Boulden fields (2010)

Field	Variables	Date	Min.	Max.	Mean	CV (%)	Skewness
BEEC	WTD from ground surface (cm)	Jun 29[a]	10.0	183.0	68.9	69.8	0.7
		Jun 30	17.0	193.0	78.2	60.2	0.7
		Jul 01	20.0	196.0	82.5	55.6	0.7
		Jul 13[b]	1.0	130.5	37.6	96.4	1.3
		Jul 14	8.5	147.5	49.1	73.2	1.2
		Jul 15	12.0	159.0	57.1	63.3	1.1
		Oct 17[c]	3.0	172.0	58.0	93.5	0.9
		Oct 18	9.0	182.0	69.3	74.7	0.8
		Oct 19	19.0	193.0	79.3	61.8	0.8
	HCP (mS/m)	Jun 29[a]	7.7	39.8	24.0	40.5	0.1
		Jun 30	6.6	38.4	20.8	43.3	0.5
		Jul 01	6.4	37.9	18.8	45.1	0.6
		Jul 13[b]	7.6	41.5	23.9	43.6	0.1
		Jul 14	7.2	40.4	20.3	48.7	0.6
		Jul 15	6.5	38.8	17.6	50.2	0.8
		Oct 17[c]	6.9	42.4	23.4	43.5	0.2
		Oct 18	6.5	40.9	21.8	47.0	0.4
		Oct 19	6.1	38.7	21.0	47.6	0.2
Boulden	WTD from ground surface (cm)	Jun 29[a]	77.0	188.0	110.8	31.9	1.2
		Jun 30	83.0	189.0	115.7	29.1	1.2
		Jul 01	84.5	192.0	119.6	27.4	1.2
		Jul 13[b]	1.0	172.0	61.0	83.3	1.1
		Jul 14	25.5	174.5	76.3	59.7	1.1
		Jul 15	49.0	178.0	92.4	42.4	1.0
		Oct 17[c]	90.0	222.0	131.2	32.8	1.0
		Oct 18	91.0	223.0	138.2	29.1	1.0
		Oct 19	97.0	224.0	143.6	26.7	1.0
	HCP (mS/m)	Jun 29[a]	13.0	28.4	21.6	21.6	-0.3
		Jun 30	12.3	28.0	20.1	23.0	-0.1
		Jul 01	11.1	25.7	18.3	22.9	-0.1
		Jul 13[b]	15.7	32.3	24.4	19.6	-0.1
		Jul 14	14.4	30.5	22.2	18.6	-0.3
		Jul 15	13.2	28.6	20.7	20.2	-0.2
		Oct 17[c]	13.6	33.1	23.1	21.6	0.0
		Oct 18	12.5	32.4	21.6	23.1	0.4
		Oct 19	11.7	31.2	20.0	21.8	0.6

a, 39.2 mm precipitation; b, 42.4 mm precipitation; c, 44.7 mm precipitation

Table 6-2 Descriptive statistics for BEEC and Boulden fields (2011)

Field	Variables	Date	Rain	Min.	Max.	Mean	CV (%)	Skewness
BEEC	WTD from ground surface (cm)	May 08	Before[a]	27.9	209.4	106.5	50.9	0.3
		May 10	After	16.2	208.0	94.6	61.5	0.3
		May 11	After	22.2	209.0	99.8	55.8	0.3
		May 12	After	25.3	209.4	104.6	51.8	0.3
		Jun 14	Before[b]	48.8	210.4	113.4	44.0	0.4
		Jun 16	After	26.7	194.4	97.8	51.9	0.4
		Jun 17	After	39.1	199.3	104.7	46.9	0.4
		Jun 18	After	45.5	208.2	111.4	45.4	0.4
		Aug 01	Before[c]	31.6	187.2	88.3	54.8	0.7
		Aug 03	After	0.0	178.4	63.7	88.0	0.8
		Aug 04	After	13.7	180.2	76.0	68.0	0.7
		Aug 05	After	28.4	184.4	85.5	56.8	0.6
	HCP (mS/m)	May 08	Before[a]	5.8	35.7	20.0	45.4	0.2
		May 10	After	7.1	37.5	21.5	42.4	0.2
		May 11	After	6.6	36.8	21.0	42.9	0.2
		May 12	After	6.4	36.5	20.3	43.9	0.2
		Jun 14	Before[b]	6.5	33.7	19.7	41.2	0.2
		Jun 16	After	7.1	35.6	21.2	40.2	0.2
		Jun 17	After	6.8	34.8	21.0	39.2	0.2
		Jun 18	After	6.4	34.2	19.9	41.3	0.2
		Aug 01	Before[c]	8.4	42.7	23.7	42.9	0.2
		Aug 03	After	10.3	43.4	24.8	40.5	0.3
		Aug 04	After	9.5	42.1	23.9	42.0	0.2
		Aug 05	After	8.4	41.8	23.0	43.3	0.2
Boulden	WTD from ground surface (cm)	May 08	Before[a]	36.5	119.0	65.8	34.4	1.1
		May 10	After	0.0	95.1	43.3	65.5	0.3
		May 11	After	17.0	98.0	53.3	45.3	0.4
		May 12	After	26.2	106.8	62.1	34.7	0.6
		Jun 14	Before[b]	31.1	124.3	73.0	34.6	0.6
		Jun 16	After	0.0	102.1	36.2	91.6	0.6
		Jun 17	After	0.0	112.2	52.0	62.8	0.2
		Jun 18	After	26.7	121.1	70.3	36.9	0.4
		Aug 01	Before[c]	14.6	95.5	50.3	47.6	0.4
		Aug 03	After	0.0	88.3	30.6	97.9	0.6
		Aug 04	After	7.0	91.3	40.9	64.0	0.5
		Aug 05	After	13.3	93.8	49.2	47.8	0.4
	HCP (mS/m)	May 08	Before[a]	14.9	25.3	20.2	13.5	0.1
		May 10	After	15.6	26.0	21.9	12.6	-0.5
		May 11	After	15.4	25.5	20.9	12.4	-0.1
		May 12	After	15.2	25.4	20.7	12.7	-0.1

a, 22.7 mm precipitation; b, 22.1 mm precipitation; c, 30.9 mm precipitation

Field	Variables	Date	Rain	Min.	Max.	Mean	CV (%)	Skewness
Boulden	HCP (mS/m)	Jun 14	Before[b]	14.9	26.2	19.4	13.8	0.6
		Jun 16	After	16.0	26.9	21.9	13.4	-0.3
		Jun 17	After	15.8	24.2	19.6	13.0	0.2
		Jun 18	After	15.1	22.5	18.7	11.8	0.1
		Aug 01	Before[c]	15.3	23.9	19.9	11.4	0.2
		Aug 03	After	16.6	24.7	21.9	11.0	-0.8
		Aug 04	After	15.0	24.6	20.3	11.8	-0.4
		Aug 05	After	14.3	23.4	19.4	11.2	-0.4

a, 22.7 mm precipitation; b, 22.1 mm precipitation; c, 30.9 mm precipitation

WTD was below than 195-cm depth of a well and this well was located at highest elevation of the field while the data were collected from all wells in Boulden field in 2010. In the next year, data were collected from 26 to 29 wells at BEEC site (Table 6-4) because of less precipitation and those wells were installed at high elevation areas but at Boulden site, there were only 27 wells (Table 6-4). A logarithmic regression resulted in a slightly better fit than a linear regression in both fields, probably due to non-linear response of the instrument as indicated by Schumann and Zaman (2003). The accuracy of the regression models to predict WTD in both fields was calculated by RMSE and ranged from 12.50 to 22.00 cm for BEEC field and 11.20 to 22.10 cm for Boulden field over different dates (Table 6-3; Figure 6-5 and Table 6-4; Figure 6-6). These RMSE values were less than the RMSE values found by Coulibaly et al., 2001; Daliakopoulos et al., 2005; Vasquez-Amabile and Engel, 2005; Krishna et al., 2008 and Sethi et al., 2010. Based upon the results of the study, EMI was considered reasonable considering that the technique has the enormous advantages of being non-destructive and very rapid response, and it could be used to assess the spatial trend of water table depth.

Table 6-3 Regression equations for predicting WTD from HCP (2010)

BEEC				
Date	Equation	n	R^2	RMSE (cm)
June 29	WTD = 357.1 – 215.2 log (HCP)	29	0.81	20.6
June 30	WTD = 363.4 – 223.4 log (HCP)	29	0.93	12.5
July 01	WTD = 333.4 – 204.2 log (HCP)	29	0.90	14.5
July 13	WTD = 235 – 148.3 log (HCP)	30	0.80	15.7
July 14	WTD = 229.3 – 143.5 log (HCP)	30	0.76	17.2
July 15	WTD = 226.3 – 141.9 log (HCP)	30	0.76	17.3
Oct 17	WTD = 378 – 241.8 log (HCP)	29	0.88	18.2
Oct 18	WTD = 345.1 – 214.4 log (HCP)	29	0.89	17.1
Oct 19	WTD = 316 – 186.9 log (HCP)	29	0.79	22.0
Boulden				
Date	Equation	n	R^2	RMSE (cm)
June 29	WTD = 528.8 – 315.8 log (HCP)	30	0.81	15.1
June 30	WTD = 479.3 – 281.5 log (HCP)	30	0.77	15.8
July 01	WTD = 469.5 – 279.8 log (HCP)	30	0.80	14.2
July 13	WTD = 789.6 – 528.5 log (HCP)	30	0.85	19.0
July 14	WTD = 731.7 – 489.3 log (HCP)	30	0.83	18.2
July 15	WTD = 568.2 – 364.1 log (HCP)	30	0.75	19.2
Oct 17	WTD = 634.6 – 372.1 log (HCP)	30	0.72	22.2
Oct 18	WTD = 572.9 – 328.4 log (HCP)	30	0.69	21.9
Oct 19	WTD = 580 – 337.8 log (HCP)	30	0.70	20.5

The R^2 range indicates that WTD account for 76 to 93% of EC_a variation in BEEC and 58 to 85% in Boulden Field. It suggested that factors other than WTD may have some effect on the EC_a of these fields and these other factors must be soil properties (Allred et al., 2005). It may also expected that with a low WTD, values of EC_a can be high or low based on moisture conditions in unsaturated soil above water table as described by Allred et al. (2005). HCP explained seventy-one percent of variation in WTD during the all six datasets in BEEC field ($n = 598$; $R^2 = 0.71$; $p < 0.01$) (Figure 6-7) while this variation was fifty-three percent in WTD in Boulden field ($n = 600$; $R^2 = 0.53$; $p < 0.01$) (Figure 6-8).

Table 6-4 Regression equations for predicting WTD from HCP (2011)

BEEC				
Date	Equation	n	R^2	RMSE (cm)
May 08	WTD = 379.2 – 218.2 log(HCP)	28	0.84	20.7
May 10	WTD = 432.3 – 262.0 log (HCP)	29	0.87	20.0
May 11	WTD = 402.3 – 237.0 log (HCP)	28	0.84	21.4
May 12	WTD = 392.9 – 228.7 log (HCP)	28	0.84	20.8
Jun 14	WTD = 406.8 – 234.0 log(HCP)	26	0.86	18.3
Jun 16	WTD = 403.8 – 237.9 log (HCP)	27	0.85	18.8
Jun 17	WTD = 413.6 – 240.3 log (HCP)	26	0.85	18.2
Jun 18	WTD = 407.3 – 234.8 log (HCP)	26	0.84	19.5
Aug 01	WTD = 380.9 – 219.7 log(HCP)	29	0.86	18.2
Aug 03	WTD = 435.3 – 273.8 log (HCP)	29	0.85	20.9
Aug 04	WTD = 401.1 – 243.2 log (HCP)	29	0.87	18.0
Aug 05	WTD = 374.6 – 219.4 log (HCP)	29	0.86	17.6
Boulden				
Date	Equation	n	R^2	RMSE (cm)
May 08	WTD = 476.6 – 315.6 log(HCP)	27	0.69	11.9
May 10	WTD = 596.1 – 413.3 log (HCP)	28	0.68	15.2
May 11	WTD = 526.8 – 359.4 log (HCP)	27	0.67	13.1
May 12	WTD = 479.0 – 317.9 log (HCP)	27	0.69	11.2
Jun 14	WTD = 501.2 – 333.4 log(HCP)	27	0.61	15.1
Jun 16	WTD = 688.2 – 487.6 log (HCP)	30	0.78	14.9
Jun 17	WTD = 693.2 – 497.9 log (HCP)	28	0.75	15.5
Jun 18	WTD = 614.1 – 428.8 log (HCP)	27	0.73	12.8
Aug 01	WTD = 554.5 – 389.3 log(HCP)	27	0.65	13.4
Aug 03	WTD = 709.1 – 507.3 log (HCP)	28	0.72	15.0
Aug 04	WTD = 555.6 – 394.5 log (HCP)	27	0.65	14.8
Aug 05	WTD = 506.7 – 356.0 log (HCP)	27	0.58	14.5

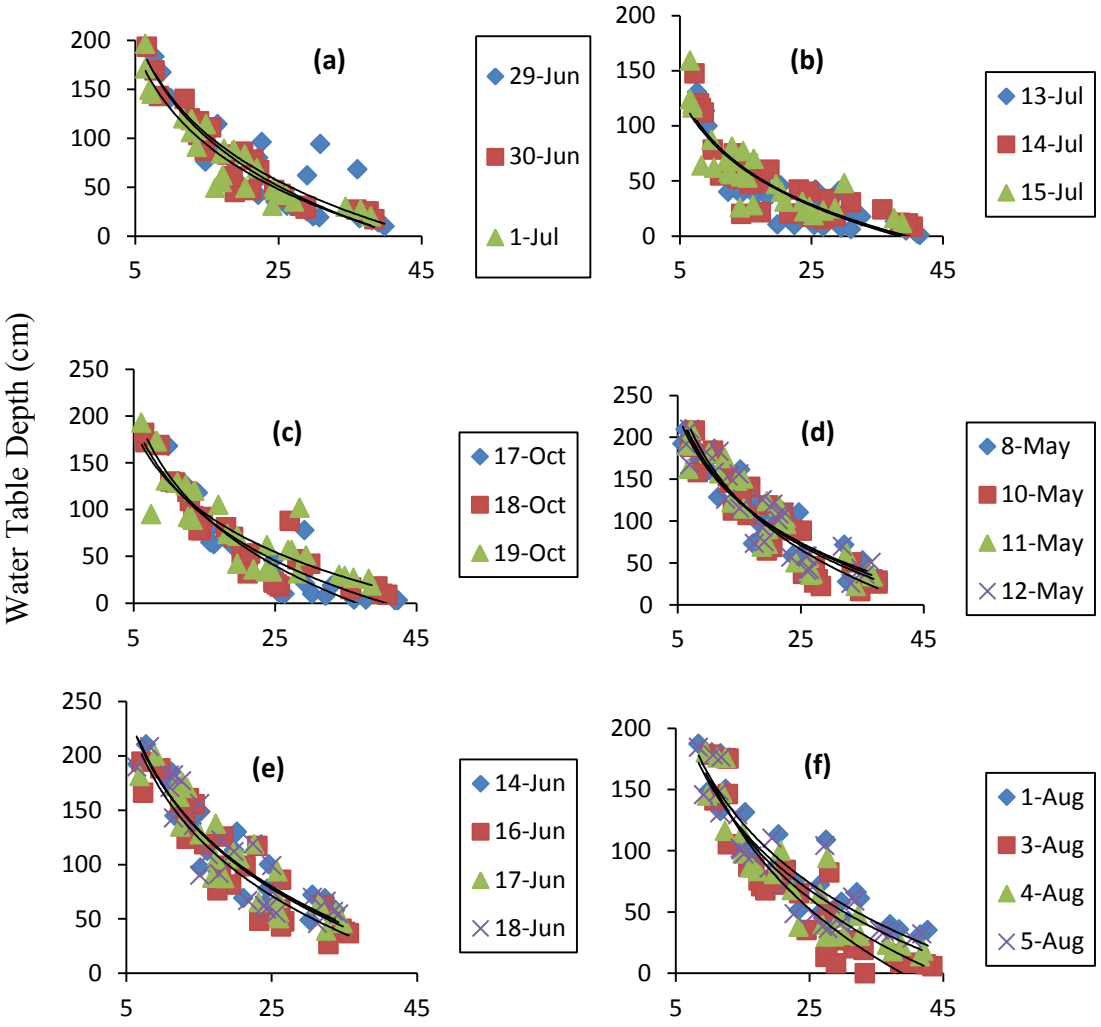

Figure 6-7 Regression curves developed for predicting water table depth from HCP (2010; a, b, c) and (2011; d, e, f) in the BEEC Field. Regression equations are in Tables 3 and 4.

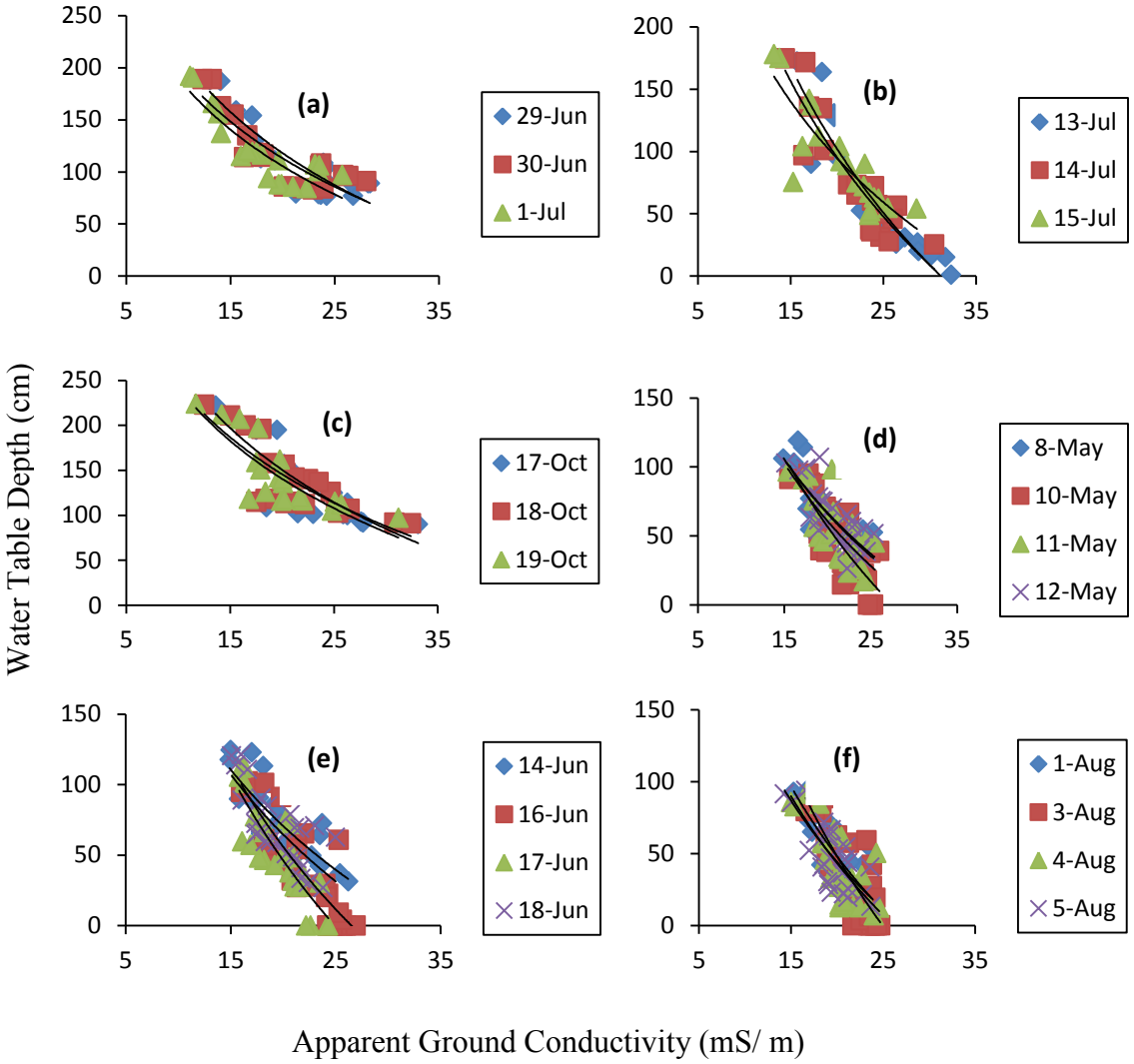

Figure 6-8 Regression curves developed for predicting water table depth from HCP (2010; a, b, c) and (2011; d, e, f) in the Boulden Field. Regression equations are in Tables 3 and 4.

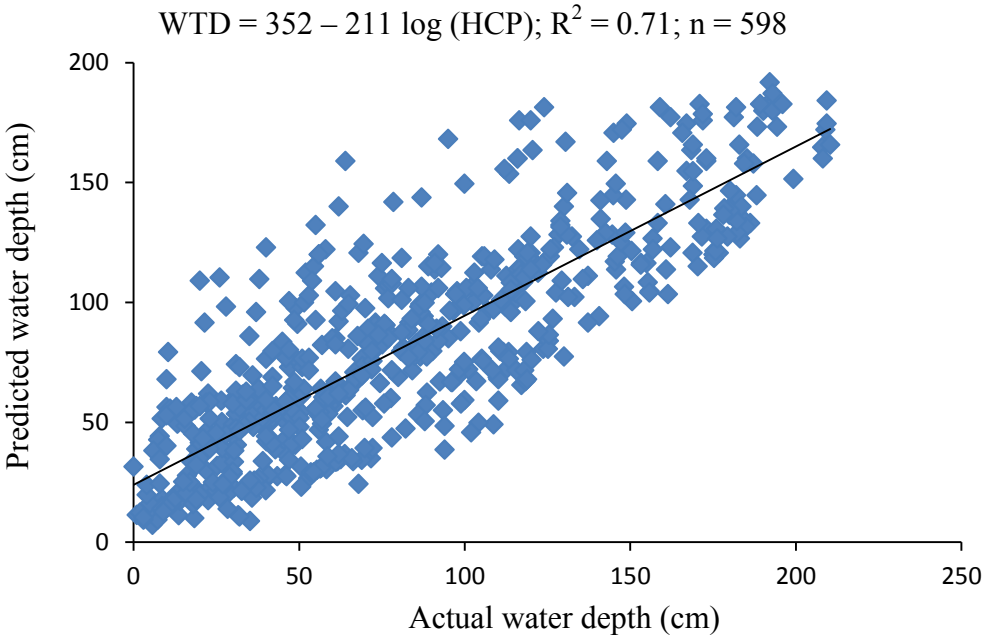

Figure 6-9 Validation of the regression model for DualEM-2 at BEEC Site

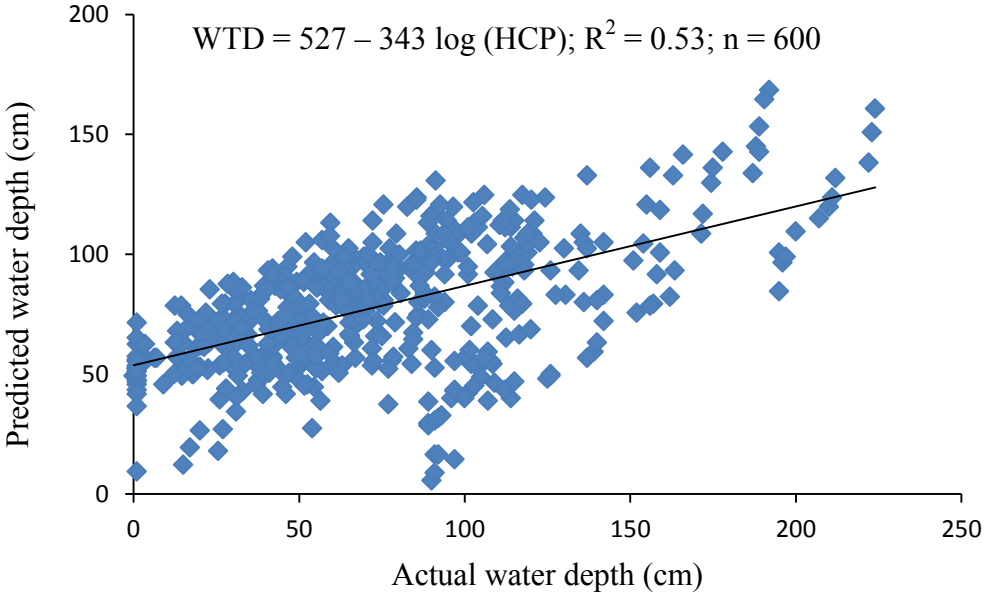

Figure 6-10 Validation of the regression model for DualEM-2 at Boulden Site

Geo-statistical analysis was performed to generate semivariogram in order to observe the spatial variation in WTD and HCP. In BEEC Site; gaussian, spherical and linear models were found best fit with the data (Tables 6-5 and 6-6). The best fitted

Table 6-5 Semivariogram of WTD and HCP (2010)

BEEC							
Parameter	Date	Nugget	Sill	Range (m)	Nugget Sill ratio	R^2	Model
WTD	June 29	640.0	4018	66.6	15.9	0.98	Gaussian
	June 30	408.0	3459	55.9	11.8	0.99	Gaussian
	July 01	28.0	3133	48.6	0.9	0.98	Gaussian
	July 13	1.0	2782	43.3	0.1	0.98	Gaussian
	July 14	180.0	2702	45.9	6.3	0.98	Gaussian
	July 15	132.0	2581	44.7	5.1	0.98	Gaussian
	Oct 17	40.0	2264	41.6	1.8	0.95	Gaussian
	Oct 18	1.0	2106	40.1	0.1	0.96	Gaussian
	Oct 19	1.0	2090	40.2	0.1	0.96	Gaussian
HCP	June 29	0.1	138	112.7	0.1	0.99	Spherical
	June 30	15.0	124	48.1	11.9	0.99	Gaussian
	July 01	10.0	121	46.5	8.2	0.98	Gaussian
	July 13	0.1	201	105.2	0.1	0.97	Linear
	July 14	4.5	153	52.8	2.9	0.96	Gaussian
	July 15	3.8	144	51.6	2.6	0.96	Gaussian
	Oct 17	0.1	201	143.5	0.1	0.98	Linear
	Oct 18	0.1	201	142.2	0.1	0.99	Linear
	Oct 19	0.1	161	154.0	0.1	0.98	Spherical
Boulden							
Parameter	Date	Nugget	Sill	Range (m)	Nugget Sill ratio	R^2	Model
WTD	June 29	33.00	1021	15.5	3.2	0.70	Gaussian
	June 30	1.00	898	31.8	0.1	0.66	Spherical
	July 01	1.00	871	12.9	0.1	0.62	Gaussian
	July 13	1.00	1992	16.3	0.1	0.80	Gaussian
	July 14	1.00	1724	17.2	0.1	0.82	Gaussian
	July 15	1.00	1189	15.8	0.1	0.79	Gaussian
	Oct 17	925.00	1961	62.9	47.2	0.16	Exponential
	Oct 18	1.00	1094	8.9	0.1	0.00	Spherical
	Oct 19	997.10	997	40.9	100.0	0.01	Linear
HCP	June 29	0.01	17	15.9	0.1	0.70	Gaussian
	June 30	0.01	17	19.0	0.1	0.51	Exponential
	July 01	0.01	21	56.5	0.1	0.85	Linear
	July 13	0.01	25	22.2	0.1	0.90	Gaussian
	July 14	0.01	20	20.1	0.1	0.72	Gaussian
	July 15	0.01	18	18.5	0.1	0.84	Gaussian
	Oct 17	17.30	19	40.9	89.6	0.02	Linear
	Oct 18	5.04	28	69.1	18.0	0.61	Spherical
	Oct 19	8.02	33	59.9	24.0	0.57	Gaussian

semivariogram models for Boulden Site were linear, gaussian, spherical and exponential. The semivariogram parameters (nugget, sill and range) describe the best spatial structure of variogram uses the R^2 to select the best model.

A variable has weak spatial dependency if the ratio is greater than 75%, moderate spatial dependency if the ratio is between 25 and 75%, and strong spatial dependency for a ratio less than 25% (Cambardella et al., 1994). Semivariogram of WTD and HCP in both years for BEEC Site indicated strong spatial dependence except 2nd data set of WTD in 2011 (Tables 6-5 and 6-6). Intrinsic soil properties such as texture, mineralogy and microorganisms may control strong spatial dependent variable. Semivariogram of WTD and HCP in 2010 and 2011 for Boulden Site indicated strong spatial dependency except for WTD on Oct 17th and 19th in 2010 and for HCP on Oct 17th, 2010 (Tables 6-5 and 6-6). Weak to moderate spatial dependent variables may be controlled by extrinsic properties such as weather conditions, topography and farming practices.

The semivariogram range of influence of WTD (40.10 to 125.7 m) and HCP (46.50 to 154.0 m) showed moderate variation within BEEC Field in both years (Tables 6-5 and 6-6) and these ranges were somewhat consistent during different time of observations. High variability was observed at Boulden Site for WTD and HCP in both years as the average range of influence for WTD was 20.74 m and 34 m, respectively (Tables 6-5 and 6-6).

Table 6-6 Semivariogram of WTD and HCP (2011)

BEEC							
Parameter	Date	Nugget	Sill	Range (m)	Nugget Sill ratio	R^2	Model
WTD	May 08	250.0	4930	125.7	5.07	0.96	Spherical
	May 10	1560.0	7230	76.7	21.58	0.94	Gaussian
	May 11	1360.0	5425	69.8	25.07	0.94	Gaussian
	May 12	180.0	4897	123.6	3.68	0.96	Spherical
	Jun 14	1281.0	3699	44.20	34.63	0.95	Gaussian
	Jun 16	1476.0	4211	63.0	35.05	0.89	Gaussian
	Jun 17	1374.0	3666	51.9	37.48	0.94	Gaussian
	Jun 18	1295.0	3723	45.0	34.78	0.95	Gaussian
	Aug 01	850.0	4810	76.1	17.67	0.96	Gaussian
	Aug 03	1310.0	6730	90.6	19.46	0.96	Gaussian
	Aug 04	1140.0	6390	91.5	17.84	0.94	Gaussian
	Aug 05	830.0	4770	75.1	17.40	0.96	Gaussian
HCP	May 08	5.9	125	57.1	4.72	0.98	Gaussian
	May 10	5.2	129	56.9	4.03	0.98	Gaussian
	May 11	5.1	128	57.8	3.98	0.98	Gaussian
	May 12	4.0	120	54.8	3.33	0.98	Gaussian
	Jun 14	2.2	110	54.5	1.99	0.97	Gaussian
	Jun 16	5.1	113	56.4	4.49	0.97	Gaussian
	Jun 17	5.1	109	55.0	4.65	0.97	Gaussian
	Jun 18	5.1	106	53.70	4.81	0.98	Gaussian
	Aug 01	6.1	162	58.1	3.76	0.98	Gaussian
	Aug 03	6.8	163	57.9	4.17	0.98	Gaussian
	Aug 04	7.7	162	58.4	4.73	0.98	Gaussian
	Aug 05	6.4	158	58.2	4.05	0.98	Gaussian
Boulden							
Parameter	Date	Nugget	Sill	Range (m)	Nugget Sill ratio	R^2	Model
WTD	May 08	0.10	254	17.4	0.04	0.97	Gaussian
	May 10	41.00	474	23.5	8.65	0.88	Gaussian
	May 11	15.30	317	17.4	4.82	0.89	Gaussian
	May 12	0.10	239	16.4	0.04	0.89	Gaussian
	Jun 14	0.10	314	15.3	0.03	0.86	Gaussian
	Jun 16	57.00	626	13.9	9.10	0.92	Gaussian
	Jun 17	1.00	513	12.1	0.19	0.68	Gaussian
	Jun 18	1.00	320	14.0	0.31	0.80	Gaussian
	Aug 01	11.10	306	16.2	3.62	0.90	Gaussian
	Aug 03	13.00	540	25.0	2.40	0.98	Gaussian
	Aug 04	8.00	401	24.0	1.99	0.97	Gaussian
	Aug 05	15.80	295	17.4	5.35	0.86	Gaussian

Parameter	Date	Nugget	Sill	Range (m)	Nugget Sill ratio	R^2	Model
HCP	May 08	1.22	19	29.4	6.37	0.86	Gaussian
	May 10	1.28	18	28.8	6.93	0.83	Gaussian
	May 11	2.12	20	33.5	10.50	0.84	Gaussian
	May 12	2.34	21	34.8	11.10	0.85	Gaussian
	Jun 14	0.01	21	66.5	0.05	0.92	Spherical
	Jun 16	0.86	18	20.5	4.64	0.92	Gaussian
	Jun 17	0.01	22	20.9	0.04	0.95	Gaussian
	Jun 18	0.72	22	21.9	3.14	0.96	Gaussian
	Aug 01	2.32	18	29.8	12.30	0.82	Gaussian
	Aug 03	2.85	21	33.0	13.50	0.79	Gaussian
	Aug 04	3.80	21	35.9	18.00	0.76	Gaussian
	Aug 05	3.66	22	36.7	16.30	0.81	Gaussian

Comprehensive EMI surveys were conducted in both fields. DualEM-2 survey collected 1022 geo-referenced HCP values, by walk, taking 28 min to complete the survey of 2.78 ha field. After interpolation, a continuous WTD surface was mapped for entire field (Figure 6-9). Interpolation process removed most of the erroneous data (Schumann and Zaman, 2003). WTD ranged from 10 to 160 cm on 1st July (Figure 6-9). The shallow WTD was observed in the north-east side of the field because this area has lower elevation and EC_a values were also higher in this region. The area located at high elevation zone showed higher values of WTD towards west in the maps. Most of the area had shallow WTD below than 100 cm. The WTD agree with the survey results but there are still some spatial variations in WTD (Figure 6-9), probably due to number of wells installed in the field and the area might not be well represented by the number of wells.

A comparison of the WTD map for BEEC field developed from the manual measurement of 30 wells (1st July; Figure 6-9) showed a high resolution for using EMI technique. Most of the within-soil type variation in WTD is lost due to the large separation between wells

during manual measurements where 30 wells were 20 m apart. In comparison, EMI provided a better than 3-m resolution.

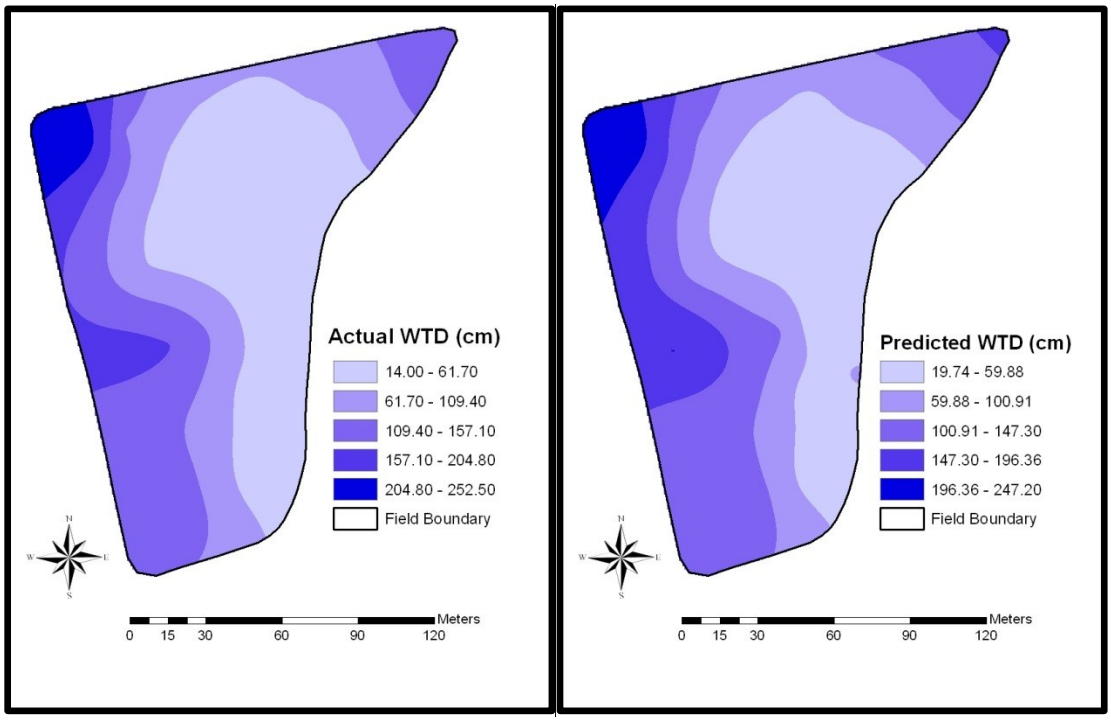

Figure 6-11 Interpolated water table depths in the BEEC Field

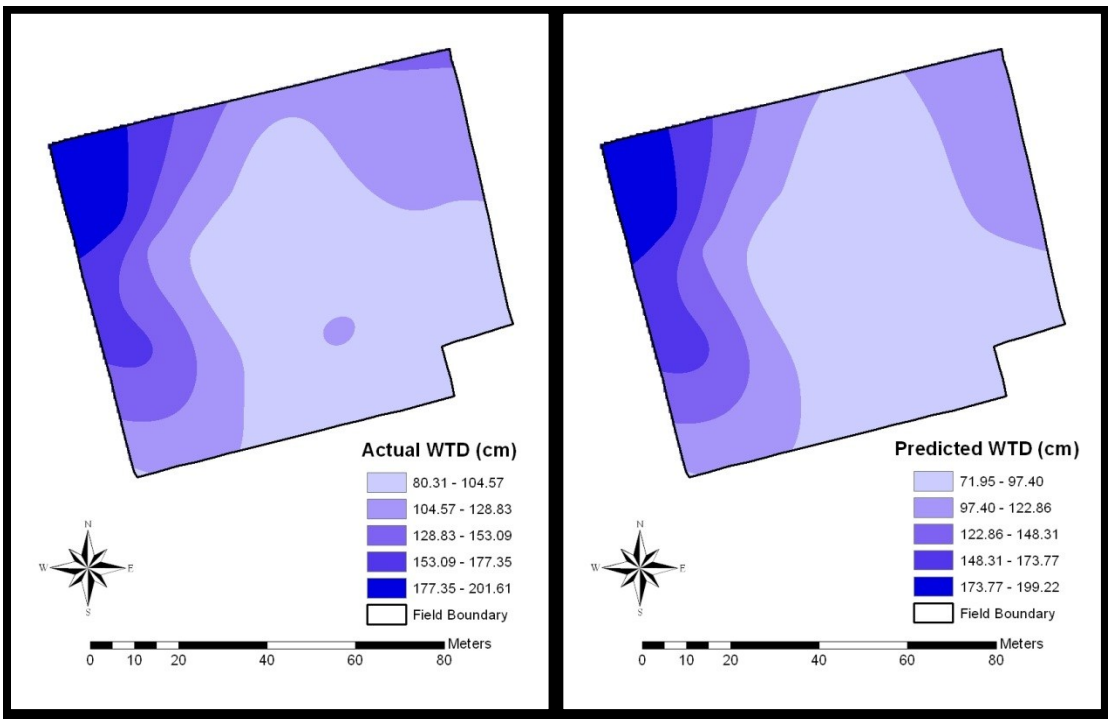

Figure 6-12 Interpolated water table depths in the Boulden Field

6.5 Conclusion

EC_a mapping is a useful tool in precision agriculture as measurement of WTD was rapid and non-destructive. HCP component of DualEM-2 instrument was better to estimate WTD because of greater sensing depth. The performance of the DualEM-2 in predicting groundwater table depth was not as good as for drainage purposes. However, the instrument was able to predict seasonal variation/ oscillations and spatial distribution of the ground water table over time, with R^2 that varied from 0.76 to 0.93 in BEEC Site and from 0.58 to 0.85 in Boulden Site. Underlying drainage designs and lack of evapotranspiration data were identified as the source of error in predicting the ground water table. This study is suitable when the focus is the quantity and quality of the water that flows through the streams of the watershed. Engineers, who design flood control structures, researchers and technicians who deal with environmental pollution carry out their analysis from this perspective. However, if soil moisture, water table depth, and suitability with a greater accuracy for farm activities throughout the year are of interest, perhaps new types of analysis with a lot of data are needed to generate appropriate outputs. Based on the above results, it is concluded that EMI is a useful tool to estimate and map water table depths in a rapid and non-intrusive manner.

CHAPTER 7 CONCLUSIONS AND RECOMMENDATIONS

Based on the results, it was concluded that electromagnetic induction (EMI) methods provide the opportunity of obtaining high resolution apparent electrical conductivity (EC_a) data across a field that can be related with soil properties, such as soil texture, moisture content, organic matter, electrical conductivity and pH, and depths to the gravel and water table depths, and can identify variations in subsurface soil profile and lateral movement of shallow ground water. Several factors influence EC_a measurements including moisture content, soil salinity, porosity, soil structure, temperature, clay content, mineralogy, cation exchange capacity, and bulk density. EMI is a technique which is suitable for field scale measurement due to its rapid response, ease of integration into mobile platforms, and non-destructive and non-contact nature.

The study can be used to develop sampling schemes, especially in untouched environments, by delivering an extra layer of information on soil variability and defining locations where minimum or maximum variation occurs. This information can be very useful for the possible location of monitoring equipment and sensors for observing soil hydrological processes in situ.

The results showed that estimation of depth to gravel layer in wild blueberry fields may be an important factor in addition to pruning, pollination by bees, weeds and insect management practices, fertilizers etc. because shallow gravel depth (0-15 cm) areas in the field showed zero or less blueberry yield accompanying grasses and bare patches.

It was also concluded that EMI mapping provide information that can improve the quality and resolution of spatially-detailed soil and water table maps that are used in hydrology, environment, and agriculture. Such spatially-detailed maps can be useful in studying the

inconsistency between measured and model predictions, where mean values used for soil parameters and water table depths can lead to large deviations. EMI methods can also be used to see the fluctuations in water table depths after rainfall event and spatial trend of water table depth can be visualized for a large area.

BIBLIOGRAPHY

Abdu, H., D. A. Robinson, and S. B. Jones. 2007. Comparing bulk soil electrical conductivity determination using the DUALEM-1S and EM38-DD electromagnetic induction instruments. Soil Sci. Soc. Am. J. 71: 189-196.

Abdu, H. 2009. Characterizing Subsurface Textural Properties Using Electromagnetic Induction Mapping and Geostatistics. PhD Thesis, Utah State University, Logan, Utah, USA.

Allred, B. J., M. R. Ehsani, and D. Saraswat. 2005. The impact of temperature and shallow hydrologic conditions on the magnitude and spatial pattern consistency of electromagnetic induction measured soil electrical conductivity. Trans. of the ASAE. 48(6): 2123-2135.

Amezketa, E. 2006. An integrated methodology for assessing soil salinization, a pre-condition for land desertification. J. Arid Environ. 67: 594-606.

Amezketa, E. 2007. Use of an electromagnetic technique to determine sodicity in saline-sodic soils. Soil Use Manage. 23: 278-285.

Anderson-Cook, C. M., M. M. Alley, J. K. F. Roygard, R. Khosla, R. B. Noble, and J. A. Doolittle. 2002. Differentiating soil types using electromagnetic conductivity and crop yield maps. Soil Sci. Soc. Am. J. 66: 1562-1570.

Arshad, M., Q. U. Zaman, A. Madani, A. W. Schumann, and K. C. Swain. 2009. Electromagnetic Induction Methods for Water Management Enhancement. ASABE Paper Number: 09558. (ASAE, St. Joseph, MI, USA).

Banin, A. and A. Fish. 1995. Secondary desertification due to salinization of intensively irrigated lands: The Israeli experience. Environ. Monit. Assess. 37: 17-37.

Banton, O., M. K. Seguin, and M. A. Cimon. 1997. Mapping field-scale physical properties of soil with electrical resistivity. Soil Sci. Soc. Am. J. 61(4): 1010-1017.

Baver, L. 1961. Soil Physics. 3rd Edition. John Wiley and Sons, Inc. USA.

Bennett, S. J., E. G. Barrett-Lennard, and T. D. Colmer. 2009. Salinity and waterlogging as constraints to saltland pasture production: a review. Agric. Ecosys. and Environ. 129: 349-360.

Black, C. 1957. Soil-Plant Relationships. 2nd Edition. John Wiley and Sons, Inc. USA.

Blackmore, S., H. Greipentrog, S. Pedersen, S. Fountas. 2002. Precision Farming in Europe. Precision Farming; A global perspective. The Haworth Press Inc. USA.

Blake, G. R. and K. H. Hartge. 1986. Physical and mineralogical methods. Pp. 363-375. Methods of Soil Analysis: Part 1. Soil Sci. Soc. Am. and Am. Soc. Agron., Madison, WI.

Boettinger, J. L., J. A. Doolittle, N. E. West, E. W. Bork, and E. W. Schupp. 1997. Nondestructive assessment of rangeland soil depth to petrocalcic horizon using electromagnetic induction. Arid Soil Res. Rehab. 11: 375-390.

Bork, E. W., N. E. West, J. A. Doolittle, and J. L. Boetttinger. 1998. Soil depth assessment of sagebrush grazing treatments using electromagnetic induction. J. Range. Manage 51: 469-474.

Bouma, J., 1997. Precision Agriculture: Introduction to the Spatial and Temporal Variability of Environmental Quality. Pp. 5-17. In: Lake, J. V., Bock, G. R., and Goode, J. A. (Eds.), Precision Agriculture: Spatial and Temporal Variability of Environmental Quality, 210. John Wiley and Sons.

Brady, N. C. and R. R. Weil. 2000. Elements of the Nature and Properties of Soils. Prentice-Hall, Upper Saddle River, NJ.

Brejda, J. J., D. L. Karlen, J. L. Smith, and D. L. Allan. 2000. Identification of regional soil quality factors and indicators: II. Northern Mississippi loess hills and Palouse prairie. Soil Sci. Soc. Am. J. 64: 2125-2135.

Brevik, E. C., T. E. Fenton, and A. Lazari. 2003. Differences in EM-38 readings taken above crop residues versus readings taken with instrument-ground contact. Preci. Agric. 4: 351-358.

Brevik, E. C., T. E. Fenton, and A. Lazari. 2006. Soil electrical conductivity as a function of soil water content and implications for soil mapping. Preci. Agric. 7: 393-404.

Brune, D. E. and J. Doolittle. 1990. Locating lagoon seepage with radar and electromagnetic survey. Environ. Geol. Water Soc. 16: 195-207.

Buchanan, S and J. Triantafilis. 2009. Mapping water table depth using geophysical and environmental variables. Ground Water. 47(1): 80-96.

Callegary, J. B., T. P. A. Ferre, and R. W. Groom. 2007. Vertical spatial sensitivity and exploration depth of low-induction-number electromagnetic induction instruments. Vadose Zone J. 6: 158-167.

Cambardella, C., T. Moorman, J. Novak, T. Parkin, D. Karlen, R. Turco, and A. Konopka. 1994. Field-scale variability of soil properties in central Iowa soils. Soil Sci. Soc. Am. J. 58:1501-1501.

Campbell, J. E. 1990. Dielectric properties and influence of conductivity in soils at one to fifty megahertz. Soil Sci. Soc. Am. J. Proc. 54: 332- 341.

Cannon, M. E., R. C. McKenzie, and G. Lachapelle. 1994. Soil salinity mapping with electromagnetic induction and satellite based navigational methods. Can. J. Soil Sci. 74: 335–343.

Chaves, J. S. 1995. Variability in Hydraulic Conductivity and Soil Salinity in a Flood-Irrigated Field: The Las Nutrias Groundwater Project. M.Sc. Thesis, New Mexico Institute of Mining and Technology, Socorro, New Mexico.

Colvin, T. S., D. B. Jaynes, D. L. Karlen, D. A. Laird, J. R. Ambuel. 1997. Yield variability within a central Iowa field. Trans. Of the ASAE 40(4): 883-889.

Cook, P. G., M. W. Hughes, G. R. Walker, and G. B. Allison. 1989a. The calibration of frequency-domain electromagnetic induction meters and their possible use in recharge studies. J. Hydro. 107: 251-265.

Cook, P. G., G. R. Walker, and I. D. Jolly. 1989b. Spatial variability of groundwater recharge in a semiarid region. J. Hydro. 111: 195-212.

Cook, P. G., D. E. R. Fett, G. Buselli, I. Potts, and A. R. Dodds. 1992. The application of groundwater recharge in a semiarid region. J. Hydro. 130: 201-229.

Cook, P. G. and G. R. Walker. 1992. Depth profiles of electrical conductivity from linear combinations of electromagnetic induction measurements. Soil Sci. Soc. Am. J. 56:1015-1022.

Cook, P. G. and B. G. Williams. 1998. Electromagnetic Induction Techniques. Pp. 1-16. In: L. Zhang and G. Walker (Eds.) Studies in Catchment Hydrology: The Basics of Recharge and Discharge. CSIRO Publishing, Australia.

Corwin, D. L. and S. M. Lesch. 2003. Application of soil electrical conductivity to precision agriculture: theory, principles, and guidelines. Agron. J. 95(3): 455-471.

Corwin, D. L. 2005. Applications of apparent soil electrical conductivity in precision agriculture. Comput. Electron. Agric. 46: 1-10.

Corwin, D.L. and S. M. Lesch. 2005a. Characterizing soil spatial variability with apparent soil electrical conductivity. Part I Survey Protocols. Comput. Electron. Agric. 46: 103-133.

Corwin, D.L. and S. M. Lesch. 2005b. Characterizing soil spatial variability with apparent soil electrical conductivity. Part II Case Study. Comput. Electron. Agric. 46: 135-152.

Corwin, D. L. 2006. Delineating site specific crop management units. Available from: www.ars.usda.gov/research/publications.htm?SEQ-NO-115=181958.

Coulibaly, P., F. Anctil , R. Aravena, and B. Bobee. 2001. Artificial neural network modeling of water table depth fluctuations. Water Reso. Res. 37(4): 885-896.

Daliakopoulos, I. N., P. Coulibaly, I. K. Tsanis. 2005. Groundwater level forecasting using artificial neural networks. J. Hydro. 309: 229-240.

Davies, B. E. 1974. Loss-on-ignition as an estimate of soil organic matter. Soil Sci. Soc. Am. Proc. 38: 150-151.

Davis, J. G., N. R. Kitchen, K. A. Sudduth, and S. T. Drummond. 1997. Using electromagnetic induction to characterize soils. Better Crops Plant Food. 81(4): 6-8.

Davis, K. M. 2007. Using Apparent Electrical Conductivity (EC_a) via Electromagnetic Induction (EMI) to Characterize Soils and the Stratigraphy for Wetland Restoration. M.Sc. Thesis, North Carolina State University, Raleigh, North Carolina, USA.

Day, P. R. 1965. Particle Fractionation and Particle-size Analysis. Pp. 545-567. In: Carter, M. R (Ed.). Methods of Soil Analysis. Part 1. Agron. Monogr. 9. Am. Soc. Agron.

Doolittle, J. A., K. A. Sudduth, N. R. Kitchen, and S. J. Indorante. 1994. Estimating depth to claypans using electromagnetic induction methods. J. Soil Water Cons. 49: 572-575.

Doolittle, J. A., R. Murphy, G. Parks, and J. Warner. 1996. Electromagnetic induction investigations of soil delineation in Reno County, KS. Soil Surv. Horiz. 37(1): 11-20.

Doolittle, J. A. and M. E. Collins. 1998. A comparison of EM induction and GPR methods in areas of karst. Geoderma 85: 83-102.

Doolittle, J. A., C. Noble, and B. Leinard. 2000. An electromagnetic induction survey of a riparian area in southwest Montana. Soil Surv. Horiz. 41(2): 27-36.

Doolittle, J., M. Petersen, and T. Wheeler. 2001. Comparison of two electromagnetic induction tools in salinity appraisals. J. Soil Water Cons. 56: 257-262.

DualEM, Inc. 2005. DUALEM-1S and DualEM-2S User's Manual. Milton, Ontario, Canada.

Eaton, L. J. and K. Jensen. 1996. Protection of Lowbush Blueberry Soils from Erosion. Lowbush Blueberry Fact Sheet. Nova Scotia Dept. Agr. Mktg.

Eigenberg, R. A., J. A. Nienaber, B. L. Woodbury, and R. B. Ferguson. 2006. Soil conductivity as a measure of soil and crop status- A four year summary. Soil Sci. Soc. Am. J. 70: 1600-1611.

Esau, T. 2012. Development and Evaluation of a Prototype Variable Rate Sprayer for Spot-Application of Agrochemicals in Wild Blueberry Fields. M.Sc. Thesis, Dalhousie University, Nova Scotia, Canada.

Farahani, H. J. and G. W. Buchleiter. 2004. Temporal stability of soil electrical conductivity in irrigated sandy fields in Colorado. Trans. of the ASAE. 47: 79-90.

Farkas, C. S., A. Ristolainen, and L. Alakukku. 2006. Simulation Modeling of Soil Water Regime of Heavy Clay Soil in Southern Finland. Pp. 249-255. In: G. Józefaciuk, C. Slawinski, and R. T. Walczak (Eds.). Review of Current Problems in Agrophysics. Institute of Agrophysics Polish Academy of Sciences.

Farooque, A. A. 2010. Effect of Soil Variability on Wild Blueberry Fruit Yield. M.Sc. Thesis, Dalhousie University, Nova Scotia, Canada.

Farooque, A. A., Q. U. Zaman, A. W. Schumann, A. Madani, and D. C. Percival. 2011. Response of wild blueberry yield to spatial variability of soil properties. Soil Sci. 177(1): 56-68.

Farooque, A. A., Q. U. Zaman, A. W. Schumann, A. Madani, and D. C. Percival. 2012. Delineating management zones for site specific fertilization in wild blueberry fields. Trans. Of the ASABE. 28(1): 57-70.

Fleming, K. L., D. G. Westphall, D. W. Wiens, L. E. Rothe, J. E. Cipra, and D. F. Heerman. 1998. Evaluating Farmer Developed Management Zone Maps for Precision Farming. Proc. 4th Int. Conf. Prec. Agric. St. Paul, MN, 335-343.

Flynn, E. S., C. T. Dougherty, and B. K. Koostra. 2006. GPS-Enabled Rising Plate Meter With Data Logging Capability. Plant Management Network.

Fraisse, C. W., K. A. Sudduth, and N. R. Kitchen. 2001. Delineation of site-specific management zones by unsupervised classification of topographic attributes and soil electrical conductivity. Trans. of the ASAE. 44(1): 155-166.

Freeland, R. S. 1989. Review of soil moisture sensing methods using soil electrical conductivity. Trans. of the ASAE. 32: 2190–2194.

Freeland, R. S., J. L. Branson, J. T. Ammons, and L. L. Leonard. 2001. Surveying perched water on anthropogenic soils using non-intrusive imagery. Trans. of the ASAE. 44(6): 1955-1963.

Friedman, S. P. 2005. Soil properties influencing apparent electrical conductivity: A review. Comput. Electron. Agric. 46: 45–70.

Fukue, M., T. Minatoa, H. Horibe, and N. Taya. 1999. The microstructure of clay given by resistivity measurements. Eng. Geol. 54: 43-53.

Gagnon, B., R. R. Simard, R. Lalande, and J. Lafond. 2003. Improvement of soil properties and fruit yield of native lowbush blueberry by papermill sludge addition. Can. J. Soil Sci. 83: 1-9.

Ganatsas, P. and I. Spanos. 2005. Root system asymmetry of Mediterranean pines. Plant and Soil. 278: 75-83.

Gebbers, R., E. Luck, and K. Heil. 2007. Depth Sounding With the EM38-Detection of Soil Layering by Inversion of Apparent Electrical Conductivity Measurements. Pp. 95-102. In: J. V. Stafford (Ed.). Proc. Prec. Agric. 07. Wageningen Acad. Publ., Wageningen, the Netherlands.

Gee, G. W. and J. W. Bauder. 1986. Particle-Size Analysis. Pp. 383-423. In: A. Klute (Ed.). Methods of Soil Analysis. Part 1. 2nd ed. Agron. Monogr. 9. Am. Soc. Agron., Soil Sci. Soc. Am. J., Madison, WI.

Geonics Limited. 1997. Applications of Electromagnetic Methods: Soil Salinity. GIS Applications in Agriculture. CRC Press. Mississauga, ON, Canada. Pp. 141-162.

Geonics, 2005. EM38. Available from: http://www.geonics.com/html/em38.html (Accessed 17 February 2005).

Ghassemi, F., A. J. Jakeman, and H. A. Nix. 1995. Salinization of Land and Water Resources. CAB Int., Wallingford, U.K. 526 pp.

Gordon, S. 2005. Assessing temporal stability and spatial variability of soil water patterns with implications for precision water management. Agric. Water Manage. 223-243.

Greenhouse, J. P. and D. D. Slaine. 1983. The use of reconnaissance electromagnetic methods to map contaminant migration. Ground Water Monit. Rev. 3: 47-59.
Gundogdu, K.S. and H. Degirmenci. 2006. WATMAPGIS, preparing of groundwater map by using geographical information system. J. Agron. 5(2): 262-266.

Hache, C. 2003. Site-specific Crop Response to Soil variability in an Upland Field. M.Sc. Thesis, Tokyo University of Agriculture and Technology, Tokyo, Japan.

Havlin, J., J. Beaton, S. Tisdale, W. Nelson. 2005. Soil Fertility and Fertilizers: An Introduction to Nutrient Management. 7th Edition. Pearson Prentice Hall, Inc.

Hedley, C. B., I. J. Yule, C. R. Eastwood, T. G. Shepherd, and G. Arnold. 2004. Rapid identification of soil texture and management zones using electromagnetic induction sensing of soils. Aust. J. Soil Res. 42: 389-400.

Hendrickx, J. M. H., B. Baerends, Z. I. Rasa, M. Sadig, and M. A. Chaudhry. 1992. Soil salinity assessment by electromagnetic induction of irrigated land. Soil Sci. Soc. Am. J. 56(6): 1933-1941.

Hendrickx, J. M. H., B. Borchers, D. L. Corwin, S. M. Lesch, A. C. Hilgendorf, and J. Schlue. 2002. Inversion of soil conductivity profiles from electromagnetic induction measurements: Theory and experimental verification. Soil Sci. Soc. Am. J. 66: 673-685.

Hendrickx, J. M. H. and R. G. Kachanoski. 2002. Nonintrusive Electromagnetic Induction. Pp. 1297-1306. In: J. H. Dane and G. C. Topp (Eds.). Methods of Soil Analysis. Part 4. Physical Methods. Soil Sci. Soc. Am.

Hillel, D. 1998. Salinity Management for Sustainable Irrigation: Integrating Science, Environment, and Economics. PN 20842. The World Bank. Washington, D.C.

Hurn, J. 1993. Differential GPS Explained. PN 2306. Trimble Navigation Ltd., Sunnyvale, CA. 55 pp.

Huth, N. I. and P. L. Poulton. 2007. An electromagnetic induction method for monitoring variation in soil moisture in agroforestry systems. Aust. J. Soil Res. 45: 63-72.

Inman, D. J., R. S. Freeland, J. T. Ammons, and R. E. Yoder. 2002. Soil investigations using electromagnetic induction and ground-penetrating radar in southwest Tennessee. Soil Sci. Soc. Am. J. 66(1): 206-211.

Jaynes, D. B., T. S. Colvin, and J. Ambuel. 1993. Soil type and crop yield determinations from ground conductivity surveys. ASAE Paper 933552.

Jaynes, D. B., T. S. Colvin, J. Ambuel. 1995. Yield mapping by electromagnetic induction. Proc. of the 2nd Int. Conf. on Site-specific manag. agri. systems. 383-394.

Johnson, C. K., J. W. Doran, H. R. Duke, B. J. Wienhold, K. M. Eskridge, and J. F. Shanahan. 2001. Field-scale electrical conductivity mapping for delineating soil condition. Soil Sci. Soc. Am. J. 65(6): 1829-1837.

Johnson, C. K., J. W. Doran, B. Eghball, R. A. Eigenberg, B. J. Wienhold, and B. L. Woodbury. 2003. Status of soil electrical conductivity studies by central state researchers. Trans. of the ASAE 48(3): 979-989.

Jung, W. K., N. R. Kitchen, K. A. Sudduth, R. J. Kremer, and P. P. Motavalli. 2005. Relationship of apparent soil electrical conductivity to claypan soil properties. Soil Sci. Soc. Am. J. 69: 883-892.

Kachanoski, R. G., E. G. Gregorich, and I. J. Van Wesenbeeck. 1988. Estimating spatial variations of soil water content using no contacting electromagnetic inductive methods. Can. J. Soil Sci. 68: 715-722.

Kerry, R. and M. A. Oliver. 2003. Variograms of ancillary data to aid sampling for soil surveys. Preci. Agric. 4:261-278.

Kettler, T. A., D. J. Lyon, J. W. Doran, W. L. Powers, and W. W. Stroup. 2000. Soil quality assessment after weed-control tillage in a no-till wheat–fallow cropping system. Soil Sci. Soc. Am. J. 64: 339-346.

Khakural, B. R., P. C. Robert, and D. R. Hugins. 1998. Use of non-contacting electromagnetic inductive method for estimating soil moisture across a landscape. Comm. Soil Sci. Plant Anal. 29 (11/14): 2055-2065.

Khan, F. S., Q. U. Zaman, A. W. Schumann, A. Madani, D. C. Percival, and A. A. Farooque. 2011. Mapping Water Table Depths Using Electromagnetic Induction Methods to Develop Variable Rate Technologies. Annual Meeting ASABE, Louisville, Kentucky. August 7-10. Paper Number: 1110632.

Kitchen, N. R and K. A. Sudduth. 1996. Predicting Crop Production Using Electromagnetic Induction. Info. Agri. Conf. Proc., Urbana IL.

Kitchen, N. R., K. A. Sudduth, and S. T. Drummond. 1996. Mapping of sand deposits from 1993 Midwest floods with electromagnetic induction measurements. J. Soil Water Conserv. 51: 336–340.

Kitchen, N. R., K. A. Sudduth, and S. T. Drummond. 1999. Soil electrical conductivity as a crop productivity measure for clay pan soils. J. Prod. Agric. 12(4): 697-617.

Kravchenko, A. N. and D. G. Bullock. 2000. Correlation of corn and soybean grain yield with topography and soil properties. Agron. J. 92: 75-83.

Kravchenko, A. N., G. A. Bollero, R. A. Omonode, and D. G. Bullock. 2002. Quantitative mapping of soil drainage classes using topographical data and soil electrical conductivity. Soil Sci. Soc. Am. J. 66 (1): 235-243.

Kravchenko, A.N., K.D. Thelen, D.G. Bullock, and N.R. Miller. 2003. Relationship among crop grain yield, topography, and soil electrical conductivity studied with cross-correlograms. Agron. J. 95: 1132-1139.

Krishna, B., Y. R. S. Rao, T. Vijaya. 2008. Modelling groundwater levels in an urban coastal aquifer using artificial neural networks. Hydrol. Processes. 22: 1180-1188.

Lesch, S. M., J. D. Rhoades, L. J. Lund, and D. L. Corwin. 1992. Mapping soil salinity using calibrated electronic measurements. Soil Sci. Soc. Am. J. 56(2): 540-548.

Lesch, S. M., J. Herrero, and J. D. Rhoades. 1998. Monitoring for temporal changes in soil salinity using electromagnetic induction techniques. Soil Sci. Soc. Am. J. 62: 232-242.

Lesch, S. M., D. L. Corwin, and D. A. Robinson. 2005. Apparent soil electrical conductivity mapping as an agricultural management tool in arid zone soils. Comput. Electron. Agric. 46: 351-378.

Li, Y., Z. Shi, C. F. Wu, H. Y. Li, and F. Li. 2008. Determination of potential management zones from soil electrical conductivity, yield and crop data. J. Zhejiang Univ. Sci. 9: 68-76.

Lopez-Granados, F., M. Jurado-Exposito, J. M. Pena-Barragan, and L. Garcia-Torres. 2005. Using geostatistical and remote sensing approaches for mapping soil properties. Euro. J. Agron. 23: 279-289.

Lund, E. D., C. D. Christy, and P. E. Drummond. 1998. Applying Soil Electrical Conductivity Technology to Precision Agriculture. Pp. 1089-1100. In: Proc. 4th Int. Conf. Prec. Agri., St. Paul MN.

Lund, E. D., C. D. Christy, and P. E. Drummond. 1999. Practical Applications of Soil Electrical Conductivity Mapping. Pp. 1-9. In: Proc. 2nd Eurp. Conf. Prec. Agri., Salina Kansas, USA.

Lund, E. D., C. D. Christy, and P. E. Drummond. 2000. Using Yield and Soil Electrical Conductivity (EC) Maps to Derive Crop Production Performance Information. Pp. 1-8. In: Proc. 5th Int. Conf. Prec. Agri., Salina Kansas, USA.

Lutticken, R. E. 1998. Implementation of Precision Fertilizing Concepts on Practical Farms in Western Germany. Pp. 859-867. In: Proc. 4th Int. Conf. Prec. Agri., St. Paul MN.

Mann, K. K. 2009. Characterization and Amelioration of Yield Limiting Soil Variability in Florida Citrus Production. Ph.D. Dissertation, University of Florida, USA.

Marschner, H. 1995. Mineral Nutrition of Higher Plants. 2nd Edition. Academic Press Limited, London.

McBratney, A., B. Minasny, and B. M. Whelan. 2005. Obtaining 'Useful' High-Resolution Soil Data from Proximally-Sensed Electrical Conductivity/Resistivity (PSEC/R) Surveys. Pp. 503-510. In: Proc. 5th Euro. Prec. Agri. Conf., J. V. Stafford (Ed.). Wageningen Acad. Publ., Wageningen, the Netharlands.

McBride, R. A., A. M. Gordon, and S. C. Shrive. 1990. Estimating forest soil quality from terrain measurements of apparent electrical conductivity. Soil Sci. Soc. Am. J. 54: 290-293.

McKenzie, R. C., R. J. George, S. A. Woods, M. E. Cannon, and D. L. Bennett. 1997. Use of the electromagnetic-induction meter (EM38) as a tool in managing salinization. Hydrogeol. J. 5(1): 37-50.

McLean, E. O. 1982. Soil pH and Lime Requirement. Pp. 199-223. In: A. L. Page (Ed.). Methods of Soil Analysis. Part II. Am. Soc. Agron., Crop Sci. Soc. Am., and Soil Sci. Soc. Am., Madison, WI.

McNeill, J. D. 1980a. Electrical Conductivity of Soils and Rocks. Tech. Note-5. Geonics Ltd, Mississauga, ON, Canada.

McNeill, J. D. 1980b. Electromagnetic Terrain Conductivity Measurements at Low Induction Numbers. Geonics Ltd. Tech. Note-6. Mississauga, ON, Canada.

McNeill, J. D. 1986. Geonics EM38 Ground Conductivity Meter Operating Instructions and Survey Interpretation Techniques: Geonics Ltd. Tech. Note-21. Mississauga, ON, Canada.

McNeill, J. D. 1990. Use of Electromagnetic Methods for Groundwater Studies. Pp. 191-218. In: S. H. Ward (Ed.). Investigations in Geophysics No. 5: Geotechnical and Environmental Geophysics. Soc. of Expl. Geophysicists.

McNeill, J. D. 1992. Rapid, Accurate Mapping of Soil Salinity by Electromagnetic Ground Conductivity Meters. Pp. 209-229. In: G.C. Topp, W. D. Reynolds, and R. E. Green (Eds.). Advances in Measurement of Soil Physical Properties: Bringing Theory into Practice. Soil Sci. Soc. Am. Spec. Publ. No. 30.

McNeill, J. D. 1997. The application of electromagnetic techniques to environmental geophysical surveys. Eng. Geo. Spec. 12: 103-112.

McNeill, J. D. and M. Bosnar. 1999. Application of "dipole-dipole" Electromagnetic Systems for Geological Depth Sounding: Geonics Ltd. Tech. Note-31. Mississauga, ON, Canada.

Mengel, K. and E. Kirby. 2001. Principles of Plant Nutrition. Kluwer Academic Publishers. Dordretcht, The Netherlands.

Miller, W. M. and J. D. Whitney. 1999. Evaluation of weighing systems for citrus yield monitoring. App. Eng. Agric. 15(6): 609-614.

Morgan, M. and D. Ess. 1997. The Precision Farming Guide for Agriculturists. John Deer Publishing. Pp.124.

Mueller, T. G., N. J. Hartsock, T. S. Stombaugh, S. A. Shearer, P. L. Cornelius, and R. I. Barnhisel. 2003. Soil electrical conductivity map variability in limestone soils overlain by loess. Agron. J. 95: 496-507.

Mueller, T. G., B. Mijatovic, B. G. Sears, N. Pusuluri, and T. S. Stombaugh. 2004. Soil electrical conductivity map quality. Soil Sci. 169 (12): 841-851.

Mulla, D. J., A. U. Bhatti, M. W. Hammond, and J. A. Boason. 1992. A comparison of winter wheat yield and quality under uniform versus spatially variable fertilizer management. Agric. Ecosys. Environ. 38: 301-311.

Nadler, A. and H. Frenkel. 1980. Determination of soil solution electrical conductivity from bulk soil electrical conductivity measurements by the four-electrode method. Soil Sci. Soc. Am. J. 44: 1216-1221.

Newton, P. and B. Williams. 2006. Conceptual Implications for Water Use of Cereals Derived from Spatial Variability in Yield Maps. In: Unkovich, M. and G. O'Leary (Eds.). Solutions for a Better Environment. Proc. 11th Aust. Agron. Conf., Geelong, Victoria, Australia.

Paine, J. G. 2003. Determining salinization extent, identifying salinity sources, and estimating chloride mass using surface, borehole, and airborne electromagnetic induction methods. Water Reso. Res. 39(3): 1-10.

Paine, J. G., W. A. White, R. C. Smyth, J. R. Andrews, and J. C. Gibeaut. 2004. Mapping coastal environments with LIDAR and EM on Mustang Island, Texas, U.S. The Leading Edge. 23(9): 894-898.

Patzold, S., F. M. Mertens, L. Bornemann, B. Koleczek, H. Feilhauer, and G. Welp. 2008. Soil heterogeneity at the field scale: a challenge for precision crop protection. Preci. Agric. 9:367-390.

Pivot, J. M., E. Josien, and P. Martin. 2002. Farms adaptation to changes in flood risk: A management approach. J. Hydro. 267(12): 12-25.

Potash and Phosphate Institute (PPI). 1996. Soil electrical conductivity mapping. Available from http://www.ppi-far.org/ssmg (Accessed May, 2002).

Reedy, R. C. and B. R. Scanlon. 2003. Soil water content monitoring using electromagnetic induction. J. Geotech. Geoenviron. Eng. 129: 1028-1039.

Rhoades, J. D. and R. D. Ingvalson. 1971. Determining salinity in field soils with soil resistance measurements. Soil Sci. Soc. Am. Proc. 35: 54-60.

Rhoades, J. D., P. A. Raats, and R. J. Prather. 1976. Effects of liquid phase electrical conductivity, water content, and surface conductivity. Soil Sci. Soc. Am. J. 40: 651-655.

Rhoades, J. D. and D. L. Corwin. 1981. Determining soil electrical conductivity–depth relations using an inductive electromagnetic soil conductivity meter. Soil Sci. Soc. Am. J. 45: 255-260.

Rhoades, J. D. 1982. Soluble Salts. Pp. 167-178. In: A. L. Page (Ed.). Methods of Soil Analysis. Part II. Am. Soc. Agron., Crop Sci. Soc. Am., and Soil Sci. Soc. Am., Madison, WI.

Rhoades, J. D., N. A. Manteghi, P. J. Shouse, and W. J. Alves. 1989. Soil electrical conductivity and soil salinity: New formulations and calibrations. Soil Sci. Soc. Am. J. 53: 433-439.

Rhoades, J. D. 1990a. Overview: Diagnosis of Salinity Problems and Selection of Control Practices. Pp. 18-41. In: K.K. Tanji (Ed.). Agricultural Salinity Assessment and Management. Manuals Pract. No. 71., Am. Soc. Civ. Eng.

Rhoades, J. D. 1990b. Soil Salinity: Causes and Controls. Pp. 109-134. In A.S. Goudie (Ed.). Techniques for Desert Reclamation. John Wiley & Sons, New York.

Rhoades, J. D., F. Chanduvi, and S. M. Lesch. 1999. Soil Salinity Assessment: Methods and Interpretation of Electrical Conductivity Measurements. Food and Agricultural Organization (FAO) Publ. No. 57.

Ristolainen, A., C. Farkas, and T. Tóth. 2009. Prediction of soil properties with field geo-electrical probes. Commun. Soil Sci. Plant Analysis. 40: 555-565.

Roberto, G. and A. Guida. 2006. Field measurements of topsoil moisture profiles by vertical TDR probes. J. Hydro. 348: 442-451.

Saey, T., D. Simpson, U. Vitharana, H. Vermeersch, J. Vermang, and M. VanMeirvenne. 2008. Reconstructing the paleotopography beneath the loess cover with the aid of an electromagnetic induction sensor. Catena 74: 58-64.

Saey, T., D. Simpson, H. Vermeersch, L. Cockx, and M. V. Meirvenne. 2009. Comparing the EM38DD and DUALEM-21S sensors for depth-to-clay mapping. Soil Sci. Soc. Am. J. 73: 7-12.

Samouelian, A., I. Cousin, A. Tabbagh, A. Bruand, and G. Richard. 2005. Electrical resistivity survey in soil science: A review. Soil Tillage Res. 83: 173-193.

Sanderson, K. R., M. R. Carter, and J. A. Ivany. 1996. Effects of gypsum on yield and nutrient status of native lowbush blueberry. Can. J. Plant Sci. 76: 361-366.

Saunders, S. P., G. Larschied, and B. S. Blackmore. 1996. A Method for Direct Comparison of Differential Global Positioning Systems Suitable for Precision Farming. Pp. 663-671. In: Proc. 3rd Int. Conf. Prec. Agri., Minneapolis, Minnesota.

Scanlon, B. R., R. S. Goldsmith, and J. G. Paine. 1997. Analysis of focused unsaturated flow beneath fissures in the Chihuahuan Desert, Texas, USA. J. Hydro. 203: 58-78.

Scanlon, B. R., J. G. Paine, and R. S. Goldsmith. 1999. Evaluation of electromagnetic induction as a reconnaissance technique to characterize unsaturated flow in an arid setting. Groundwater. 37(2): 292-300.

Schueller, J. K. 1992. A review and integrating analysis of spatially variable control of crop production. Fert. Res. 33: 1-34.

Schumann, A. W. and Q. U. Zaman. 2003. Mapping water table depth by electromagnetic induction. Trans. of the ASAE. 19(6): 675-688.

Sethi, R. R., A. Kumar, S. P. Sharma, and H. C. Verma. 2010. Prediction of water table depth in a hard rock basin by using artificial neural network. Int. J. Water Reso. Environ. Eng. 2(4): 95-102.

Sheets, K. R. and J. M. H. Hendrickx. 1995. Non-invasive soil water content measurement using electromagnetic induction. Water Reso. Res. 31: 2401–2409.

Shenk, H. J. and R. B. Jackson. 2002. Rooting depths, lateral root spreads, and belowground/aboveground allometries of plants in water-limited environments. J. Ecol. 90: 480-494.

Shenk, H. J. 2008. Soil depth, plant rooting strategies and species niches. New Physio. 178: 223-225.

Sherlock, M. D., and J. J. McDonnell. 2003. A new tool for hillslope hydrologists: spatially distributed groundwater level and soil water content measured using electromagnetic induction. Hydro. Process. 17: 1965-1977.

Slavich, P. G. 1990. Determining EC_a-depth profiles from electromagnetic induction measurements. Aust. J. Soil Res. 28: 443-452.

Smith, S. T. 1962. Some Aspects of Soil Salinity in Western Australia. MSc. Thesis. University of Western Australia.

Sophocleous, M. A. 1991. Combining the soil water balance and water table fluctuation methods to estimate natural groundwater recharge. Practical aspects. J. Hydro. 124: 229-241.

Sudduth, K. A., and N. R. Kitchen. 1993. Electromagnetic induction sensing of claypan depth. ASAE Paper 93-1550.

Sudduth, K. A., S. T. Drummond, and N. R. Kitchen. 2001. Accuracy issues in electromagnetic induction sensing of soil electrical conductivity for precision agriculture. Comput. Electron. Agric. 31: 239-264.

Sudduth, K. A., N. R. Kitchen, G. A. Bollero, D. G. Bullock, and W. J. Wiebold. 2003. Comparison of electromagnetic induction and direct sensing of soil electrical conductivity. Agron. J. 95: 472-482.

Sudduth, K. A., N. R. Kitchen, W. J. Wiebold, W. D. Batchelor, G. A. Bollero, D. G. Bullock, D. E. Clay, H. L. Palm, F. J. Pierce, R. T. Schuler, and K. D. Thelen. 2005. Relating apparent electrical conductivity to soil properties across the north-central USA. Comput. Electron. Agric. 45: 263-283.

Tatabatai, M. 1996. Soil Organic Matter Testing: An Overview. Soil Sci. Soc. Am. 14: 1-9.

Triantafilis, J., I. A. Huckel, and I. O. A. Odeh. 2003. Field-scale assessment of deep drainage risk. Irrig. Sci. 21: 183-192.

Triantafilis, J., I. O. A. Odeh, A. L. Jarman, M. G. Short, and E. Kokkoris. 2004. Estimating and mapping deep drainage risk at the district level in the lower Gwydir and Macquarie Valleys, Australia. Aust. J. Exp. Agric. 44(9): 893-912.

Triantafilis, J. and S. M. Lesch. 2005. Mapping clay content variation using electromagnetic induction techniques. Comput. Electron. Agric. 46: 203-237.

Usery, E. L., S. Pocknee, and B. Boydell. 1995. Precision farming data management using Geographical Information System. Photogram. Eng. Remote Sens. 61(11): 1383-1391.

Vazquez-Amabile, G. G. and B. A. Engel. 2005. Use of SWAT to compute groundwater table depth and streamflow in the Muskatatuck River Watershed. Trans. of the ASABE. 48(3): 991-1003.

Wait, J. R. 1962. A note on the electromagnetic response of a stratified earth. Geophysics 27: 382-385.

Wander, M. M. and G. A. Bollero. 1999. Soil quality assessment of tillage impacts in Illinois. Soil Sci. Soc. Am. J. 63: 961–971.

Warman, P. R. 1987. The effects of pruning, fertilizers, and organic amendments on lowbush blueberry production. Plant and Soil. 101: 67-72.

Webb, K.T., R. L. Thompson, G. J. Beke, and J. L. Nowland. 1991. Soils of Colchester County, Nova Scotia. Report No. 19. Nova Scotia Soil Survey. Research Branch, Agriculture Canada, Ottawa, ON. 1991, pp. 201.

Webb, K. T. and D. R. Langille, 1996. Soils of the Fiddes and Brookside Research Fields, Colchester County, Nova Scotia – Revised. Research Branch, Agriculture and Agri-Food Canada.

Wilding, L. 1985. Spatial Variability: Its Documentation, Accommodation and Implication to Soil Surveys. Pp. 166-189. In: D. R. Nielsen and J. Bouma (eds.). Soil Spatial Variability, Centre for Agricultural Publishing and Documentation, Wageningen, the Netherlands.

Williams, B. G., and G. C. Baker. 1982. An electromagnetic induction technique for reconnaissance surveys of soil salinity hazards. Aust. J. Soil Res. 20:107-118.

Williams, B. and D. Hoey. 1987. The use of electromagnetic induction to detect the spatial variability of the salt and clay content of soils. Aus. J. Soil Res. 25: 21-27.

Wong, M. T. F., and S. Asseng. 2006. Determining the causes of spatial and temporal variability of wheat yields at sub-field scale using a new method of upscaling a crop model. Plant and Soil. 283:209-221.

Yang, C., C. L. Peterson, G. J. Shropshire, and T. Otawa. 1998. Spatial variability of field topography and wheat yield in the Palouse region of the Pacific Northwest. Trans. of the ASAE. 41:17-27.

Yarborough, D. E., J. J. Hanchar, S. P. Skinner, and A. A. Ismail. 1986. Weed response, yield, and economics of hexazinone and nitrogen use in lowbush blueberry production. Weed Sci. 34(5): 723-729.

Zalasiewicz, J. A., S. J. Mathers, and J. D. Cornwell. 1985. The application of ground conductivity measurements to geological mapping. Quat. J. Eng. Geo. Hydrogeo.18: 139-148.

Zaman, Q. U., A. W. Schumann, D. C. Percival, and R. J. Gordon. 2008. Estimation of wild blueberry fruit yield using digital color photography. Trans. of the ASABE. 51(5): 1539-1544.